

**Conceptual Design for a Gamma-Ray Large Area
Space Telescope (GLAST) Tower Structure**

Daniel Alex Luebke

Stanford Linear Accelerator Center
Stanford University
Stanford, CA 94309

SLAC-Report-489
August 1996

Prepared for the Department of Energy
under contract number DE-AC03-76SF00515

CONCEPTUAL DESIGN FOR A GAMMA-RAY LARGE AREA
SPACE TELESCOPE (GLAST) TOWER STRUCTURE

A THESIS
SUBMITTED TO THE DEPARTMENT OF AERONAUTICS AND
ASTRONAUTICS
AND THE COMMITTEE ON GRADUATE STUDIES
OF STANFORD UNIVERSITY
IN PARTIAL FULFILLMENT OF THE REQUIREMENTS
FOR THE DEGREE OF
ENGINEER

By
Daniel Alex Luebke
August 1996

I certify that I have read this thesis and that in my opinion it is fully adequate, in scope and in quality, as a thesis for the degree of Engineer.

Robert Twiggs
(Academic Advisor)

Elliott Bloom
(Research Advisor)

Stephen Tsai
(Principal Advisor)

Approved for the University Committee on Graduate
Studies:

Abstract

The main objective of this work was to develop a conceptual design and engineering prototype for the Gamma-ray Large Area Space Telescope (GLAST) tower structure. This thesis describes the conceptual design of a GLAST tower and the fabrication and testing of a prototype tower tray.

The requirements were that the structure had to support GLAST's delicate silicon strip detector array through ground handling, launch and in orbit operations as well as provide for thermal and electrical pathways. From the desired function and the given launch vehicle for the spacecraft that carries the GLAST detector, an efficient structure was designed which met the requirements.

This thesis developed in three stages: design, fabrication, and testing. During the first stage, a general set of specifications was used to develop the initial design, which was then analyzed and shown to meet or exceed the requirements. The second stage called for the fabrication of prototypes to prove manufacturability and gauge cost and time estimates for the total project. The last step called for testing the prototypes to show that they performed as the analysis had shown and prove that the design met the requirements.

As a spacecraft engineering exercise, this project required formulating a solution based on engineering judgment, analyzing the solution using advanced engineering techniques, then proving the validity of the design and analysis by the manufacturing and testing of prototypes. The design described here met all the requirements set out by the needs of the experiment and operating concerns. This strawman design is not intended to be the complete or final design for the GLAST instrument structure, but instead examines

some of the main challenges involved and demonstrates that there are solutions to them. The purpose of these tests was to prove that there are solutions to the basic mechanical, electrical and thermal problems presented with the GLAST project.

Acknowledgments

There are many people and agencies who made this work possible. This long list is only a partial list of the most notable contributors.

I'd like to thank my advisors, Elliott Bloom, Stephen Tsai; and Bob Twiggs; Stanford Linear Accelerator Center's (SLAC) Terry Anderson, Bill Atwood, Joe Ballam, John Broeder, Lynn Cominsky, Linda Lee Evans, Bruce Feerick, Gary Godfrey, John Hanson, Chad Jennings, Y.C. Lin, Peter Michaleson, and Pat Nolan; Stanford Satellite Systems Development Lab's (SSDL) Raj Batra, Jeff Chan, and Alison Nordt; Stanford Structures And Composites Lab's (SACL) Sung Ahn, Tracy Colwell, Steve Huybrechts, George Springer and Qiuling Wang; Lockheed-Martin's Dave Chenette, Eric Herzberg, George Nakano, and Jeff Tobin; Space Systems Loral's Steve Berglund, and Fred Wooley; The National Aeronautics and Space Administration's (NASA Ames) Roger Arno, and Gary Langford; Stanford Center for Integrated Systems (CIS) Nanofabrication Lab's Nancy Latta, Mary Martinez , and Bob Wheeler; Aptos Corporation's Scott Graham; Promex Corporation's Bill Stansbury, and Glen Stansbury; DynaFlex Corporation's Scott Russel; Merlin Technologies' Walt Wilson; The International Center for Theoretical Physics' (ICTP) Andreas Cicuttin, Alberto Colavita, and Fabio Fratnik; The Italian Center for Nuclear Physics' (INFN) Guido Barbullini; San Francisco State's Abraham Anapolsky, and Barbara Neuhauser; University of Santa Cruz's Robert Johnson; University of Chicago's Renee Ohn, and Mark Oreglia; University of Tokyo's Tune Kamae; The Navel Research Lab's (NRL) Neil Johnson, Michael Lovellett, and Kent Wood; The Department Of Energy (DOE); Bryte Technologies; Stanford University's Department of Aeronautics and Astronautics, Department of Physics and Department of Mechanical Engineering; and all other businesses and associates who helped on this project and to all my friends at Stanford and around the world.

Most importantly my thanks to Brad “swing jumper” Betts, Rick “danger seeker” Lu, James “the man” Myatt, my Mom, Dad, sister Aviva and Debbie for their help and support.

List of Symbols

a	Albedo (30% of direct solar, 407 W/m ²)*
a_g	Acceleration in gravities
A_{sc}	Radiator area for spacecraft (m ²)
α	Solar absorptivity (0.15 for radiators, 0.01 for thermal blankets)
c_{max}	Maximum distance from neutral axis
D	Flexural stiffness modulus matrix
δ	Deflection (meters)
δ_{max}	Maximum deflection (meters)
ε	Mechanical strain = σ/E
ε^o	Constant strain component
ε_{SSD}	Strain in silicon strip detector
ε_t	Solar Emissivity (0.8 for radiators, 0.01 for thermal blankets)
E	Modulus of elasticity (Pa)
g	Gravity of acceleration (9.8 m/s ²)
G_s	Solar constant (1358 W/m ²)
h_{core}	Thickness of composite core (meters)
I	Area moment of inertia (meters ⁴)
H	Altitude of orbit (600 km)

* MKS units used except when English units are given as standard for manufacturing

k	Thermal conductivity ($\text{W cm}^{-1} \text{K}^{-1}$)
K_a	$0.664+0.521\rho_e-0.203\rho_e$, a factor which accounts for the reflection of collimated incoming solar energy off a spherical Earth.
K_{mn}	Fourier coefficients
K_{trayn}	Curvature of tray
L	Length of side of tray
L_{trak}	Length of the tracker section (meters)
M_{max}	Maximum moment (N m)
m_{cal}	Mass of calorimeter section (N m)
m_{trak}	Mass of tracker section (N m)
P_o	Distributed Load (Pa)
Q	Composite stiffness matrix
ρ	Mass density (kg/cm^3)
ρ_e	Angular radius of Earth ($R_e/(H + R_e)$)
q_1	Earth IR emission (237 W/m^2)
R_e	Radius of Earth (6378 km)
σ	Mechanical stress (Pa)
σ_{max}	Maximum mechanical stress
σ_s	Stefan-Boltzmann constant ($5.67\text{E-}8 \text{ W m}^{-2}\text{K}^{-4}$)
t_{SSD}	Thickness of silicon strip detector (m)
t_{face}	Thickness of composite facesheet (meters)
X	X silicon layer, bottom layer of detectors on tray
Y	Y silicon layer, top layer of detectors on tray
Z	Elemental number on periodic chart (radiation length)

List of Acronyms

- CsI.....Cesium Iodide crystals, used in calorimeter
- CTE.....Coefficient of Thermal Expansion, describes amount materials expand when exposed to temperature gradients
- CTT.....Conductive Transfer Tape, double sided tape which offers high thermal conductivity
- CVCM.....Collectable Volatile Condensable Materials, percentage of evaporated material that is condensable
- EOL.....End Of Life, design condition exemplifying changes in materials over time
- ESDElectrostatic Discharge, the transfer of potential static electricity by an electrical spark
- FEM.....Finite Element Model, engineering computer tool to analyze physical systems
- GEVS.....General Environmental Vehicular Specifications, report put out by NASA which lists basic requirements for spacecraft

GLAST.....Gamma-ray Large Area Space Telescope

IDL.....Interactive Design Language

IR.....Infrared, energy range exemplified by heat emittance

MLI.....Multilayer Insulation, thermal insulation blankets

NASA.....National Aeronautics and Space Administration, the principal space agency responsible for defining spacecraft requirements

RVC.....Reticulated Vitreous Carbon, expanded carbon foam structural spacer material

SSD.....Silicon Strip Detector, device for measuring the passage of charged particals en-mass

SSM.....Second Surface Mirror, device used to radiate heat energy

TABTape Automated Bonding system for providing electrical connections

TML.....Total Mass Loss, percentage of mass lost due to evaporation

UVUltra Violet, range of electromagnetic energy emission

Contents

1 Introduction	1
<i>Statement of Problem</i>	1
Design Concept Summary.....	3
The Space Environment.....	4
<i>Contributions of Dissertation</i>	5
2 : Tower Design Issues	6
<i>Tower Design</i>	6
<i>Layup of SSDs on Tray</i>	7
Tray Mounting	7
SSD Mounting	9
Electrical Connections	10
<i>Calorimeter and Tower Wall Design</i>	11
<i>Instrument Strong-back Design</i>	11
<i>Satellite Bus Design</i>	12
3 : Design Specifications	14
<i>Material Audit</i>	14
<i>Attitude and Thermal Control</i>	15
<i>Orbit, Size, and Weight</i>	15
<i>Expected Loads</i>	15
<i>Operating temperatures</i>	16
4 : Thermal, Material, and Electrical Considerations	17
<i>Thermal Considerations to meet Specifications</i>	17
Thermal Conditions.....	17
Thermal Subsystem.....	18
Thermal Contact Resistance and Heat Pipes	20

<i>Spacecraft Materials to meet Specifications</i>	21
Composites	22
Metals	24
Adhesives.....	24
Other materials	25
<i>Electrostatic Discharge</i>	25
5 : Analysis of Design	27
<i>Finite Element Model</i>	27
<i>Structural Analysis: Strength and Deflection</i>	28
SSD Tray	28
Tower	30
Grid.....	32
<i>Vibrational Analysis: Natural Frequency Estimates</i>	34
SSD Tray	34
Tower Structure.....	36
Grid Structure	37
<i>Thermal Analysis, Operating Temperature Estimates</i>	38
SSD Tray	38
Tower Wall.....	39
Grid.....	41
<i>On Orbit Temperatures</i>	43
6 : Fabrication of Prototypes	47
<i>Space Qualification</i>	47
<i>Built in Testing Schemes</i>	47
Back-plane continuity check	47
Back-plane design	48
Dummy detector.....	50
<i>Manufacturing of a Tray</i>	51
Manufacturing processes.....	51
7 : Testing of Prototypes	53
<i>Random Vibration Tests</i>	53
Vibration Equipment Setup	53
Shake Test	54
<i>Thermal Cycling under Vacuum</i>	55
Thermal Equipment Setup	55
Thermal/vacuum Tests	55

8 : Final Results	57
<i>Post test</i>	57
<i>Mass Estimates</i>	58
<i>Physics Performance Numbers</i>	60
<i>Concluding Remarks</i>	60
BIBLIOGRAPHY	61
APPENDIX A - ANSYS STATIC DEFLECTION AND FREQUENCY GRID CODE	62
APPENDIX B - ANSYS TRAY CODES	68
APPENDIX C - ANSYS TOWER CODES	72
APPENDIX D - ANSYS THERMAL AND RADIATION GRID CODES	78
APPENDIX E - MATLAB THERMAL CODE FOR WALL	84
APPENDIX F - ANSYS THERMAL WALL FEM	88
APPENDIX G - IDL CODE FOR ON ORBIT TEMPERATURES	92

List of Figures

Figure 1-1 - Artists concept of GLAST (showing tracker and calorimeter).....	2
Figure 1-2 - Layout of towers.....	3
Figure 2-1 - Lay-up of tray (exploded view)	8
Figure 2-2- Electrical connection of Silicon Strip Detectors (SSDs).....	9
Figure 2-3 - Structural grid design.....	12
Figure 2-4 - Schematic of GLAST.....	13
Figure 4-1 - Composite core laminate	23
Figure 5-1 - FEM stress analysis of structural grid.....	33
Figure 5-2 - FEM modal analysis of structural tray.....	35
Figure 5-3 - FEM modal analysis of tower	36
Figure 5-4 - FEM modal analysis of structural grid	37
Figure 5-5 - Temperature distribution down tower wall	39
Figure 5-6 - FEM thermal analysis for temperature rise down tower wall	40
Figure 5-7 - FEM thermal analysis for temperature distribution across grid.....	42
Figure 5-8 - Maximum temperatures of GLAST radiator surface as function of rotations. .	44
Figure 5-9- Maximum temperatures of GLAST radiator surface as function of rotations..	45
Figure 6-1 - Circuit design for electrical connection of back-plane	49
Figure 6-2 - Dummy detector testing scheme.....	50
Figure 7-1 - Response of center of tray under random vibration.....	54
Figure 7-2 - Sample thermal vacuum temperature cycle.....	56

List of Tables

Table 4-1 - Spacecraft material properties.....	22
Table 8-1 - Mass and radiation lengths in tray.....	58
Table 8-2 - Mass estimates for GLAST.....	59

1 Introduction

Statement of Problem

The main objective of this work was to develop a conceptual design and engineering prototype for the Gamma-ray Large Area Space Telescope (GLAST, Figure 1-1) tower structure. This thesis describes the conceptual design of a GLAST tower and the fabrication and testing of a prototype tower tray.

The novelty of the GLAST instrument is that it is a high energy gamma-ray telescope based on silicon strip detector (SSD) technology. This new technology provides an effective way to measure the passage of charged particles while still allowing for a highly modular structure.

Because of the Earth's atmosphere, only the highest energy gamma-rays are detectable by ground based observatories. By using detectors in orbit, gamma-rays can be viewed before they are absorbed by the atmosphere. The purpose of the GLAST instrument is to measure the interaction of gamma-rays in the detector in order to determine their energy and direction. From this information we might further understand the physics of gamma-ray emissions from astrophysical sources such as relativistic jets emanating from active galactic nuclei, gamma-ray bursts, pulsing neutron stars, and the diffuse galactic and extragalactic emission. The combination of wide field of view, high angular resolution, good sensitivity, and a wide-energy bandwidth make telescopes based on silicon strip technology well suited for the observation of such sites of cosmic particle acceleration [<http://www-glast.stanford.edu>].

The basic component of the GLAST instrument is a tower which is composed of a tracker and a calorimeter (see Figure 1-2). The tracker section is used to convert the incoming gamma-rays to electrons and positrons and then track the paths of the subsequent electromagnetic shower of these particles. The calorimeter is then used to measure all the remaining energy from the electromagnetic shower and thus make an energy measurement of the gamma-rays. The work presented here focuses on the design and prototyping of the tracker section of the GLAST tower -

CHAPTER 5. ANALYSIS OF DESIGN

specifically the mechanical support of the SSDs. Additionally, to provide accurate models for the tray analysis, detailed designs were done for electrical connections and mechanical bonding of detectors, as well as the main structural support for the instrument.

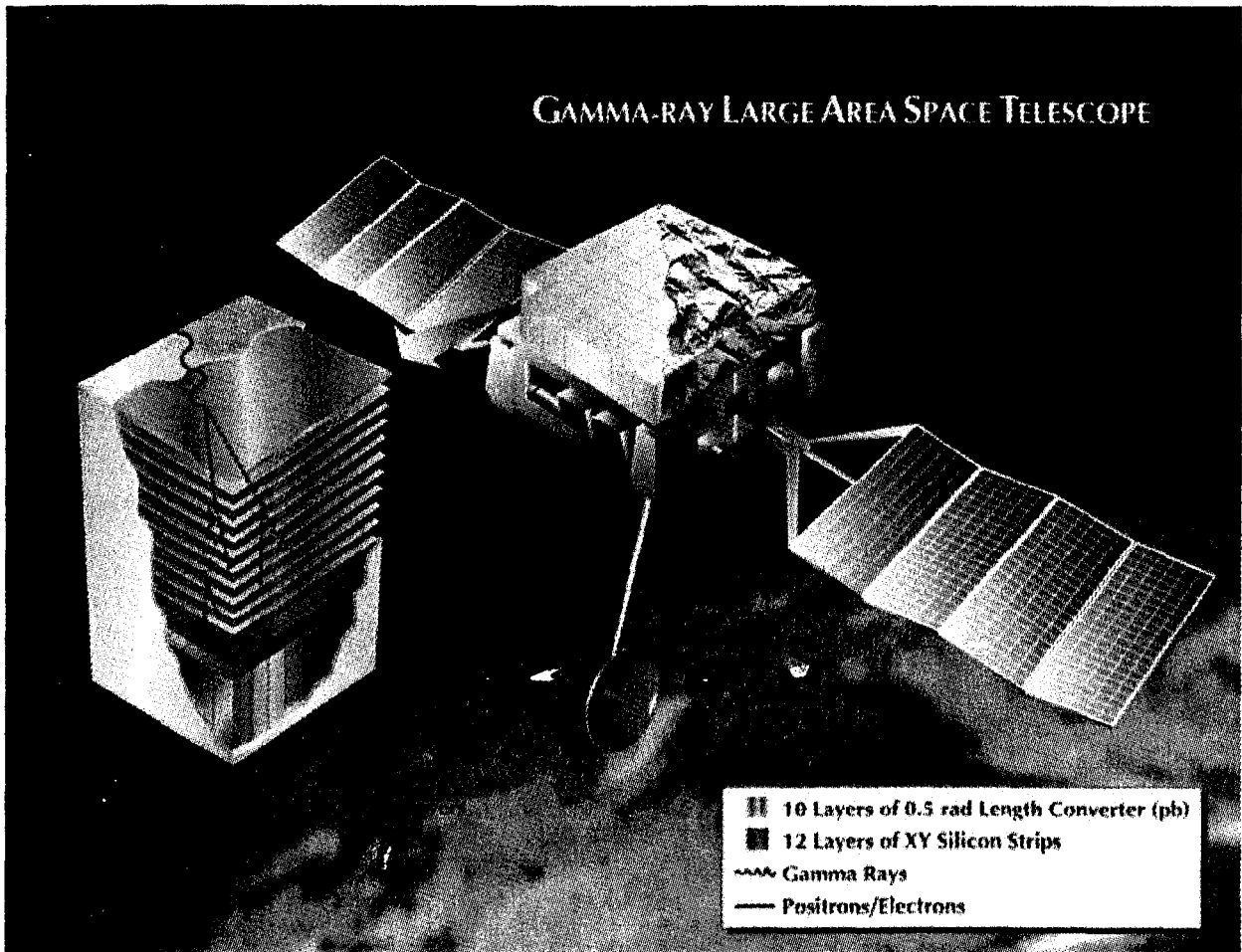


Figure 1-1 - Artists concept of GLAST (showing tracker and calorimeter).

CHAPTER 1. INTRODUCTION

Design Concept Summary

The proposed GLAST instrument consists of a 7x7 array of towers, each with a stack of silicon detectors (tracker section) followed by an array of Cesium Iodide (CsI) crystal detectors (calorimeter section). These towers are supported on a mounting structure (grid) that sits above the spacecraft bus (see Figure 1-2).

In designing the GLAST structure, two critical design criteria for components were identified -- modularity and accessibility. These criteria led to an identical design for each of the towers, resulting in straightforward manufacturing, assembly, and disassembly of the instrument. This design philosophy also extends into the tower itself, where each tracker tray is nearly identical, as is each calorimeter detector. Although there are many benefits for this modular structure, it introduces a difficulty in designing for robust thermal and mechanical connections.

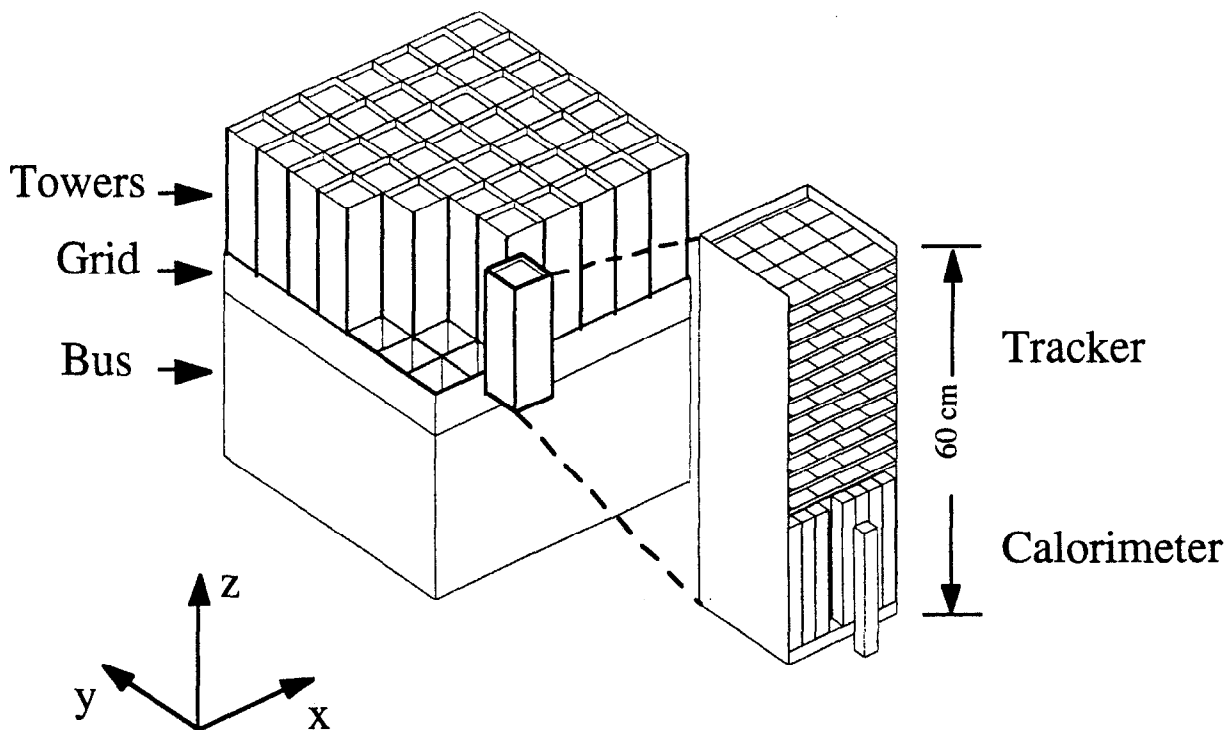


Figure 1-2 - Layout of towers

CHAPTER 1. INTRODUCTION

The trays in the tracker section required substantial engineering. The purpose of the trays is to support the delicate SSDs through ground handling, launch and on orbit operations. The requirement for the tower structures are high stiffness, good thermal pathways, and maximum transparency to gamma-rays. This last requirement was a main driver in the tower designs, requiring minimal material (in-line with the detectors) that might cause the gamma-rays to convert to electrons and positrons before reaching the SSDs.

The solution was for the trays to utilize composites. The directional nature of composites allowed the strength, stiffness, and thermal properties to be tailored to meet the requirements. Additionally, by using a laminate consisting of a core spacer in-between thin layers of high modulus composite fibers, high strength and stiffness was achievable using minimal material mass and volume. Advanced composites also offer excellent thermal conductivities, rivaling the most conductive metals.

The Space Environment

Because this instrument must operate in the harsh environment of outer space, the demands of space must be understood and accounted for in the design. The most obvious characteristic of space is the hard vacuum. The problem here is that many materials (resins, adhesives, liquid lubricants and even some metals) evaporate (outgas) in a vacuum. Excessive outgassing can lead to the degradation of material properties and can also affect other components. For example, since there is no force to carry the outgassed particles away from the spacecraft, these particles remain in a cloud around it or condense onto its colder surfaces. In this way, outgassing can degrade optical surfaces, radiators and solar arrays, and even cause shorting of electrical circuits and promote corona or electrical discharge [Williamson, 1990, pg. 29]. The high vacuum poses another problem by severely reducing thermal conduction between components.

The temperature regime of space must also be accounted for, or serious problems can arise. In orbit, the temperature range is much larger than normally experienced on Earth and, without air for convective cooling, the differentials can be extreme. These extremes in temperature cause many problems. Thermal cycling can produce fatigue, fracture and de-bonding through differential expansion and contraction. In addition, low temperature promotes condensation while high temperature increases outgassing. While this can pose serious problems for some components, the main structure is generally not exposed to these extreme temperatures because the spacecraft core temperature is controlled to protect the payload and subsystem equipment.

CHAPTER 1. INTRODUCTION

Radiation such as x-rays, gamma rays, alpha particles, protons, and electrons can affect many systems on a spacecraft, including the structural subsystem. Ultra violet (UV) radiation can degrade polymeric materials while x- and gamma radiation can scatter electrons in metals. This scattering of electrons may eventually decrease electrical conductivity, a particularly undesirable effect in materials which transmit low signal currents [Williamson, 1990, pg. 31].

In space, physical properties of material may also degrade over time. It is therefore critical for all calculations to be designed with end of life (EOL) properties in mind. This is particularly true when calculating solar cell efficiencies, radiator efficiencies, thermal surface properties and heat generation in electronics.

However, there are some advantages of the space environment. There is no corrosion and space offers inherently good electrical insulation, meaning that high voltage electrical components can be positioned closer together before arcing problems occur [Williamson, 1990, pg. 31].

Contributions of Dissertation

In summary, there are several factors which must be considered in designing the GLAST instrument tower. The tower structure must be designed to support all the tower components while not interfering with the experiments. It must be versatile and allow for easy assembly, disassembly and modifications. Because of the large size of the instrument and the tight tolerances between components, special production techniques must be accounted for in the designs. All this must be accomplished with minimal cost and time constraints.

This thesis offers a basic concept for designing and manufacturing the GLAST instrument structure and defines some of the specifications that will be needed to for the final design. While the solutions offered in this thesis do not necessarily provide the best designs, they have demonstrated the feasibility of the GLAST tower system.

2 : Tower Design Issues

In this chapter, many issues for the GLAST instrument are examined, including SSD mounting and electrical connections, designs for the tracker, calorimeter, tower wall, structural strong-back, and satellite bus. While not all aspects or issues of the instrument are explored, the main issues are addressed sufficiently well to obtain a “big” picture of the system.

Tower Design

The basic configuration of the GLAST instrument is based on five design criteria: performance, cost, ease of manufacturing, ease of assembly (serviceability), and versatility of design. Trade studies were performed using the above design parameters to address two critical design issues: the method for holding the trays in the tracker section, and configuration of the tower walls.

The first set of trade studies assessed two designs for the mounting of trays. The competing designs were for the “rack” and the “stack” tower designs where trays are either slid into place like shelves or stacked on top of one another, respectively. Because of thermal contact and ease of assembly reasons, the rack design was chosen.

The second trade study was performed to determine the most suitable configuration for the tower walls. The tower walls must provide structural support for trays, thermal pathways for heat dissipation, and space for electrical cables. They must do all this with minimum interference to the gamma-rays products being measured. The three basic configurations for the tower walls had to do with the number of walls. A two walled tower had the lowest material audit and was sufficient for thermal needs but mechanically weak. While three walls improved the mechanical properties, for robustness, the design selected as the baseline was with four walls. Although this design resulted in an increased material audit for the tower, this effect was offset by the selection of higher performance materials (higher strength, stiffness and radiation length).

CHAPTER 2. TOWER DESIGN ISSUES

Layup of SSDs on Tray

SSD layup and corresponding electrical connections drive the mechanical requirements for the structural tray. The tray must be stiff and strong enough to protect the detectors and electrical connections when loaded.

Tray Mounting

A honeycomb composite tray provided the required properties of strength and stiffness to protect the SSDs and wirebonds. The need to mechanically attach and thermally couple the tray to the walls still remained. A simple solution was to add a “close-out” around the tray (see Figure 2-1). The close-out provided secure mounting points for bolts and also provided enough material and surface area to transfer heat to the tower walls. The relatively large amount of concentrated material in the close-out, however, required a good low Z, thermally conductive material. Because GLAST will have a 2π field of view, gamma-rays can penetrate tower walls before registering on the SSDs. Also, because the walls offer the only thermal path from the readout electronics to the satellite bus, the walls will have to be good conductors of heat. The challenge is to find a suitable low Z, thermally conductive material (e.g., Be, composites; See Chapter 4).

The “active” area is defined as the area of the SSD minus a small inactive border on the edges of the detectors. All other area within the instrument is classified as “dead” area, because it cannot register particle tracks. The efficiency of the GLAST instrument increases proportionally to the active area of the SSDs. In order to minimize dead area, clearances between components in the tower and clearances between towers must be kept to a minimum. To reduce dead area created by the readout electronics, the SSDs will be daisy chain bonded together, requiring only one set of readout electronics per four detectors.

The readout electronics (pre-amplifier, shaper, filter, etc.) are 2 mm wide silicon devices that lie on the periphery of two sides of a tray. These electronics are the main source of the heat generated in GLAST and thus drive the thermal design. To reduce problems resulting from heat generation and dead area, these devices have been designed to be as small and efficient as possible.

CHAPTER 2. TOWER DESIGN ISSUES

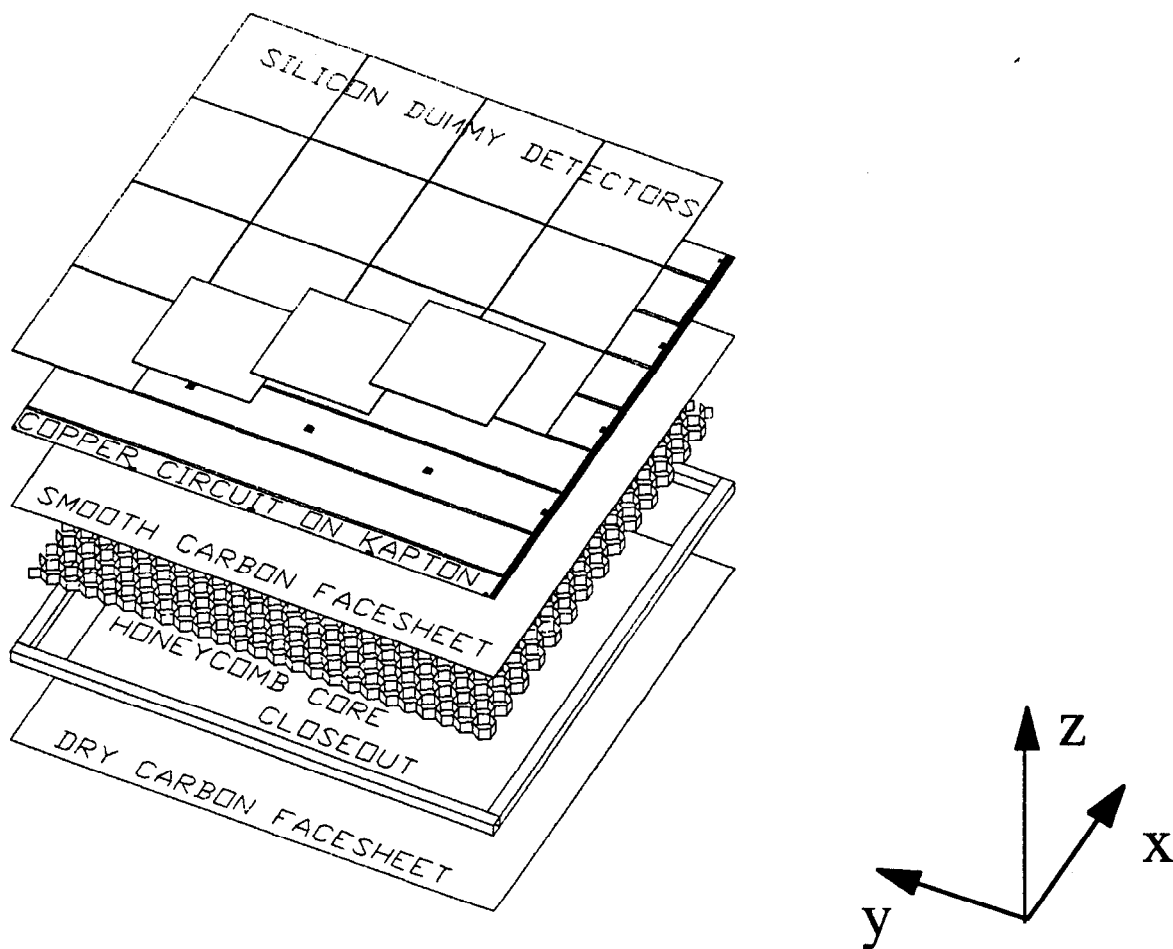


Figure 2-1 - Lay-up of tray (exploded view)

The area in the tower includes four 2 mm walls, 3.5 mm on two edges for electronics and electrical connection, and 416 μm between all components. This design gives exactly the equivalent of 43 dead strips between active area in adjacent towers. In the current design, with a 736 μm dead band around the periphery of each detector, the dead area in the instrument is 11%.

The design of the tracker section, as discussed earlier, is a vertical array of 12 horizontal trays, spaced apart by 3 cm and held together by four walls. These walls offer structural support in addition to thermal and electrical pathways. Each horizontal tray in the tracker section holds 32 SSDs. Each SSD is a 6x6 cm square pieces of 500 μm thick, high resistivity silicon with 249 parallel strip implants nearly 6 cm in length and 236 μm apart (see Figure 2-2).

CHAPTER 2. TOWER DESIGN ISSUES

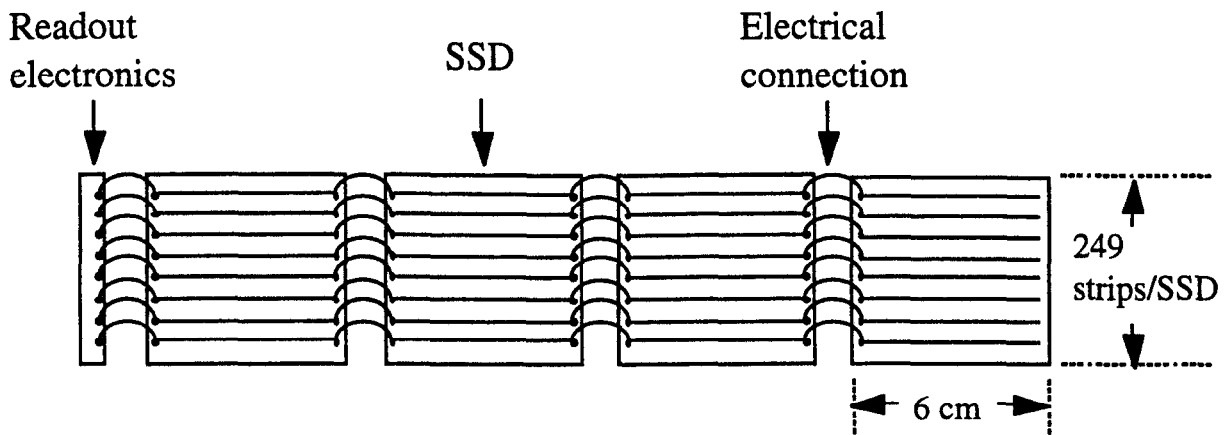


Figure 2-2- Electrical connection of Silicon Strip Detectors (SSDs)

SSD Mounting

Another trade study was done for establishing the specific method for configuring the SSDs on the each tray. As the SSDs have been selected to be single sided (for reasons of cost, versatility and ease of handling), two complete layers are required to determine X and Y coordinates for an incoming gamma-ray. One important design factor is that these layers be as close together as possible (directly on top of each other) to insure a good coordinate value for three dimensional tracking.

There are two basic concepts for mounting the two SSD layers. The first is to produce two trays each with 16 detectors mounted upward. Tray pairs would be mounted facing each other in close proximity with one tray oriented 90 degrees from the other. This allows each tray to be manufactured separately, reducing the cost risk by 50% should a tray get damaged. Such a design leads to easier manufacturing, but will likely compromise the angular resolution of the instrument. Because of the gap that must exist between trays (primarily for vibrational clearances) in this design, the X and Y coordinates are not located at the same Z position. This complicates data analysis and reduces angular tracking resolution. The distance between detectors is a function of mounting techniques. The challenge is to find a scheme that will reduce the gap between layers to an acceptable value while still being straightforward to mount in the tower.

The second concept for mounting the two SSD layers is to mount the Y layer directly on top of the X layer. This design offers the minimum distance between layers giving the maximum

CHAPTER 2. TOWER DESIGN ISSUES

accuracy for the instrument. In this scheme, the mounting of a layer in the tower is very straightforward since it is only a single tray. However, extreme care must be taken in mounting the Y layer, as damage could be incurred on the working X layer below. If something goes wrong with a tray, a total of 32 detectors would potentially have to be scrapped, compared to only 16 detectors in the other design. Also, repair of the covered X layer becomes virtually impossible. As a baseline, this single tray design was selected.

Electrical Connections

Regardless of which concept for mounting is used, the challenge is still the making of the 4000 electrical connections per layer of SSDs. Each layer of 16 detectors is electrically bonded together in four strips of four (each strip acting as a single, long, SSD with 249 channels) with the output of each channel going to a low power pre-amplifier. Searching for solutions to the mass bonding problem led the GLAST collaboration to study such familiar techniques as Tape Automated Bonding (TAB) and Bump bonding, and to develop a combination of these two techniques that was named flex bonding. The process called for making small flexible circuits (similar to TAB circuits) which are ultrasonically welded to small Gold bumps on adjacent detectors connecting the channels. This process resulted in many excellent characteristics including high strength and allowed for rapid mass bonding with the flexibility of modifications and re-manufacturability. More testing will be required to qualify this process for the GLAST instrument. One idea, still in the conceptual stage, uses an electrically conductive thermoplastic Z-axis adhesive film (such as 3M's 5303R). Rather than using the complex ultrasonic welding to bond the mass electrical connections, this process reduces the complexity and cost of these electrical connections.

After assessing the various methods, wirebonding was selected for electrically connecting detectors because it is well known, well used in industry, cost effective and meets all of the requirements. During this process, a thin (~1 mil) Aluminum wire is ultrasonically welded to form an electrical path between two detectors. There are some trade-offs with wirebonds. They are less mechanically robust than flex (6-8 grams pull strength vs. 40-60 grams) and they must sit above the components that they are connecting, increasing the vertical distance between X and Y detector planes (reducing the angular resolution when tracking). The limit to which wirebonds can be "flattened" needs to be explored. Regardless, wirebonds meet the requirement of this project.

CHAPTER 2. TOWER DESIGN ISSUES

Calorimeter and Tower Wall Design

At the base of each tower is a Cesium Iodide (CsI) calorimeter. Each calorimeter consists of an 8x8 pack of CsI crystals, each measuring 3x3x19 cm. The crystals are decoupled optically from each other (wrapped in an opaque material such as Teflon or Tyvex) with a photodiode and preamplifiers on both ends of each crystal. The power required for the 128 photodiodes and their readouts can be as much as 5 watts. The purpose of the CsI is to convert the deposited shower energy into light. The photodiodes give an electrical signal proportional to the amount of light and hence the energy of the gamma-ray.

Because the calorimeter sits directly beneath the tracker section, the tower walls that hold the trays simply extend to support the calorimeter as well. The tower walls are 60 cm in length and 2 mm thick.

Instrument Strong-back Design

In order to provide a scheme for attachment of the GLAST instrument to the spacecraft and to provide boundary conditions for analysis of tower performance, a structural strong-back had to be designed. The solution, after many iterations, came in the form of a structural grid that spanned the whole area under the towers. The grid also doubled as a heat conduction path from the towers to the thermal radiators on the exterior of the spacecraft. The grid is a simple, efficient design that is relatively easy to manufacture (even out of composites), inherently stiff and strong, and is straight-forward to analyze. The configuration that was selected was a 7x7 grid of squares, each the size of a tower (see Figure 2-4), the idea being that each tower simply bolts around the lip of each grid, providing ample surface area for support and thermal contact. The thickness and height of the ribs are determined by considering the requirements for stiffness and thermal conductivity.

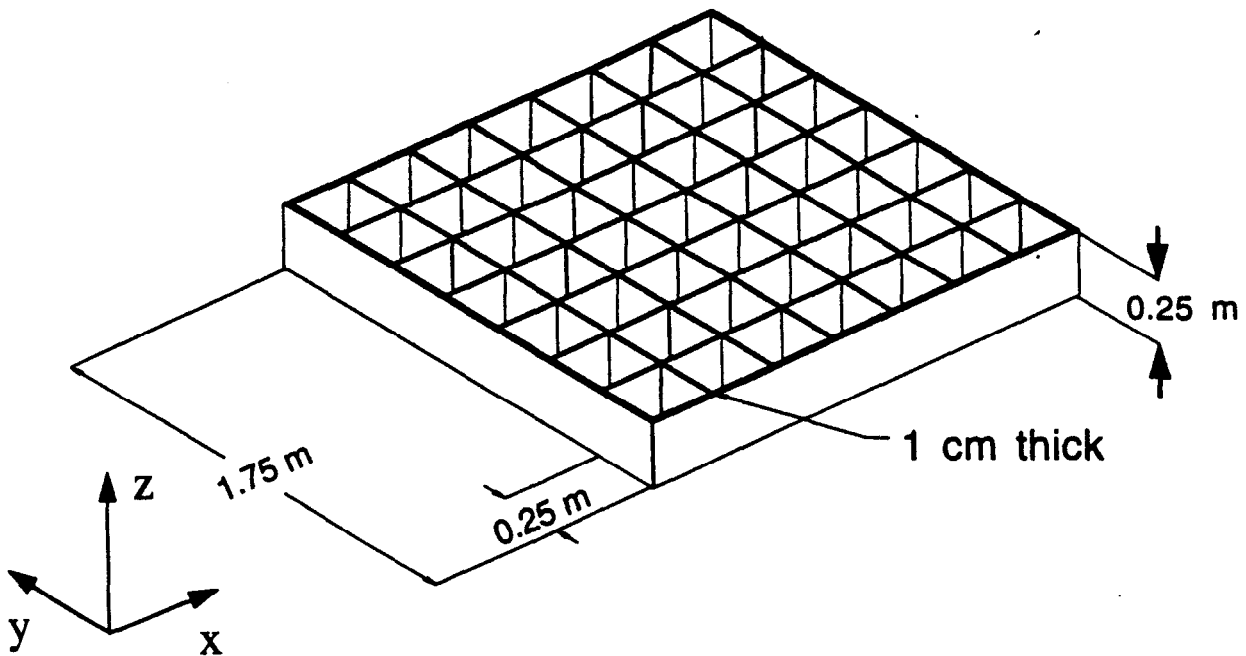


Figure 2-3 - Structural grid design

Satellite Bus Design

As long as the instrument is self-supportive, the design of the bus is not critical for the design of the instrument. When doing analyses, certain assumptions must be made for how load paths run from the instrument to the satellite bus and for the amount of heat generated by the bus. A simple design for an instrument/bus layout is shown in Figure 2-4. This design alleviates the need for the bus structure to hold the instrument. Instead, the instrument structure itself holds the bus where the components of the bus are hung onto the underside and periphery of the structural grid, making electrical connections through the grid. Thermally, the bus components conduct their heat directly to the radiators, and not through the grid. Thus, the thermal analysis for the grid does not account for heat generated by the bus. The structural analysis, however, requires the knowledge of how the structural grid is supported. While not necessarily the final bus design for GLAST, this bus design supplies the necessary compatibility information to analyze the instrument.

CHAPTER 2. TOWER DESIGN ISSUES

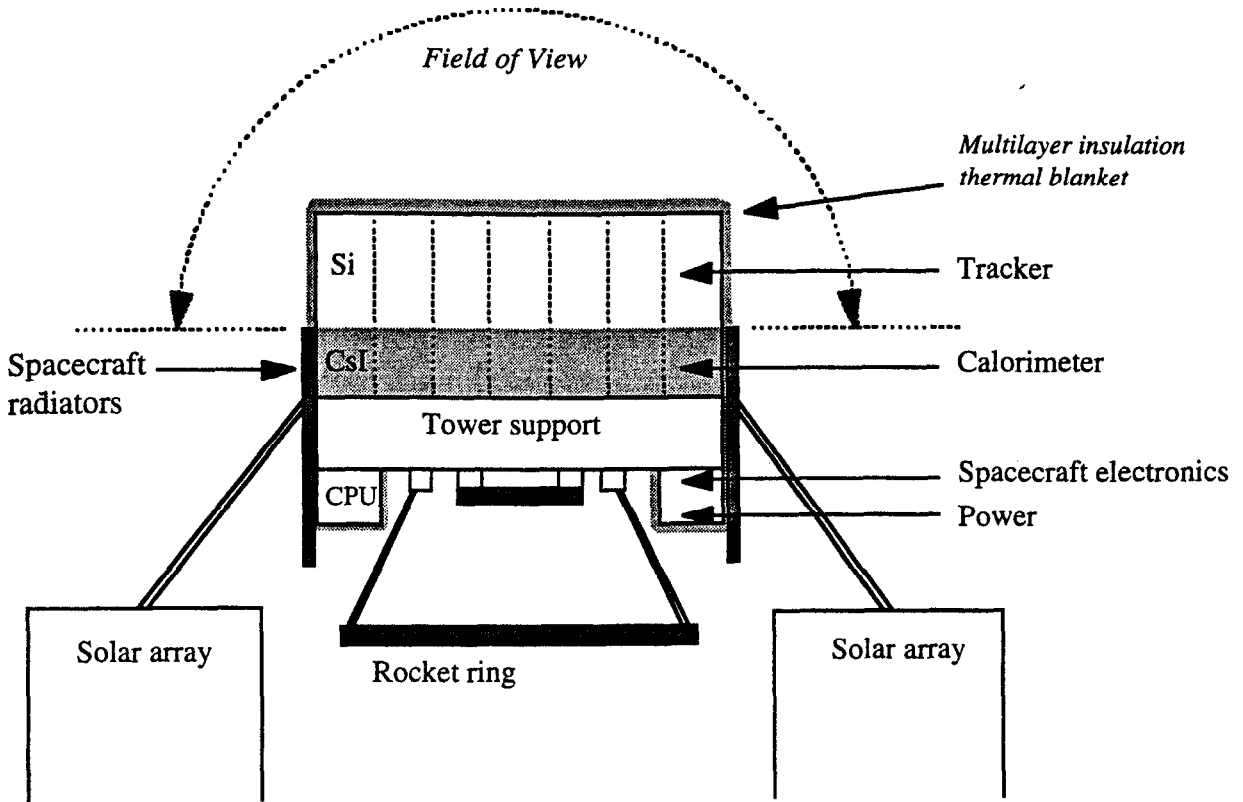


Figure 2-4 - Schematic of GLAST

3 : Design Specifications

In the previous chapter the major design issues were presented and discussed in detail, providing an in depth look at the “big picture” of the GLAST design. In this chapter, the specifications are defined which will be used to analyze and qualify designs in Chapter 5. Specifically, this chapter covers the specifications for material audit, instrument weight, expected loads, and allowable temperatures.

Material Audit

The design criteria for GLAST require that the tower structure minimally absorb or produce the photons which GLAST detects. The materials considered for the tower structure all have different radiation lengths.¹ As an example, the radiation length of Lead is 0.56 cm while that of Beryllium is 35.3 cm.

To cause a gamma-ray to convert to an electron-positron pair, a layer of converter material (280 μm , or 5% of a radiation length of Lead) is placed directly over each tray. The material used for supporting the detectors should be much less than the converter layer, preferably under 1% of a radiation length. Additional material in the supports generates background processes that degrade the performance of the instrument.

To obtain a more uniform acceptance for the instrument, the supporting materials must be spread out over the detector area rather than having it concentrated in small regions. This requirement is used to specify the material of the core spacer for the tray.

¹ The mean distance over which a high energy electron loses all but 1/e of its energy by bremsstrahlung.

CHAPTER 3. DESIGN SPECIFICATIONS

Attitude and Thermal Control

In order to have GLAST point toward specific gamma-ray sources in outer space, an active control system must be implemented. A standard three axis control system was selected, where momentum wheels are used for control and torquer coils are used to bleed off excess, built up angular momentum.

To reduce complexity and cost, a passive control system for temperatures was selected. Passive thermal control requires no energy, instead using only the thermal properties of various materials to reach the desired temperatures. Heat is transported around the satellite, by passive means, to radiators that, when pointed to objects of a lower temperature (like space), radiate the heat away from the satellite. The fact that GLAST will be three axis stabilized opens the possibility of active pointing of thermal control surfaces for better control of the spacecraft's operating temperature.

Orbit, Size, and Weight

The GLAST project is planned to be a "medium sized" NASA space mission. As a baseline, the McDonnell Douglas Delta II 7920 launch vehicle was selected to provide design specifications. For the given dimensions and weight to altitude limits of the Delta II, a Low Earth Orbit (LEO - 600 km , 28.7° inclination - allows for 4500 kg) was selected as the design orbit. The Delta II fairing limits the size of the satellite to a 100 inch diameter circle. The Delta II baseline also defined the vibration and acceleration loading during launch to orbit.

Expected Loads

The characteristics of the Delta II launch vehicle defined the structural loads for the GLAST instrument. The loads consist of steady state (axial and lateral) accelerations, acoustic vibrations, shock, and sinusoidal and random vibrations. Acoustic and shock loads are difficult to analyze and were not considered. Acceleration loads were applied to test the steady state stresses and deflections of various components. Sinusoidal and random excitations were superimposed on steady state accelerations to obtain composite accelerations for the dynamic structural design.

CHAPTER 3. DESIGN SPECIFICATIONS

Specifically, for a 4500 kg instrument, the Delta II produced a 6.0 g steady state acceleration and an expected 8.7 gRMS random vibration load [NASA GEVS, 1990, D-7,10].

The launch excitation of a spacecraft is a function of the spacecraft mass and dynamic characteristics, as well as the launch vehicle characteristics. To avoid dynamic coupling between low frequency vehicle and spacecraft modes, the stiffness of the spacecraft structure must be designed to produce fundamental frequencies above 35 Hz along the thrust axis and 15 Hz along the lateral axes for "spacecraft hard-mounted at the spacecraft separation plane" [Delta II Commercial Spacecraft Users Manual, 1987, 3-22]. To verify the robustness of designs, qualification testing for vibrations are completed (see Chapter 7). The qualification test assures that the spacecraft, even with minor weight and design variations, can withstand the most severe dynamic and environmental loads.

Operating temperatures

The temperature of the satellite varies widely both internally and around its exterior. Temperature characteristics depend on solar illumination, internal heat generation and the details of the thermal design itself. As a reasonable guide, the interior of the satellite should operate around room temperature (0 °C is the preferred temperature). For a typical spacecraft, temperatures usually range between -20 and +35 °C [Williamson, 1990, pg. 139].

The front end electronics and the SSDs themselves drive the thermal requirements. Both of these components generate noise as they heat up. For the noise requirement, a maximum temperature of +25 °C was selected as the design constraint. As electronics operate well at lower temperatures, a lower limit of -25 °C was sufficient, resulting in the final thermal design specification of ± 25 °C or lower.

4 : Thermal, Material, and Electrical Considerations

Now that the specifications have been laid out, the technological considerations need to be examined. In this chapter the thermal, material, and electrical considerations to meet the specifications are reviewed.

Thermal Considerations to meet Specifications

Because of the demanding thermal requirements in orbit, special attention must be given to the thermal subsystem. In the following section, the thermal conditions of space are discussed in detail, along with the intricacies of the thermal subsystem including contact resistances and heat pipes.

Thermal Conditions

Because GLAST will need to control its internal temperature within relatively tight tolerances, the thermal control system is a critical aspect in the design. The heat input from the Sun is 1358 W m^{-2} . In addition to the direct solar radiation heat input, there is heat input from reflected energy off the Earth (for LEO satellites only). The amount of incident solar radiation returned to space by planetary albedo (solar reflection) is 407 W m^{-2} and the input from the Earth itself from infrared thermal radiation approaches 237 W m^{-2} [Wertz and Larson, 424].

The temperature inside the spacecraft also depends on the amount of heat generated internally. This is a function of the efficiency of all the electronic components. The expected heat dissipated by the instrument is 645 watts (350 w from pre-amplifiers, 245 w from the calorimeters

CHAPTER 4. THERMAL, MATERIAL, AND ELECTRICAL CONSIDERATIONS

and 50 w from miscellaneous electronics). The spacecraft bus has been allotted 350 watts, giving a total baseline power consumption of 1 kW (EOL). This amount of heat generation drives the sizing of thermal pathways and radiative surfaces. If this value changes, simple re-sizing of radiator surfaces should compensate.

Because the GLAST instrument generates a substantial amount of heat internally, it is expected to be a "hot" satellite. To control the heat exchange with the environment, sunlit areas of the satellite should be covered by a thermal barrier while dark space pointing radiators should be used to dump thermal energy.

A very simple equation to describe the radiation and absorption of thermal energy is:

$$\alpha Q_s A_{sc} + Q_{int} - \epsilon_t \sigma_s T^4 A_{rad} = 0 \quad (4.1)$$

where α is the spacecraft absorptivity, A_{sc} is spacecraft area, ϵ_t is spacecraft emissivity, A_{rad} is radiator area, Q_s is the solar constant and σ_s is the Stefan-Boltzmann constant. The first term accounts for the rate of solar energy absorption, the second term for the rate of internal energy generation and the last term for the rate of thermal radiation. Another term that may be considered is the rate of thermal energy storage within the satellite. Once the satellite has come to equilibrium (steady state condition), however, this term can be usually ignored.

An orbit lasts approximately 90 minutes, during which time the satellite goes from its maximum temperature to minimum temperature and then back to its maximum temperature. The Sun is always shining on some part of the spacecraft except when eclipsed by the Earth or Moon. The side facing the Sun is hot while every side facing deep space is cold. The result of this situation is a steep thermal gradient which can cause misalignment of components (ruining pointing accuracy), thermal stress damage, and noise in certain arrays of electronics. Steep thermal gradients can be a serious problem if not looked at in detail.

Temperature control of the satellite is regulated by designing surfaces with specific properties for emission and absorption of thermal energy. Care must be taken, however, to consider EOL characteristics (mostly absorptivity) in these design decisions.

Thermal Subsystem

With the specification of a passively controlled thermal subsystem, different materials must be used to tailor the amount of heat absorbed and emitted from the satellite. The general

CHAPTER 4. THERMAL, MATERIAL, AND ELECTRICAL CONSIDERATIONS

components of a passive thermal control system are insulation blankets and reflective mirrors or thermal coatings (paints).

Because of material audit limitations, no radiator surfaces may surround the tracker section. In addition, no radiators are placed on the bottom, Earth facing side of the spacecraft because it will absorb heat from the Earth. To limit the heat input and to make designs easier, sections without radiators are covered with multilayer insulation (MLI). The MLI that is selected must be extremely transparent to gamma radiation since it separates the instrument from the incoming gamma rays.

Like any insulation, MLI both limits heat input and output by providing a thermal barrier. The most straightforward example of MLI consists simply of layers of synthetic polymeric material such as Kapton or Mylar foil. Each layer is about 6 μm thick, aluminized on one or both sides, and acts as a low emittance shield separated by low conductance spacers produced by crinkling the foil to create insulating voids. An alternative method uses Dacron netting as a separator between layers of foil [Williamson, 1990, pg. 132]. A typical 10 layer blanket, with a density of 0.3 kg/m^3 and a total thickness of 5 mm, would be equivalent to about 0.5 m of conventional insulation (the conductance for MLI is typically in the range $\sim 0.1\text{-}0.3 \text{ W m}^{-2} \text{ K}^{-1}$). The effectiveness of MLI is shown by the fact that a satellite's internal temperature can be controlled to $\pm 5 \text{ }^\circ\text{C}$ even when the external temperature ranges over $250 \text{ }^\circ\text{C}$ [Brooks 1985].

Heat absorbed or generated by a spacecraft must be radiated (mostly by IR radiation) to something at a lower temperature. The radiators in GLAST radiate thermal energy to the 3°C heat sink of outer space. Radiators may be fashioned into panels and serve as structural support. Because mass is at such a premium, the thermal control equipment around the bus may thus double as extra structure for the bus. Radiators are generally located on the north and south faces of a three-axis stabilized satellite to receive solar radiation obliquely. However, as a simpler design for GLAST, radiator surfaces were placed around all four sides, extending from the tracker section down (see Figure 2-5).

Second Surface Mirrors (SSM) offer a type of radiator surface with excellent properties, including low solar absorptance, high IR emittance and high reflectance and high resistance to electron and UV irradiation. They generally consist of a thin sheet of silvered or aluminized glass or quartz bonded to the exterior surface of the satellite using high conductance adhesives [Williamson, 1990, pg. 128]. The percentage of energy (primarily IR) absorbed onto its surface is only 10% ($\alpha = 0.1$) while the percentage of solar energy emitted is 85% ($\epsilon_r = 0.85$). Again it is important to design for EOL where α can be 0.25 (degrades at rate of 1-2% per year).

CHAPTER 4. THERMAL, MATERIAL, AND ELECTRICAL CONSIDERATIONS

As an example, a one meter tall radiator (80% packing factor) on each of the four faces of GLAST gives 5.6 m^2 of radiator area. SSMs typically radiate at a net rate of about 200 W m^{-2} , giving GLAST a heat rejection rate of 1.12 kW [Williamson, 1990, pg. 131]. This amount of radiation should provide the dissipative power required for GLAST and all spacecraft subsystems.

The basis for efficient, easy thermal design rests on the principles of passive control: reflect, radiate, absorb and insulate. An added benefit of GLAST's three axis attitude control is that the temperature may be controlled somewhat by active pointing of radiator surfaces. Naturally, all design solutions must be compatible with lifetime requirements and mass and power constraints.

Thermal Contact Resistance and Heat Pipes

In order to transport heat efficiently within the satellite, a good thermal conduction path must exist between items of hardware. Across each section in a thermal path and across each joint, there is a temperature rise resulting potentially in temperatures above the allowable limit. In addition, the contact resistance across mechanical joints significantly increases in a vacuum.

Although dry joints are used to ease the assembly, they only achieve about $200 \text{ W m}^{-2} \text{ K}^{-1}$ of conductance in space. To increase conductance across joints, interface or interstitial filler must be used. One such filler is the "wet joint" interface, which utilizes an unprimed thermoelastic compound such as a silicone adhesive. An alternative to this filler is a preformed conductive gasket or grease (Dow Corning 340 vacuum grease). Although the conductance depends on the pressure on the joint, values between 2 and $8 \text{ kWm}^{-2} \text{ K}^{-1}$ are typical [Wise 1985].

Another factor which contributes to temperature rise is the conduction of heat through material. To minimize this effect, designs must maximize the thermal conductivity by selection of appropriate materials and the minimization of conduction distances. Aside from the selection of materials and layout of thermal paths, another possible design solution is the use of passive heat pipes. Heat pipes are devices with a thermal conductance much higher than even the best heat conducting metals. It is a highly efficient passive device used for transferring large amounts of heat from one place to another, or simply to remove hot spots. A heat pipe contains a fluid which is vaporized by the applied heat at one end (the evaporator) and condensed at the other end where it relinquishes its heat. The condensed liquid returns to the evaporator end through a porous wick by means of capillary action. An example is an Aluminum axially grooved heat pipe with ammonia (or methanol) as the working fluid which can operate in a specific temperature range ($-70 \text{ }^\circ\text{C}$ to about $+200 \text{ }^\circ\text{C}$, 40 W m capability). A 15 mm Aluminum/ammonia pipe can transport about 200

CHAPTER 4. THERMAL, MATERIAL, AND ELECTRICAL CONSIDERATIONS

W over 1 m with a temperature difference as small as 1 °C (and a mass of 0.4 kg) [Williamson, 1990, pg. 137]. A device such as this is very mass efficient and has the “passive” advantage that it has no moving parts and uses no electrical power. The problem with heat pipes is that they are expensive.

In GLAST, the structural grid will provide the conduction path for the heat from the towers. The grid supplies material paths directly from the base of each tower (contacting through a large surface area) to the radiators on the periphery of the satellite. If needed, heat pipes can be added to complement the conductivity of the grid.

Spacecraft Materials to meet Specifications

In addition to needing the low weight and high strength required by high performance aircraft, satellite materials must be designed to survive in space. Before the satellite leaves the Earth, it is prone to a number of purely terrestrial problems such as oxidation and corrosion, water absorption or losses by evaporation, creep under load and biological attack. Some of these problems can be minimized by careful control of the satellites immediate environment. For example, keep all components in a clean-room (room where the environment is carefully controlled against contaminants). The materials that are chosen must be capable of surviving three years of manufacturing and processing, environmental testing, storage and transportation before the spacecraft even leaves the ground. Whereas the punishing launch environment exerts the maximum mechanical stress on materials, the extended period in Earth orbit (up to 10 years for GLAST) exposes materials to processes in which time is the damaging factor.

The ideal spacecraft material would have high dimensional stability under mechanical and thermal loads, low susceptibility to fatigue, radiation damage and the influences of Earth's atmosphere, and, above all, high strength, low weight and realistic cost. For this project, structural materials used in the tracker must also have long radiation lengths and uniformity. Below is a list of common aerospace materials and their pertinent properties including a comparative figure of merit between radiation length and thermal conductivity (with Beryllium equal to one, Table 4-1).

CHAPTER 4. THERMAL, MATERIAL, AND ELECTRICAL CONSIDERATIONS

Materials	Conductivity K (W/cm/°C)	Specific gravity	Elastic modulus (GPa)	Yield strength (MPa)	Radiation length, \bar{X}_0 (cm)	$K \cdot X_0$ (normalized to Be)
<i>Metals</i>						
Cu	4.0	8.8	110	69	1.4	0.07
Be	2.2	1.9	303	241	35.3	1.00
Al	1.7	2.7	69	255	8.9	0.19
Al Be	2.1	2.1	179	275	16.1	0.44
<i>Carbon fibers</i>						
T300	0.2 - 0.8 0.01 lateral	1.6	181	1500	18.8	0.04 - 0.20
Pitch based K-1100K	11.0	1.6	930	—	18.8	2.66
K-1100K/carbon 0/90 cross ply	3.6 (x,y) 0.52 (z)	—	—	—	18.8	0.87

Table 4-1 - Spacecraft material properties

Composites

Composites are typical aerospace materials with properties including high stiffness to weight ratios (with a density equal to about 65% that of Aluminum), high thermal conductivities (along the fibers) and very low coefficients of thermal expansions (CTE). The properties of a composite are dictated by the orientation of its fibers, allowing design of the material for a specific application. The production process calls for taking composite fibers (with specific properties of modulus, thermal conductivity, etc.) and impregnating them with a matrix material (usually epoxy resins). After “laying up” the composite into the desired shape, thickness and orientation, it is cured to give it its final properties.

By the addition of a core material between composite sheets (Figure 4-1), high stiffness can be achieved. For a 3% increase in weight (with twice the thickness) you can get a 200% increase in stiffness and a 350% increase in strength. Composites must generally be manufactured by hand

CHAPTER 4. THERMAL, MATERIAL, AND ELECTRICAL CONSIDERATIONS

and cured in very controlled environments. Although this increases manufacturing costs, as time progresses and manufacturing processes become more standard costs should decrease.

When using a composite core laminate for space applications, the walls of the core must allow for the escape of trapped gasses once in orbit. Some examples of acceptable cores include vented Nomex honeycomb, Hexcell carbon fiber honeycomb, and Reticulated Vitreous Carbon expanded foam (RVC). Carbon fiber honeycomb (like Hexcell's HFT-GP-327) has mechanical properties similar to Nomex, thermal conduction properties rivaling Aluminum (5052) and is naturally vented for release of trapped gasses. The disadvantage of honeycomb cores is that all the material is concentrated in the thin vertical walls of each cell rather than spread out over the area of the tray. A new material like RVC, however, would yield superior performance because of its good mechanical properties, natural venting and uniform distribution of mass. But, because it is a new technology, initial costs are high.

For the test trays, 3/8 inch cell Nomex honeycomb (without venting) was used because of the ready availability, low cost and ease of handling. Any of these core materials are acceptable structurally and meet the requirements for the experiment.

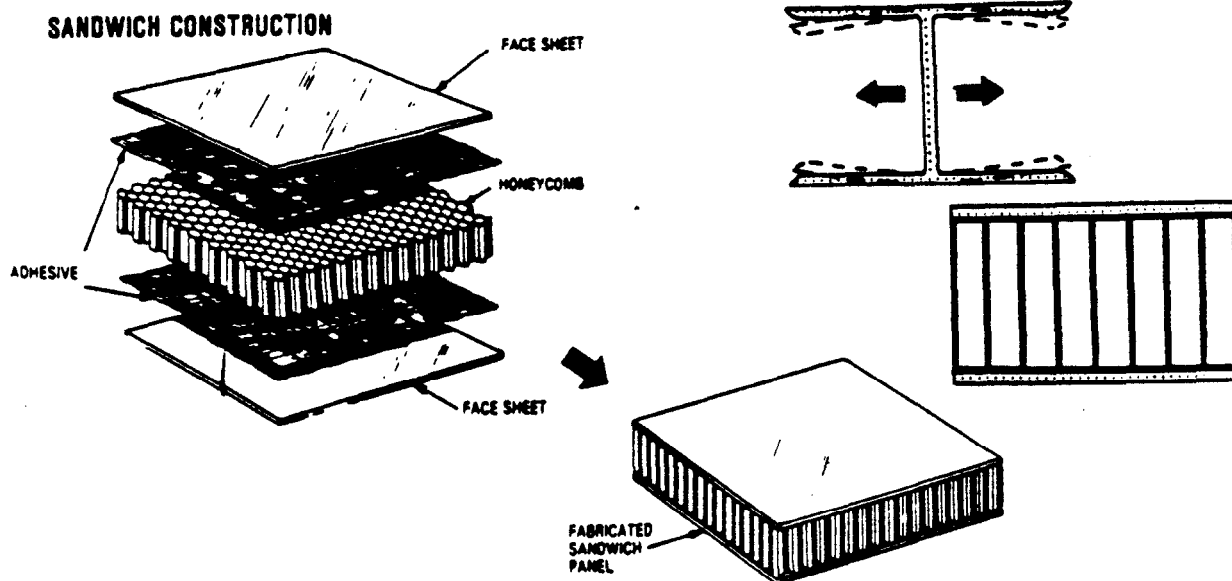


Figure 4-1 - Composite core laminate

CHAPTER 4. THERMAL, MATERIAL, AND ELECTRICAL CONSIDERATIONS

Metals

Another material with high stiffness to weight ratio, high thermal conductivity and shorter radiation length is Beryllium (Be). Because of these excellent properties, Beryllium was selected as the baseline material for the tower walls and the tray close-outs. Because of its toxicity, however, special safety procedures must be applied during manufacturing and only a limited number of sites are available for manufacturing. In addition, because of its brittleness, an etching process is required to remove crack propagation sites. Due to these manufacturing complications, Beryllium is an expensive material to use.

Three additional metals were considered: magnesium, titanium, and Aluminum alloys. Magnesium alloy is not used because of its low resistance to surface corrosion and stress corrosion cracking which results from a combination of corrosion and mechanical stress [Williamson, 1990, pg. 33]. Titanium, another excellent material with high stiffness to weight properties, was not selected as it exhibits a short radiation length. Aluminum, one of the most widely used materials in satellites, has low density, reasonable strength and stiffness, ease of manufacturing and relatively low cost. However, it was not selected since its radiation length is fairly short.

Adhesives

All tapes and adhesives used in satellites must be selected for their properties in the environment of space. Outgassing and free oxygen can greatly degrade the properties of adhesives in space so care must be taken to verify their reliability in that environment. In the selection of materials we try not to exceed a total mass loss (TML) of 1% and a collected volatile condensable materials (CVCM) amount of under 0.1% while at 125 °C, for 24 hrs. in 2×10^{-6} Torr vacuum (NASA's SP-R-0022 or ASTM E-595 standard).

GLAST has only a few components that contain these materials including composites cured in an epoxy matrix. This does not prove to be a major design issue, however, since many epoxies exist that perform well in space.

Another component where outgassing is a concern is the conductive transfer tapes used in electrical connections. To electrically connect the back of each SSD to the high voltage bias, 3M's Scotch brand 9703 conductive adhesive transfer tape (CTT) may be used. Wirebonds cannot be used due to manufacturing issues and conductive glues offer a lower uniformity in electrical

CHAPTER 4. THERMAL, MATERIAL, AND ELECTRICAL CONSIDERATIONS

conductivity and thickness. Checking the outgassing characteristics, 9703 shows a TML at 0.7% and a CVCM amount of 0.01% which meets our requirements.

Another product under consideration is 3M's Z-axis adhesive film (ZAF) 5303R. This is a thermoplastic material that would allow for reworking. The cure temperatures and pressures are higher (180 °C, 280 psi) than for 9703 adhesive (70 °C, light pressure).

The last product under consideration for GLAST is a thermally conductive double sided tape (to reduce thermal contact resistances), such as 3M's Scotch brand thermally conductive adhesive transfer tape.

Other materials

Kapton is a thin polyimide film used extensively in satellites. One of the properties of Kapton is that it has the ability to maintain its excellent physical, electrical, and mechanical properties over a wide temperature range (-269 to +400 °C). It also has excellent chemical resistance and there are no known organic solvents for the film.

Kapton may also be bonded to metal foils using existing adhesives. Because of its insulative properties, Kapton may be used for flexible electrical circuits. The procedure calls for bonding a metal foil to a pre-cut piece of Kapton and then etching away parts of the metal leaving an exposed metal pattern (e.g., circuit design). Because it has a low density and only thin sheets are needed, a Kapton flexible circuit is used to carry the back-plane bias circuit (Kapton is available in a variety of standard thickness' from 25 μm to 125 μm).

Electrostatic Discharge

Electrostatic discharge (ESD) is generally a problem for electronic equipment [Williamson, 1990, pg. 20]. ESD may be generated by the MLI layers on the exterior of the satellite, storing static charge which, if discharged, could destroy equipment. ESD is measured on a Rosen scale of 0, no hazard, to 10, a catastrophe (1 means an outage of a second or less, 5 is an outage of a few hours).

Because of the nature of the GLAST detectors, there is a stringent requirement on ESD. The outside surface of the satellite should be conductive and grounded to avoid differential charging. Particular attention must be paid to shaded areas, which are not discharged by photo-emission. For exterior thermal control surfaces, conductive black paint on radiator surfaces

CHAPTER 4. THERMAL, MATERIAL, AND ELECTRICAL CONSIDERATIONS

could be employed, although these conductive coatings are generally expensive [Williamson, 1990, pg. 21]. The best solution is a conductive flexible second-surface mirror such as Kapton with conductive indium-tin oxide layer. For the solar panels, a carbon composite structure is recommended because it acts as a conductor which can be grounded electrically. In addition, cover glass doped with cerium should be placed over the cells to provide protection and allow conduction. A Rosen scale of less than one may be easily obtained with proper ESD protection techniques. However, charging of surfaces cannot be completely avoided, electronics that are less susceptible to ESD should be selected.

5 : Analysis of Design

There are several methods for analyzing the different components of a satellite. This thesis uses analytical and numerical methods (computer codes) including commercial finite element packages. The finite element analysis is one of the most useful modern engineering tools for analyzing complicated mechanical systems. In a finite element analysis, a computer finite element model (FEM) is generated which simulates real world mechanics and allows testing in a virtual environment.

Finite Element Model

The finite element model approximates the behavior of a system by dividing the system into a finite number of separate parts. The elements (as individual parts are called) are small enough to be assigned realistic values for loading, boundary conditions, etc., but not so numerous that the integration process becomes unwieldy. For mechanical designs at the concept stage, the FEM technique is very useful in accurately assessing structural and thermal behavior. For this project, various structural prototypes were built to confirm the predicted behavior from the FEM analysis.

Of course, there is a limit to the abilities of FEM analysis. The demand for higher complexity of models and higher accuracy of solutions has the penalty of higher processing time and the need for large data storage space. Even medium complexity devices like GLAST can tax the most powerful computer systems of this age. Regardless, finite element analyses are very powerful tools and are used heavily to help address the structural, vibration and thermal challenges in this thesis.

Structural Analysis: Strength and Deflection

SSD Tray

One of the most critical components of GLAST are the structural trays that support the delicate SSDs. These trays must be strong enough so that they do not structurally fail, and stiff enough so that they do not excessively deflect and damage the SSDs. This must all be accomplished with a minimal material audit to retain transparency to incoming gamma-rays. Since a carbon composite laminate with a core spacer meets these requirements and provides excellent mechanical properties, it was selected as the tray material.

Silicon strip detectors do not have to catastrophically fail to be destroyed. If the detectors are over strained (and not much is needed to over-strain them) they generate excessive noise and become useless. There is very little data on the limit to which detectors may be strained, so testing is needed to determine the acceptable limits. The strain in the detectors relates to the curvature of the tray by the following equation:

$$\varepsilon = \varepsilon^0 + c \cdot K_{tray} \quad (5.1)$$

The pre-strain ε^0 is zero and c is the vertical distance from the center of the tray to the top of the detector. Thus, combining the previous equations, the curvature limit corresponding to failure is determined:

$$K_{tray \max} = \frac{\varepsilon_{SSD}^{\max}}{\left[\frac{1}{2} \left(\frac{h_{core}}{2} + t_{face} \right) + t_{SSD} \right]} \quad (5.2)$$

where h_{core} is the thickness of the core material, t_{face} is the thickness of the face-sheet, t_{SSD} is the thickness of the detector and ε_{SSD}^{\max} is the maximum allowable strain for the detectors.

To find the curvature of a composite tray, a stiffness matrix must be generated. The material properties that are required to generate the matrix are supplied by the manufacturers. These properties are not always very accurate as each batch may vary in terms of mechanical

CHAPTER 5. ANALYSIS OF DESIGN

properties and flaws from handling. As a result, properties can vary greatly from tray to tray necessitating moderately large factors of safety (2.0) in the design.

The 24.6 cm (~25 cm) wide tray is composed of a single [0/90] weave ply for each face-sheet (symmetric lay-up) attached to a 1/4 inch thick Nomex honeycomb core. Analysis was needed to make sure that the deflection of the tray under static loads did not exceed the limits set by the detectors. Also, the maximum stress under loading must be below the yield strength of the materials used in the tray. To approximate the worst case, a simply supported plate was modeled to calculate the stresses and deflections. An equation for the deflection of a square composite tray of length L is given as

$$\delta_{\max} = \sum_{m=1,3,5\dots} \sum_{n=1,3,5\dots} K_{mn} \cdot \sin\left(\frac{m\pi}{2}\right) \cdot \sin\left(\frac{n\pi}{2}\right) \quad (5.3)$$

where

$$K_{mn} = \frac{16 \cdot P_o}{\pi^4} \left\{ D_{11} \left(\frac{m}{L}\right)^4 + 2(D_{12} + 2 \cdot D_{66}) \left(\frac{m}{L}\right)^2 \left(\frac{n}{L}\right)^2 + D_{22} \left(\frac{n}{L}\right)^4 \right\}^{-1} \quad (5.4)$$

where P_o is a uniform vertical load equal to the total weight of the tray and components distributed over the surface. The “ D ” matrix components (flexural stiffness modulus matrix) are a function of the geometry, lay-up and material properties [Tsai, 1980].

For the specific case of a 1/4 inch thick core spacer with symmetric [0/90] ply face-sheets of carbon composites (Hexcell 3K70 plain weave T300/F155 - properties listed in tray FEM code, Appendix B), the stiffness coefficients are:

$$\begin{aligned} D_{11} &= 726 \text{ N m}; D_{12} = 7 \text{ N m}; D_{22} = 708 \text{ N m}; D_{66} = 12 \text{ N m} \\ Q_{11} &= 6.1\text{E}10 \text{ Pa}, Q_{12} = 3.1\text{E}9 \text{ Pa}, Q_{22} = 6.1\text{E}10 \text{ Pa}, Q_{66} = 4.5\text{E}9 \text{ Pa} \end{aligned}$$

The weight of a tray and two layers of SSDs (excluding the close-out material that is concentrated on the edges; see Table 8-1) is 229 grams. Under the expected 10 g load, a distributed load of $P_o = 3.7 \text{ grams/cm}^2$ is applied to the 25x25 cm tray, resulting in a deflection of

CHAPTER 5. ANALYSIS OF DESIGN

157 μm and curvature is 0.022/m. As discussed above, this value must be compared with the critical limit for the SSDs.

The expected mode of failure for the tray is fiber breakage in the facesheets. The stress in the facesheets is obtained from Hooke's Law, which states:

$$\{\sigma\} = [Q]\{\varepsilon\} \quad (5.5)$$

where $\{\sigma\}$ is the column matrix of stresses, $\{\varepsilon\}$ is the column matrix of strains, and $[Q]$ is the stiffness matrix (values given above). For this particular design and loading configuration, the stress in the fiber direction of each layer is the same and represents the maximum stress in the laminate ($\sigma_{max} = 4.47 \text{ MPa}$). The tensile strength of the fiber is 200 MPa (120 ksi), giving a hefty factor of safety of 44. While this early design is much stronger than needed, it provides robustness and ease of manufacturing.

Tower

The strength and deflection of the tower walls are also critical to GLAST. Because the material in the walls is thin (to reduce dead area and minimize material in the instrument), careful analysis had to be performed to make sure the walls would not deform or yield during launch. As the tower structure is fairly simple in design, an analytical analysis to determine the perpendicular deflection could be performed.

Modeling the structure as a cantilevered hollow tube [Wertz & Larson, 1992, pg. 454]:

$$\delta_{max} = 0.125a_g \left(\frac{m_{cal}(L_{cal})^3 + m_{trak}(L_{trak})^3}{EI} \right) \quad (5.6)$$

where a_g is the acceleration, m_{cal} is the mass of the calorimeter, L_{cal} is the length of the calorimeter section, m_{trak} is the approximate mass of the tracker and L_{trak} is the length of the tracker section. E is the modulus of elasticity of the wall material and the I is the area moment of inertia of the tower cross section. The EI is called the "bending stiffness" of the structure and is maximized to keep the deflections low and the natural frequencies high.

CHAPTER 5. ANALYSIS OF DESIGN

The transverse (horizontal) acceleration (a_g) during a rocket launch can be as much as 4 g. To be conservative, the tower was analyzed with a fixed base under a 10 g transverse acceleration, using a calorimeter weight of 55 kg and length of 21 cm and a tracker weight of 6 kg and length of 39 cm. The tower walls were taken as Beryllium ($E = 318$ GPa) with a width of 25 cm and a 2 mm thickness giving a bending stiffness (EI) equal to $6.47E6$ N m². Using equation 5.6, the deflection of the tower is 167 μ m. Because this deflection is not excessive, even under a very harsh loading condition, it is predicted there will not be a problem with towers “bumping” into each other. To reduce the possibility of this happening, the towers could be strapped or bolted together. However, depending on how the towers are attached together, extra stresses could be induced in the tower walls if they are fixed to one-another.

The stress in a stand-alone tower wall can be found using the beam equation:

$$\sigma_{\max} = \frac{M_{\max} \cdot c_{\max}}{I} \quad (5.7)$$

where M_{\max} is the maximum moment resultant from the loads, c_{\max} is the maximum distance from the neutral axis and I is defined above. The maximum moment occurs at the base of the tower and is equal to the forces applied to the tower multiplied by the distances each force is from the base. For the conditions listed above, we obtain:

$$M_{\max} = \left\{ \left(m_{cal} \cdot L_{cal} / 2 \right) + \left(m_{trak} \left(L_{cal} + \frac{L_{trak}}{2} \right) \right) \right\} a_g \quad (5.8)$$

where the values are defined above and the acceleration, a_g , is equal to 10g.

From this calculation, M_{\max} is found to be 820.5 N m. The maximum value for c is 0.125 meters (half the width of a tower) and the value for I , as given above, is equal to $2.03E-5$ m⁴. The maximum stress in the walls is then 50.5 MPa. The yield strength of Beryllium is 241 MPa, giving a factor of safety of 4.7. This is a worst case analysis since in the real structure, the trays and calorimeter will stiffen up the structure and carry some of the loads.

CHAPTER 5. ANALYSIS OF DESIGN

Grid

An analysis of the grid determines what dimensions are required to give adequate stiffness and strength to support the instrument. The general layout of the grid was taken to be a 7x7 array of squares, each square lying directly under a tower. The design objective was to determine the thickness and height of the grid ribs.

While performing the grid analysis, a decision was made on where to place the supports for the grid, as this affects the grid deflection and natural frequency. Setting the requirement for the grid is not straightforward, since stiffness, thermal and vibrations requirements are coupled. The deflection of the grid under the weight of the instrument and a 10 g acceleration must not cause the towers to cantilever into each other.

A finite element model of the grid was analyzed to determine its deflections and stresses for any given geometry and boundary conditions. The material selected for the grid was an Aluminum alloy, 6061-T6. The dimensions used were a rib thickness of 1.0 cm and a height of 25 cm. The weight of each tower was taken as 66 kg (see Table 8-2). The boundary condition selected was to support the grid under the first ribs from the outermost elements. This boundary condition gave the lowest deflection of the grid, δ_{\max} of 189 μm , and a maximum stress of 11.2 MPa. The yield strength of the Aluminum is 255 MPa, giving a factor of safety of 22. The finite element model is shown below in Figure 5-1 (the code is in Appendix A). To decrease the deflection, a thinner, deeper grid could be used.

CHAPTER 5. ANALYSIS OF DESIGN

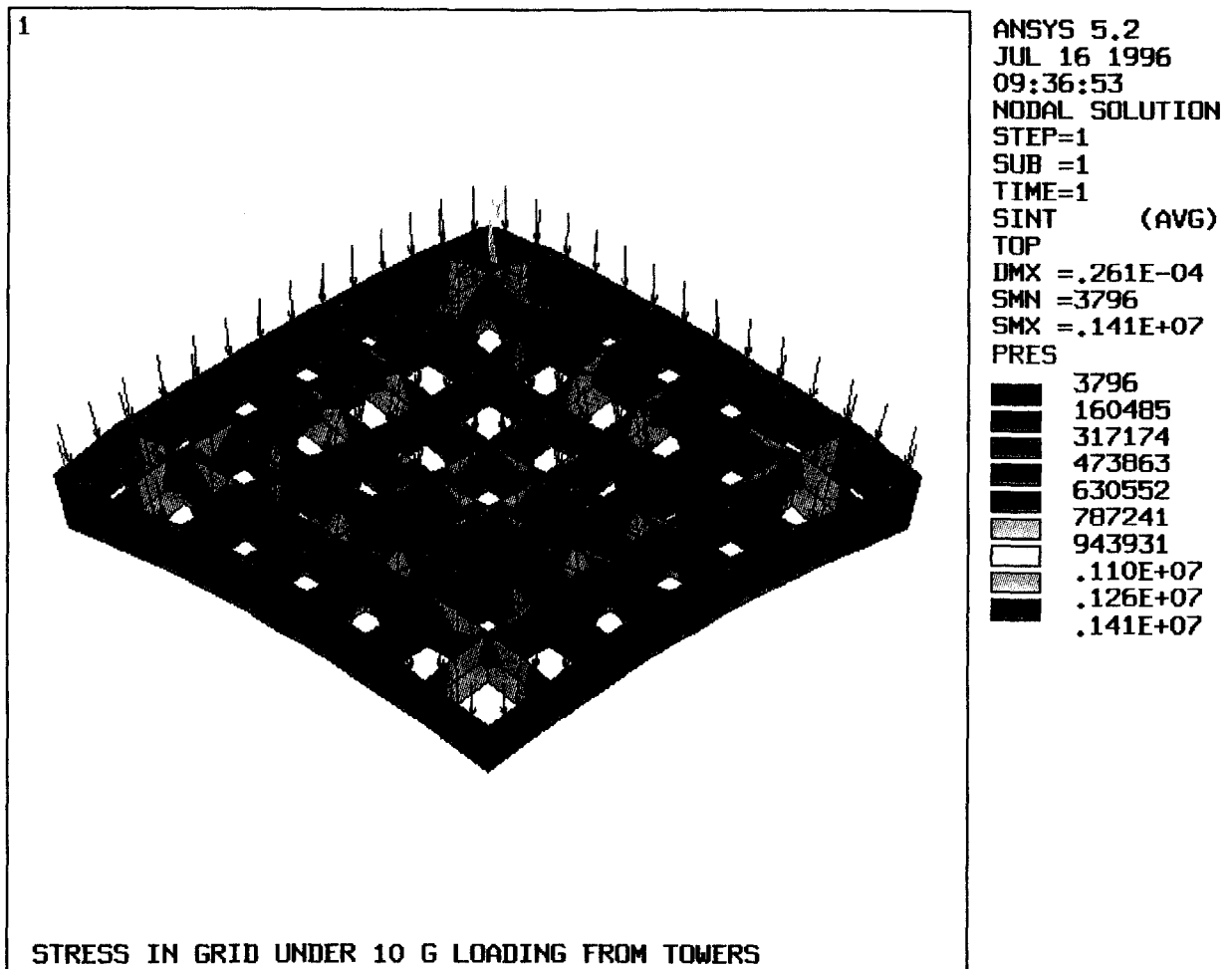


Figure 5-1 - FEM stress analysis of structural grid

Vibrational Analysis: Natural Frequency Estimates

During launch, the satellite will be excited at all frequencies, including its natural frequencies. A low natural frequency can couple with the low frequencies of the launch vehicle producing large deflections which can cause components to overstrain or, for components in close proximity, to even collide with each other. When the natural frequency occurs at higher frequencies, even if the accelerations are higher, the net movement is lower. The objective of the vibrational analysis is to determine the first natural frequency of each structure and verify that it is greater than the critical frequency of 35 Hz.

SSD Tray

Because the tray is a flat plate, it is susceptible to a low frequency vibrational mode known as "oil canning". A finite element model was produced to test the modes of the tray under various conditions (see Appendix B for code).

In the design, the bolted edges are more closely represented by a fixed boundary condition. To be conservative and give a lower fundamental frequency, however, the model used a simply supported condition as well as the maximum expected load. Using the typical maximum load expected for a tray with two layers of SSDs (229 grams total) under a 10 g acceleration, the composite tray was analyzed. The fundamental frequency was found to be 291 Hz. A picture of the deformed model including boundary conditions is shown in Figure 5-2.

Because of this high natural frequency, minimal coupling will occur between the launch vehicle and the trays. If this value had been under 35 Hz, the frequency could simply have been increased by making the core spacer thicker. Thickening the core increases the stiffness of the tray (raising the natural frequency) with only a slight increase in material.

CHAPTER 5. ANALYSIS OF DESIGN

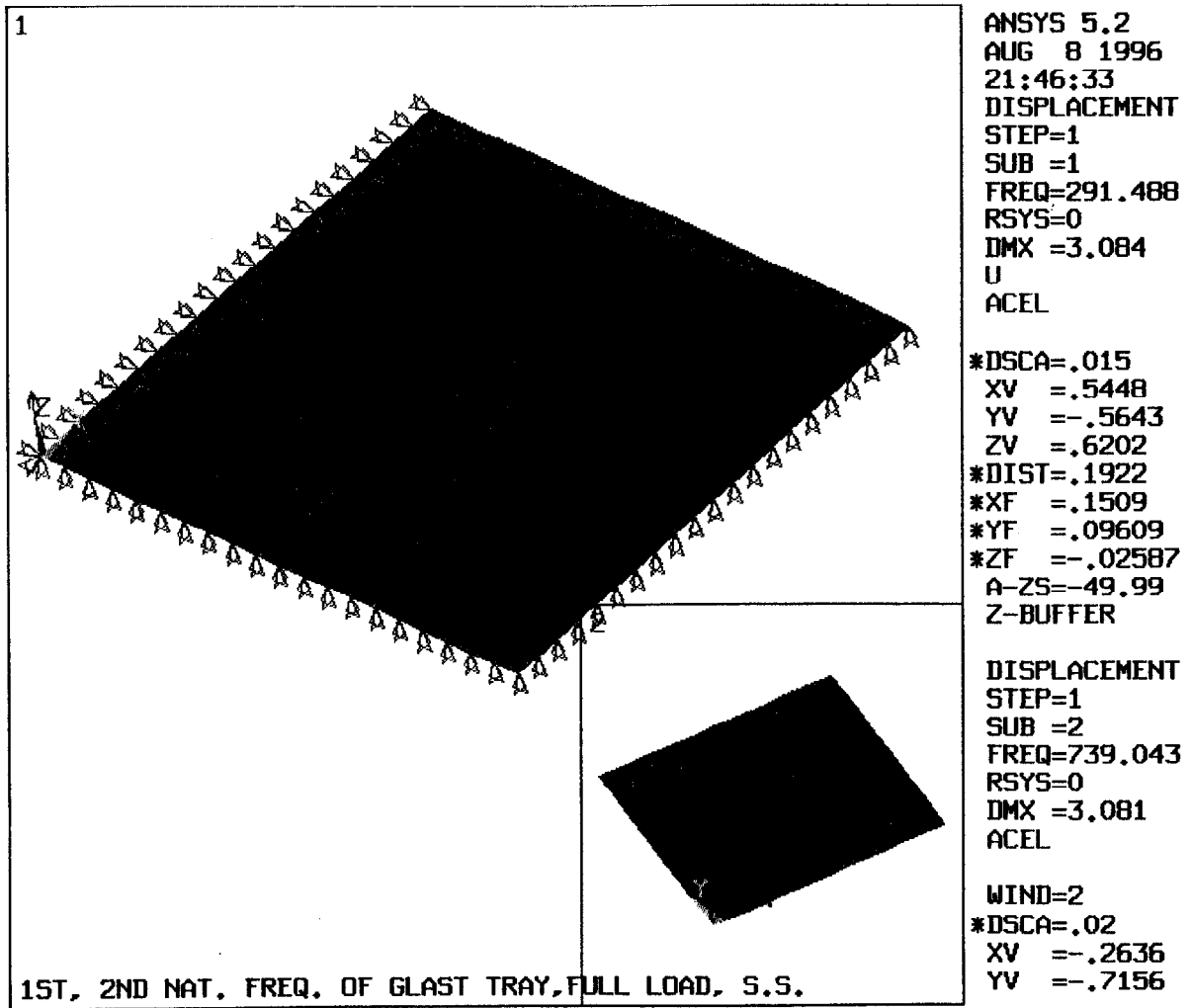


Figure 5-2- FEM modal analysis of structural tray

CHAPTER 5. ANALYSIS OF DESIGN

Tower Structure Natural Frequencies

The vibration analysis of the tower was critical in determining the number of walls used. The decision to use two, three, or four walls was based on finding a significant increase in the natural frequency with four walls (where the Beryllium walls are 2 mm thick, 25 cm wide, and 60 cm tall). The model includes 12 composite trays 3 cm apart and a 21x25x25 cm block of CsI all within the walls that are fixed at their base. The fundamental frequency for the four walled tower, in this configuration, is 604 Hz. Figure 5-3 shows the tower FEM deforming in its first resonant mode of vibration for the four walled configuration (See code in Appendix C).

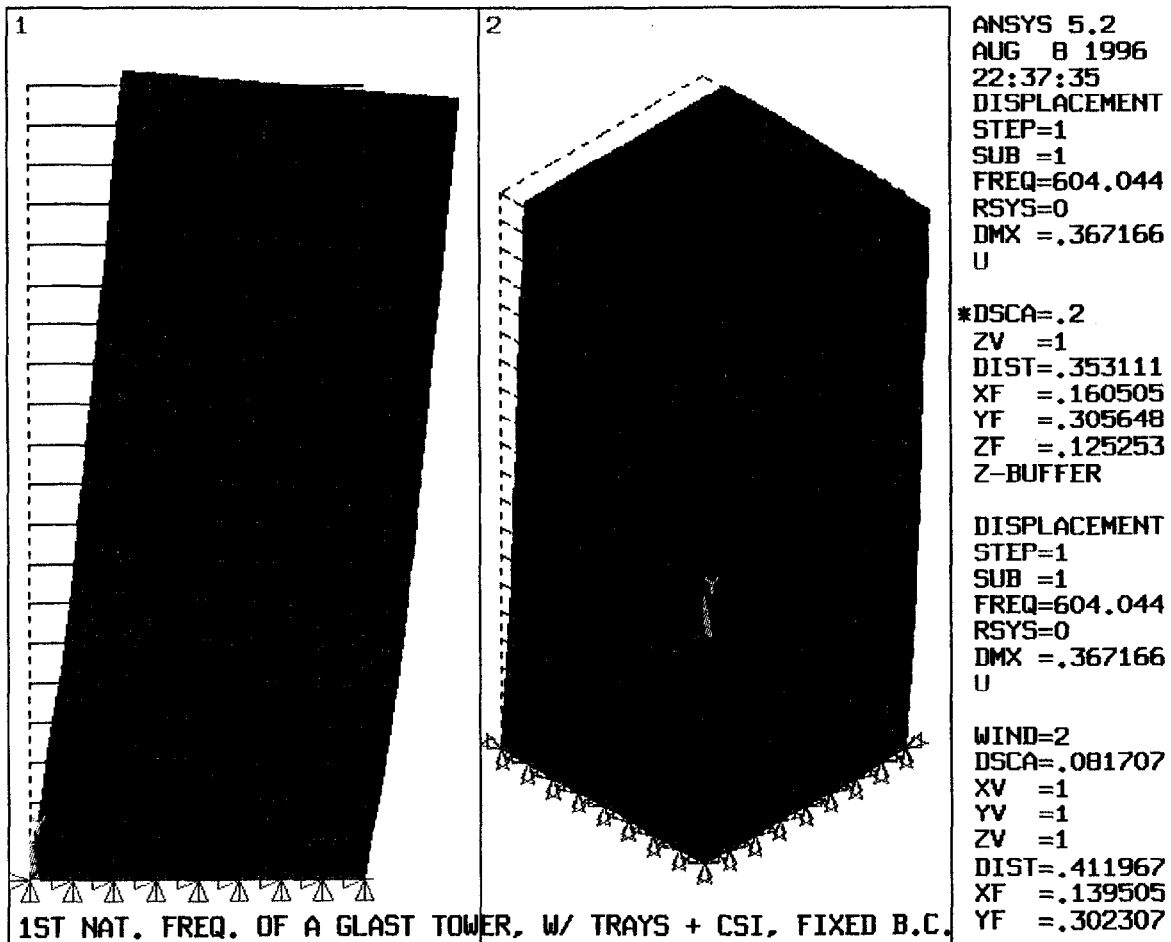


Figure 5-3 - FEM modal analysis of tower

CHAPTER 5. ANALYSIS OF DESIGN

Grid Structure Natural Frequencies

The resonant mode of the grid was critical in determining how the grid was to be supported. With the grid supported only on the borders, the natural frequency was dangerously low. By moving the supports closer to the center, the inherent stiffness of the structure was increased, raising the first fundamental frequency.

A detailed FEM was produced to analyze various structural configurations for the grid. The results show that for the 200 kg Aluminum grid in Figure 2-3, the first natural frequency is an acceptable 440 Hz. The FEM model for the grid is shown below in Figure 5-4 (code in Appendix D).

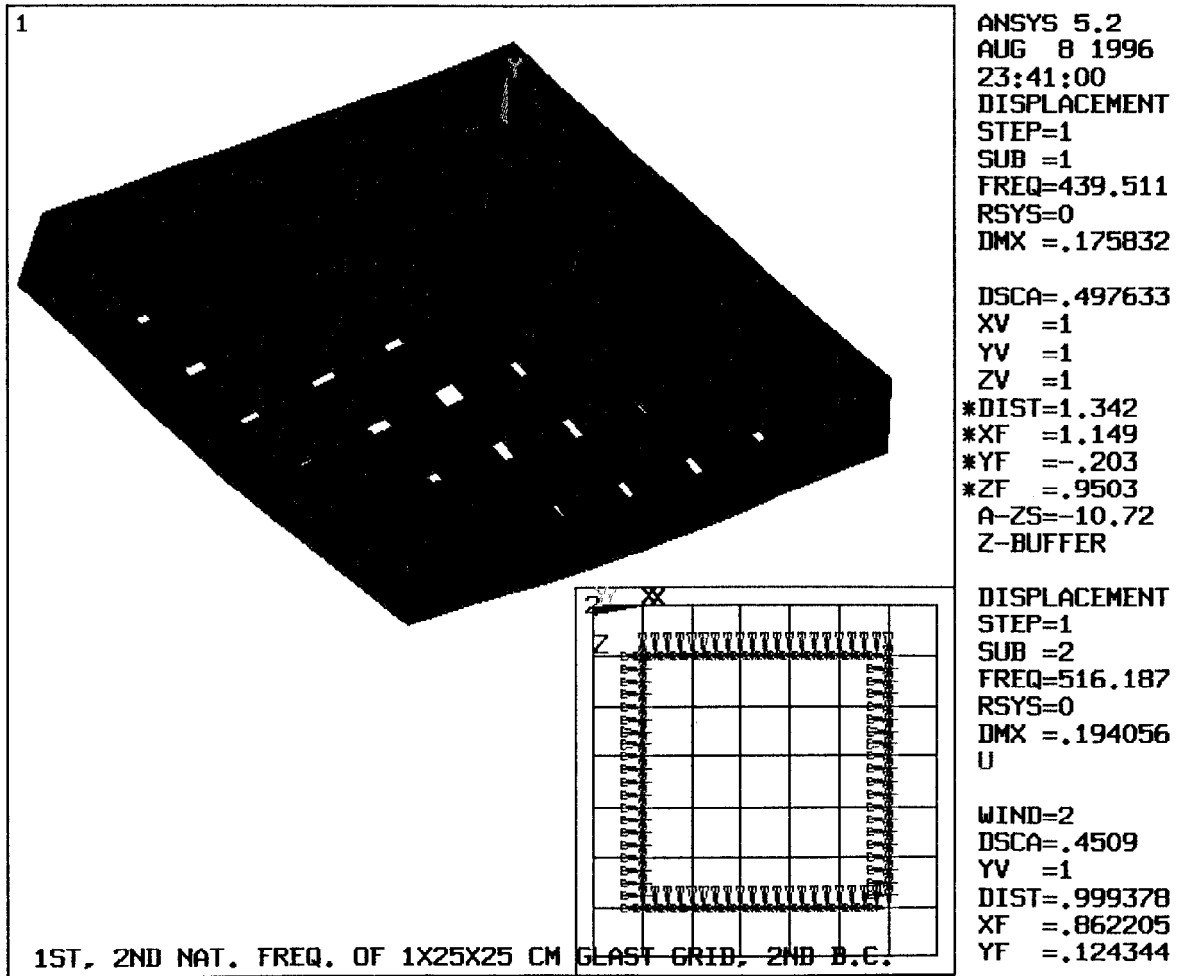


Figure 5-4 - FEM modal analysis of structural grid

CHAPTER 5. ANALYSIS OF DESIGN

Thermal Analysis, Operating Temperature Estimates

The maximum operating temperature of GLAST was the driver for many of the design decisions. This analysis was highly dependent on the amount of heat generated by the internal electronic components of GLAST, most notably the pre-amplifiers for the SSDs. The heat generated by each channel of the pre-amplifiers was conservatively taken to be $300\ \mu\text{W}$ (as opposed to the $100\ \mu\text{W}/\text{channel}$ expected for the final instrument). The amount of heat generated directly drives the thickness of the tower walls, the number of tower walls, the thickness of the structural grid and the size of radiators. The goal is to keep the temperatures in the instrument within the required ranges.

To estimate the maximum operating temperature of the satellite, an intricate analysis had to be completed. Heat that is generated inside GLAST is piped through different members and across contact points to a radiator surface. The radiator surfaces radiate as a function of their position, which is a cyclic function of their orbit.

The temperature path starts with the outermost pre-amplifiers and continues down the tower wall. Next, the heat travels through the structural grid to the radiators. Then, the heat is radiated to space as a function of orbit.

SSD Tray

The heat transfer properties of the whole tray were ignored since there is minimal contribution anywhere except the periphery of each tray. Because honeycomb has poor thermal conductivity properties and the pre-amplifiers are mounted directly onto the metal close-out where heat is directly transferred to the tower walls, thermal analysis of the tray does not reveal any pertinent information. The temperature of the tray is therefore taken to be the temperature of the pre-amplifiers. The effects of the temperature rise across the contacts and the close-out are included in the tower wall thermal analysis.

Tower Wall

The heat generated from the pre-amplifiers must travel through the closeout, across a thermal joint at the wall, down the tower wall and then through another thermal joint before entering the grid. The MATLAB code in Appendix E shows the analysis of this system. The steady state conduction model was for a 60 cm tall 2 mm thick Beryllium wall with 12 heat inputs equivalent to the layout of the trays. A large contact resistance (1.27 °C temperature rise) was used between the trays and the wall. This conservative resistance value can easily be improved with proper conditioning of surfaces and contact forces. Figure 5-5 gives the worst case temperature rise down a tower wall as 14 °C (Note: No heat loss through top of wall).

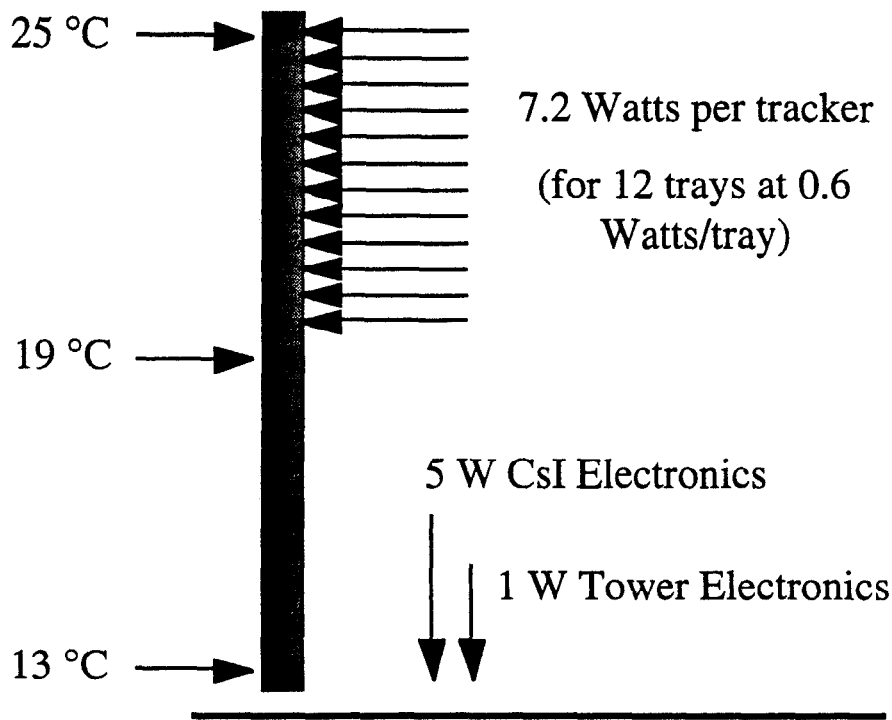


Figure 5-5 - Temperature distribution down tower wall

CHAPTER 5. ANALYSIS OF DESIGN

To check these analytical results, a FEM of a thermal tower wall was created. The FEM verified the results of the analytical model and gave a similar temperature rise of 12 °C. The contour plot of the heat distribution is given in Figure 5-6. See Appendix F for code.

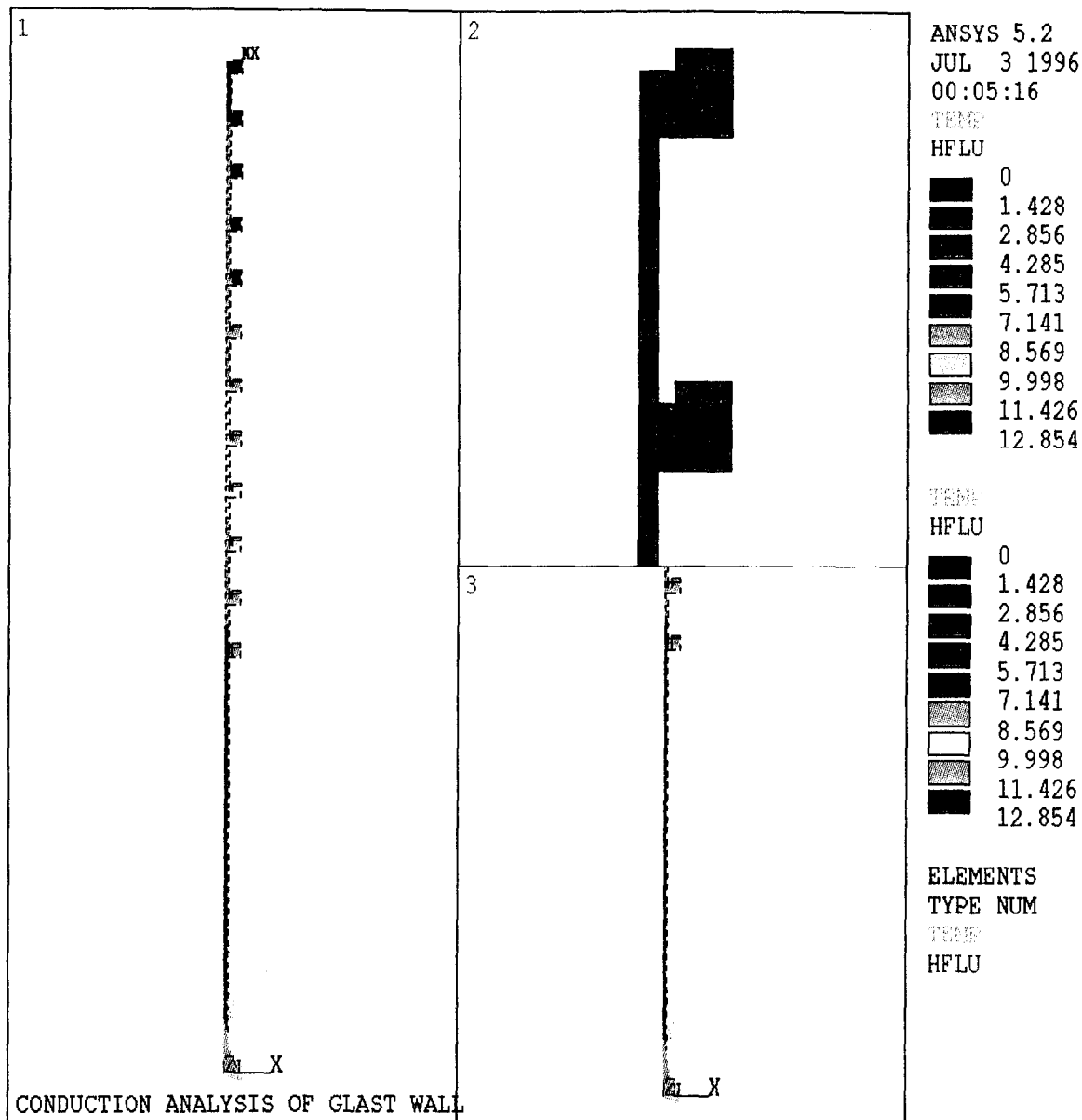


Figure 5-6 - FEM thermal analysis for temperature rise down tower wall

CHAPTER 5. ANALYSIS OF DESIGN

Grid

Once the heat has traveled down the wall and into the grid, it must travel the length of the grid and across another thermal joint before entering the radiator surface. This is a very complicated analysis since there are 49 towers dumping heat into the grid uniformly along its full length. The problem is further complicated by the fact that the radiators emit different amounts of heat as a function of their temperature.

A 7x7 Aluminum grid, 25 cm deep, with 1 cm thick walls was modeled using the coldest condition in orbit where all sides are pointing to free space (at 3 °K) and there are no heat inputs from the Sun or Earth. The heat input from the towers to the grid was 645 watts. After traveling through the grid, the heat was radiated to free space from the 0.6 meter tall radiator surface on the periphery of the instrument. The resulting temperature distribution across the grid is displayed by the FEM model output shown below in Figure 5-6 (see code in Appendix D). The cold temperature on the edge of the grid was around -20 °C (-23 °C to -17 °C) rising as much as 28 °C (-23 °C to 5 °C) across the grid. To understand how the temperature varies as a function of orbit, a more detailed analysis had to be performed.

CHAPTER 5. ANALYSIS OF DESIGN

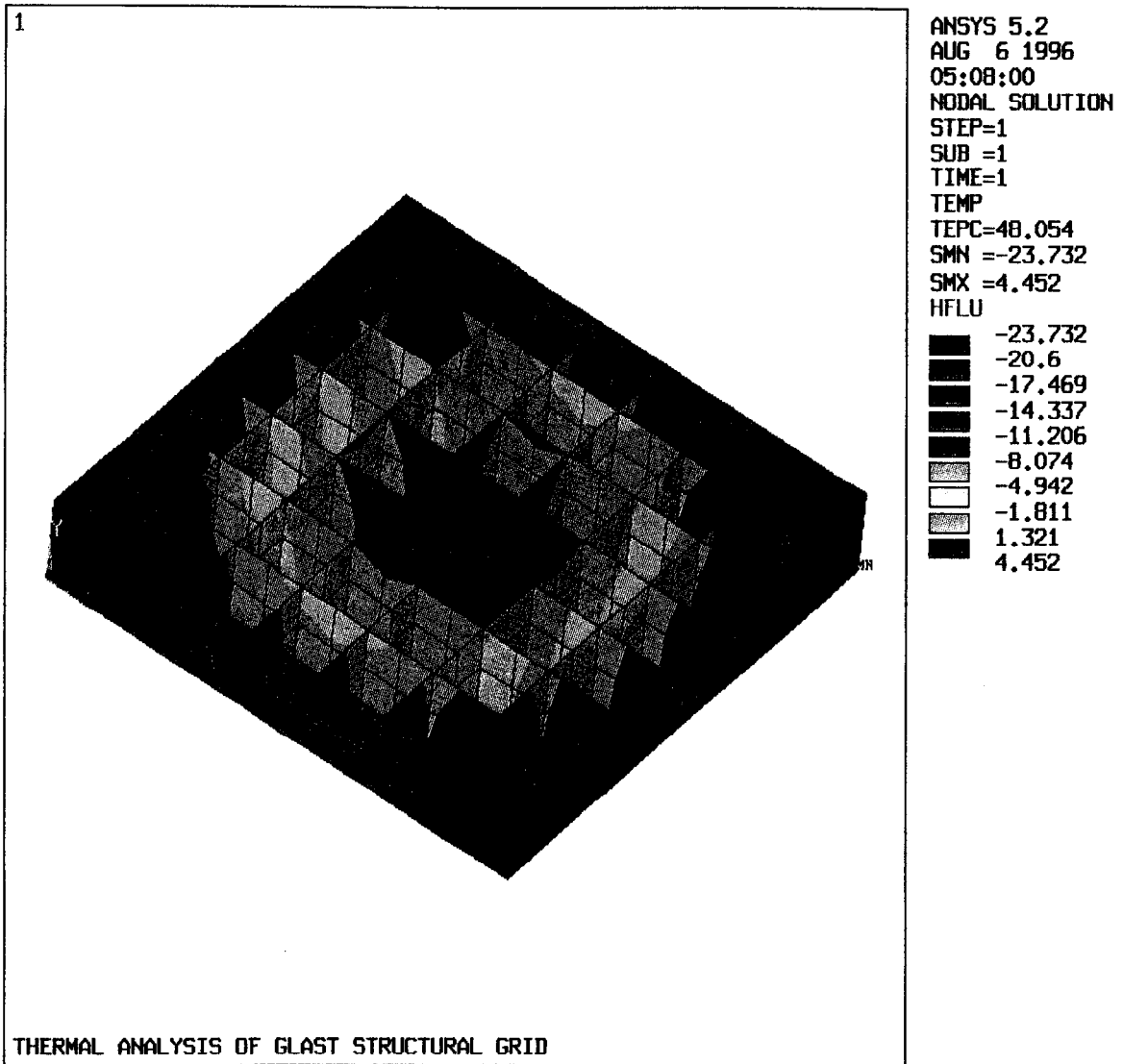


Figure 5-7 - FEM thermal analysis for temperature distribution across grid

On Orbit Temperatures

Because the spacecraft will orbit the Earth and point generally in various directions (except toward the Earth), the surfaces of the spacecraft always see different conditions. This is an extremely complicated condition where simple hand calculations will not yield much understanding. For this reason, a thermal program was written in Interactive Design Language (IDL) which simulates the expected environmental conditions in orbit. There are the heat inputs from the Sun and the Earth (which vary continuously around an orbit and for different altitudes, seasons, etc.) and the heat generated internally. An assumption was made that above the 645 w produced by the instrument, an additional 350 w is produced by other components in the spacecraft bus, giving a total of about 1 kW of power to be dissipated. The IDL analysis (see Appendix G) is based on the thermal orbit equation shown in Wertz and Larson (pg. 423):

$$T = \left[\frac{G_s \alpha + q_1 \epsilon_t \sin^2(\rho_e) + G_s a \alpha K_a \sin^2(\rho_e)}{\sigma_s \epsilon_t} \right]^{\frac{1}{4}} \quad (5.9)$$

where T is the temperature of the system and the other variables are as follows:

G_s = solar constant (1358 W/m²)

q_1 = Earth IR emission (237 W/m²)

a = albedo (30% of direct solar, 407 W/m²)

σ_s = Stefan-Boltzmann constant (5.67E-8 W m.⁻²K⁻⁴)

α = Solar absorptivity (0.15 for radiators, 0.01 for thermal blankets)

ϵ_t = Solar Emissivity (0.8 for radiators, 0.01 for thermal blankets)

R_e = Radius of Earth (6378 km)

H = Altitude of orbit (600 km)

ρ_e = Angular radius of Earth ($R_e/(H + R_e)$)

K_a = $0.664 + 0.521\rho_e - 0.203\rho_e^2$, a factor which accounts for the reflection of collimated incoming solar energy off a spherical Earth.

CHAPTER 5. ANALYSIS OF DESIGN

The analysis accounts for a 10% EOL reduction in properties. The model has the radiators extending around the periphery on the base of the spacecraft with thermal blankets over the instrument and on the bottom of the spacecraft.

The results depend highly on the type of radiator used and on the amount of surface area. By selecting standard SSM's as the radiators, the temperature of the satellite then becomes a function of the surface area of the radiators. A plot of the temperatures as a function of azimuthal and elevational rotations for the eclipse condition are plotted in Figure 5-8. In contrast, Figure 5-9 shows the response in full sun for a radiator absorptivity of 0.1 and 0.25 (beginning of life and end of life respectively). For a given temperature, if the power requirements are increased or decreased, the temperature can be controlled by simply increasing or decreasing the surface area of the radiators.

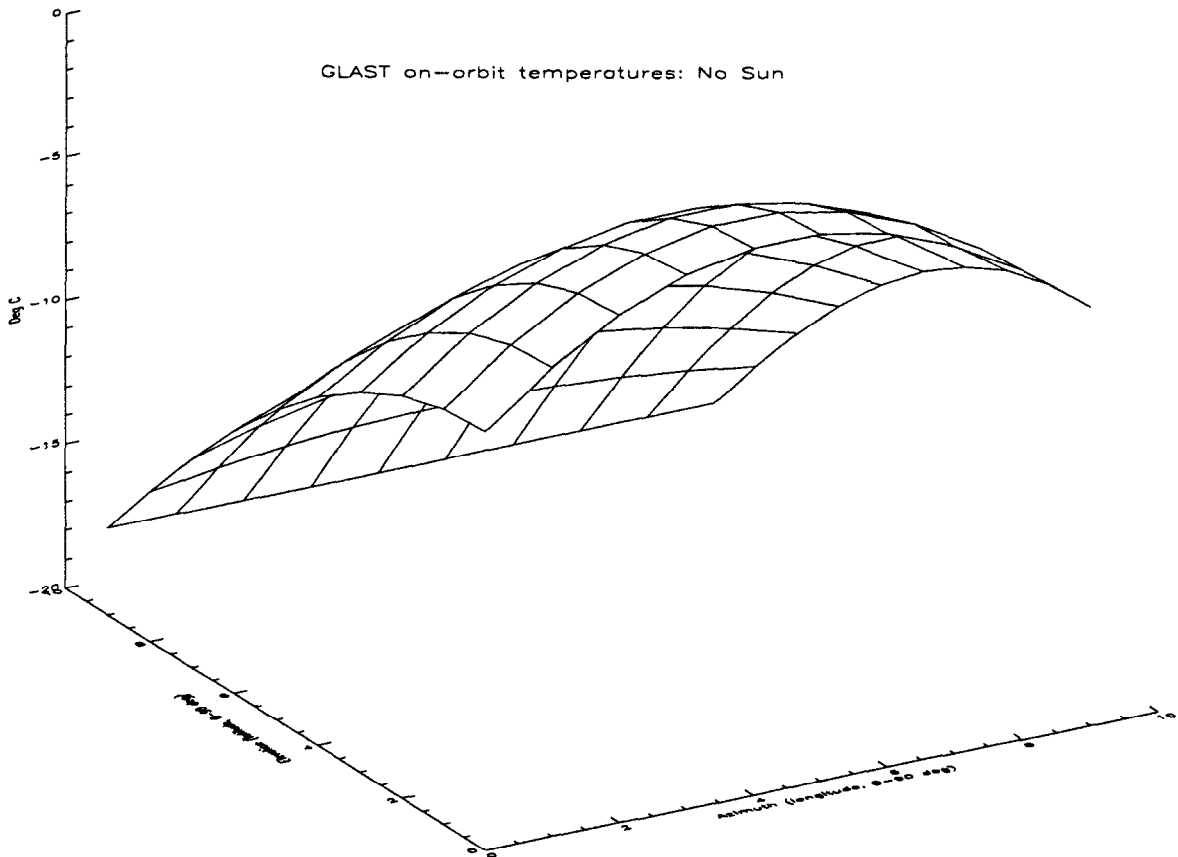


Figure 5-8 - On - orbit temperatures during eclipse

CHAPTER 5. ANALYSIS OF DESIGN

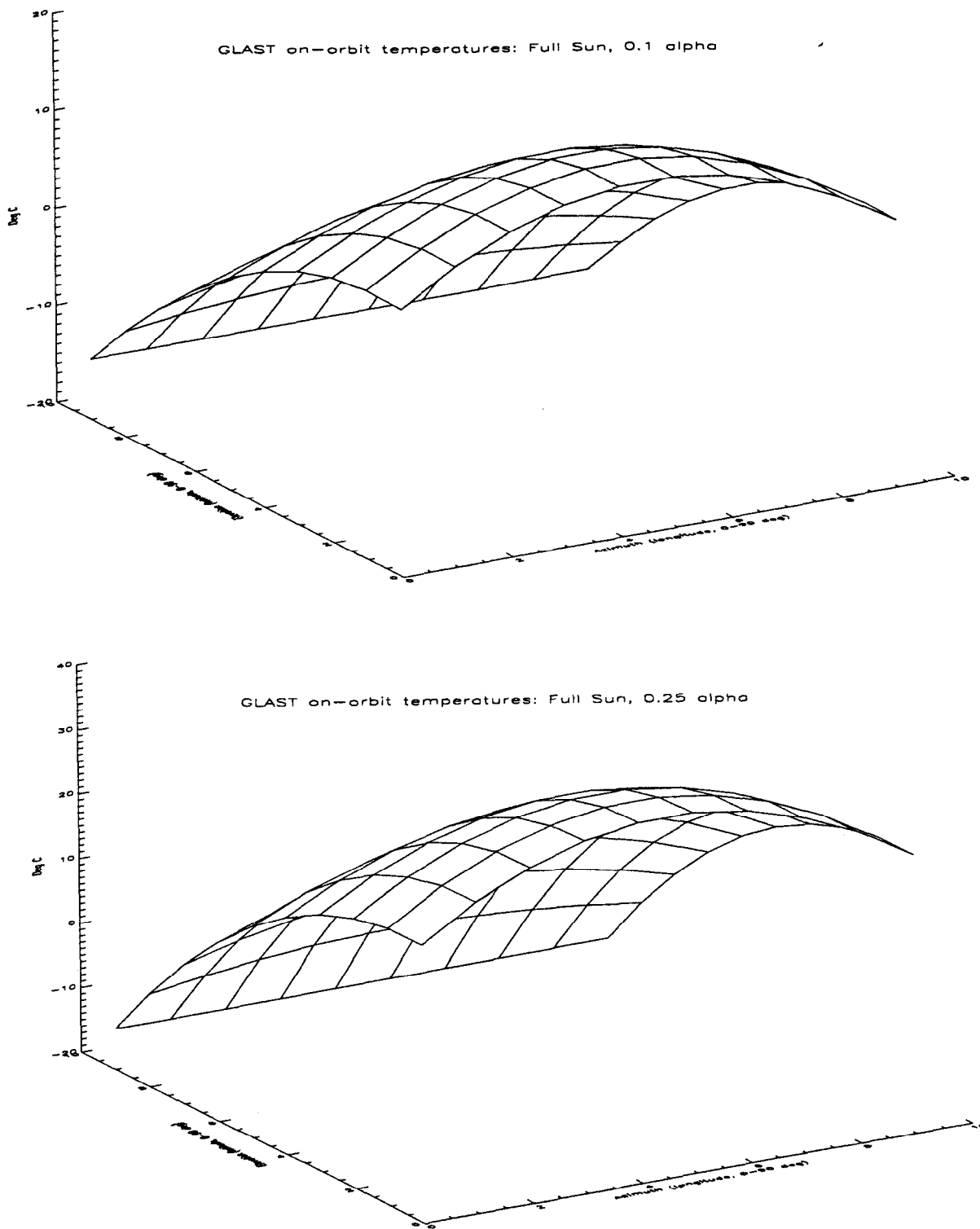


Figure 5-9 - On orbit temperatures with full sun and variable absorptivity

CHAPTER 5. ANALYSIS OF DESIGN

By controlling the pointing of the satellite, a temperature of $-17\text{ }^{\circ}\text{C}$ can be achieved at the radiators. A $28\text{ }^{\circ}\text{C}$ temperature rise across the grid and a $14\text{ }^{\circ}\text{C}$ rise up the tower wall gives a maximum temperature of $25\text{ }^{\circ}\text{C}$, just barely meeting the requirement. To lower this value, the thickness of the walls or grid ribs could be increased, superior materials (e.g., composites) could be used, heat pipes could be employed, or the radiator area could be increased.

This analysis confirms the earlier finding that for 5.6 m^2 of radiators, and for the given configuration of components, dimensions of structures and selection of materials, a temperature range within the specification ($\pm 25\text{ }^{\circ}\text{C}$) can be achieved using only passive thermal components.

6 : Fabrication of Prototypes

In order to verify the design calculations and to get realistic ideas about manufacturing, costs and schedules, prototypes of trays were manufactured and tested. Care was taken to duplicate the conditions and environments that the trays are expected to see in real use.

Space Qualification

Because of the concern about the accuracy and relevancy of the tests, special care was taken when selecting materials for prototypes to try and meet space qualifications. Tapes and adhesives with low outgassing properties were used and components exposure to hygrothermal environments was minimized.

Built in Testing Schemes

Back-plane continuity check

In order for the SSDs to work properly, the back of the detectors must be connected to high voltage bias. The back of each detector is coated with Aluminum and connected to a bias voltage source (approximately 100V). Making this connection was difficult given the layup of the detectors on the tray, but was accomplished using a double sided electrical transfer adhesive. The properties of the adhesive were unknown, so, a method was devised to test the adhesive tape under realistic conditions.

CHAPTER 6. FABRICATION OF PROTOTYPES

Back-plane design

The method for testing the back-plane connections involved placing a series of circuit lines under the detectors that, when connected through the back-plane of the detectors, would yield a continuity condition. The conductive transfer adhesive was then used to make the electrical connection from the back-plane to the grid circuit. The grid circuit was made thin and flexible by using Kapton sheets and 1 oz. Copper foil (flex circuit technology). The electrical signal enters the Copper circuit at an input, travels up through the electrical adhesive to the back of the first detector, then along the Aluminized back of the detector, down through more transfer adhesive and into the Copper circuit again (see Figure 6-1). This same signal traces its way in a zigzag pattern across all 16 detectors in the X layer before finally exiting on a Copper bus line. A continuity check from the input line to the exit bus line verifies that all detectors are electrically connected

Seven grid lines were placed on the periphery of one side of the circuit. Five of the lines were used for checking the wirebonds while two were used to check the back-plane connections. The grid lines bussed the continuity signals to the corner of the tray where they could be checked during testing.

The flex circuit was made by taking adhesive-laminated 2 mil Kapton sheet (with Pyralux adhesive), hot press bonding a 1 oz. Copper foil onto it and then resisting, masking, and etching off the Copper, leaving only the desired pattern. The outside bus lines had the added complexity of having bonding pads placed on them (thick Gold pads on thin Nickel film bonded to the Copper circuit). While this flex circuit was only used to test continuity, the purpose of the flex circuit on GLAST will be to electrically bias the back-plane of the detectors and bus signals and power to the detectors.

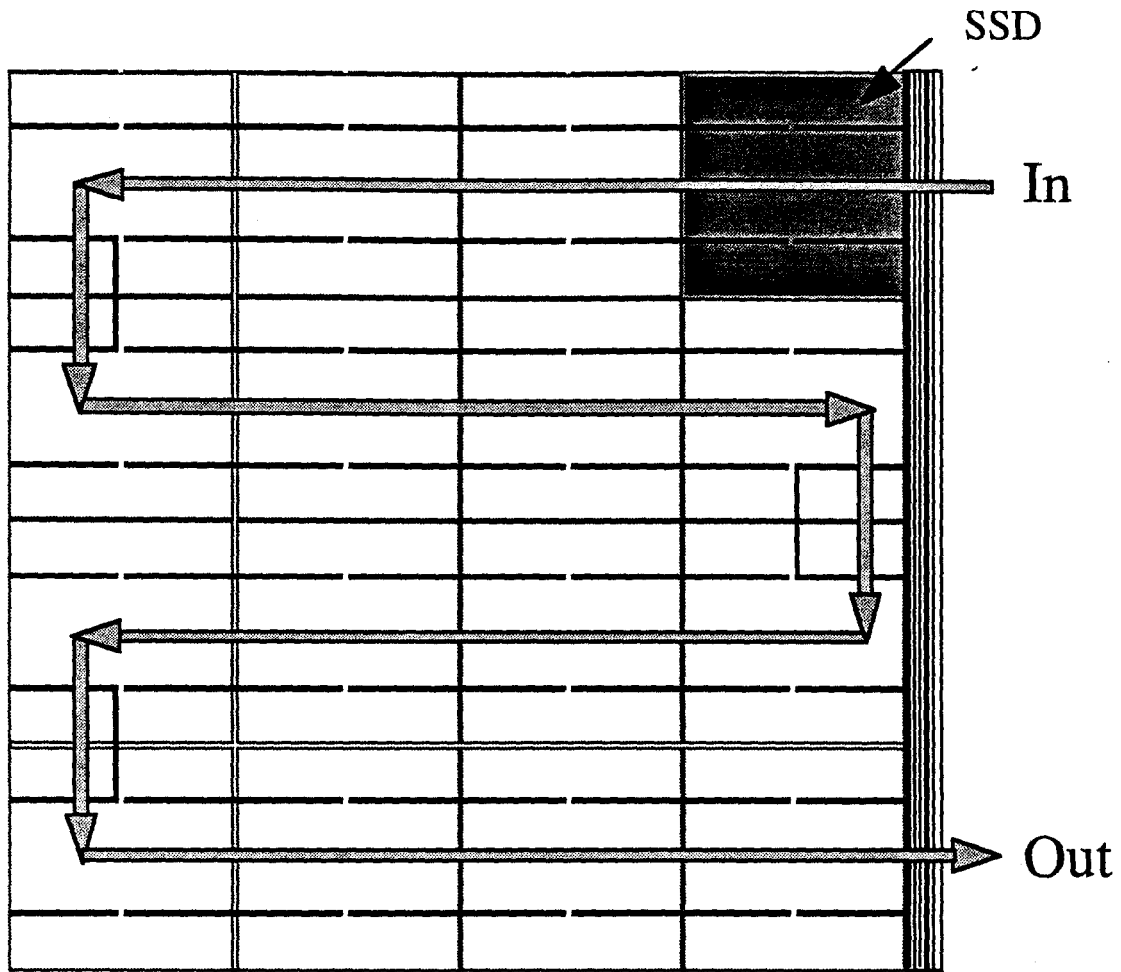


Figure 6-1 - Circuit design for electrical connection of back-plane

CHAPTER 6. FABRICATION OF PROTOTYPES

Dummy detector

To verify that SSDs survive with the prototype structures, inexpensive test dummy detectors were made. These detectors appeared like real detectors mechanically and electrically. The dummy detectors were made by cutting 4" silicon wafers into 6 cm square chips. They were then coated with 1 μm of Aluminum on both sides, coated with resist, and exposed under a mask to leave a pattern of lines and pads (on the polished side of the wafer). When etched away, small electrical connection lines and pads were left which simulated what is on the real detectors.

The pattern of lines connecting the pads is a zigzag testing scheme similar to the design used for the backplanes. The continuity check in this case consisted of testing the wirebonds that connect the detectors together. In this testing scheme, the electrical signal enters one of the dummy strips on the first detector and travels along its length until it reaches the opposite end of the detector. At each end are wire-bonding pads where wire-bonds connect two adjacent strips together. After a signal has passed through the four outermost strips, a jumper sends the signal to the next adjacent strip and the signal continues to travel, checking wirebond continuity. This process continues until all 247 strips² of the four daisy chained dummy detectors have been checked. The test of the nearly 750 bonds on one chain is a simple continuity check at the input and output of the corner strings (see Figure 6-2).

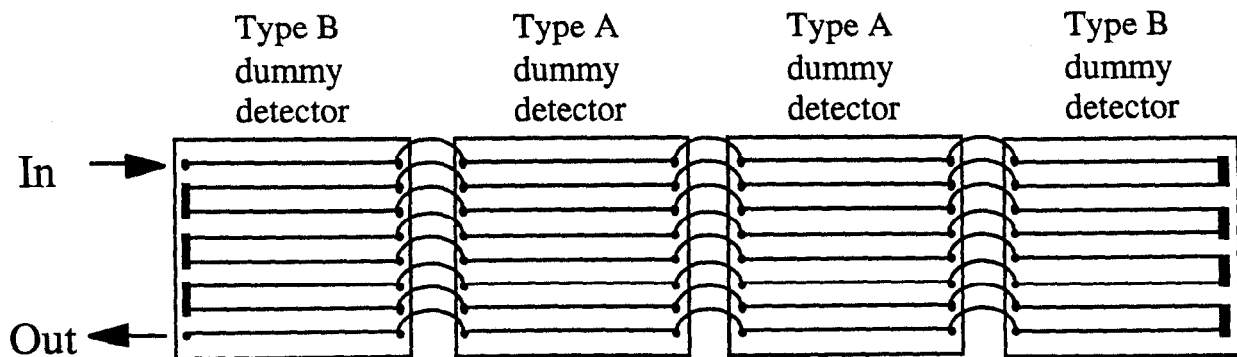


Figure 6-2 - Dummy detector testing scheme

² Because of manufacturing issues, only 247 strips were made for the dummy detectors. However, in the GLAST SSD, there will be 249 strips.

CHAPTER 6. FABRICATION OF PROTOTYPES

Because there are four sets of these serial detectors, four different continuity checks must be made to test all the nearly 3000 wirebonds on the tray. This setup allows for very rapid assessment of the condition of the tray and eases trouble-shooting if problems arise.

To reiterate: seven bus lines are on the periphery of the tray. They consist of a back-plane input and output, a common line for each input to the strips, and an output from the four detector strings.

Manufacturing of a Tray

The structural trays that were produced are composed of single ply composite weave facesheets on each side of a honeycomb core with an alodined (space grade adhesive friendly coating) Aluminum close-out. As a first cut in the design, all the test trays incorporated only a single layer of test SSDs.

Manufacturing processes

This section outlines the process for the manufacturing of the “test” GLAST trays. The purpose of these prototypes was to experiment with different manufacturing processes, technologies and materials.

In the process of making a test GLAST tray with dummy detectors, a structural tray was first produced. The tray was made as a sandwich composite laminate with a single [0/90] cloth carbon fiber face sheet (~125 μm thick) on each side of a 1/4 inch honeycomb core spacer. The face-sheets were cured as flat sheets separately. The upper face-sheet was hot press cured against a flat surface using excess resin to give the outer ply a smooth, flat surface. A threaded Aluminum insert (close-out) was placed around the periphery of the tray and bonded along with the face sheets and core. The top (smooth) face-sheet was bonded using a thin film adhesive, while the bottom, dry (porous) face-sheet was epoxied down. The close-out had four mounting points on each side (a total of 16 mounting taps) for mounting to the tower wall and the whole close-out was alodined to ensure good adhesion when gluing (Figure 2-1).

Once the structural tray was produced, the mechanical dummy detectors had to be affixed. First, the back-plane test circuit was epoxied to the smooth side of the tray. The circuit was aligned and cured with the Copper grid facing up and exposed. The next step called for placing

CHAPTER 6. FABRICATION OF PROTOTYPES

electrically conductive "double sided" transfer adhesive over the exposed circuit (3M's 9703 conductive transfer tape was used).

The single layer of "dummy" detectors was aligned and placed on the tray (because of the adhesive, they could not be moved once they touched the tray). To improve the bond between the detector ground plane and the Kapton circuit, a small amount of heat and pressure was applied to "fix" the bond (the tray was vacuum bagged and placed in an oven at 70 °C for 20 minutes

All the detectors on the X layer were then wire bonded using automated machines. Because it was planned to test the tray without a conformal coating, the exposed, free floating wire bonds were protected by placing a removable cover over the tray. At this point the tray was ready for testing.

Most of the manufacturing for the prototype was done by hand although automated techniques will have to be used for making the nearly 600 trays for the final GLAST instrument. Mass manufacturing techniques will require custom equipment to handle and align the various components that a tray (equipment like vacuum chucks). In addition, the manufacturing environment will have to be controlled to avoid contaminants.

7 : Testing of Prototypes

To verify the mechanical and electrical stability under vibrational and thermal loading as well as the robustness of the wirebonding scheme, the prototype tray was mechanically and thermally tested. The mechanical testing used loads designed to reasonably envelope those expected during launch. The thermal testing exerted thermal strains under high vacuum, simulating the worst cases of the combined thermal and vacuum loads experienced in orbit.

Random Vibration Tests

Vibration Equipment Setup

The testing setup provided the same fixed boundary conditions used in the analysis of the tray. This was done to ensure maximum compliance between the tests and the FEM analysis. One quarter inch Aluminum plates (3" tall) were bolted to the sides of the tray and secured to a one inch thick Aluminum plate which was securely fastened to the shake fixture.

Then, three accelerometers were placed on the test stand and tray. One accelerometer was placed on the solid base of the test stand as a reference, one on a corner of the tray and one in the middle of the tray. The corner accelerometer ended up being inoperative and gave no useful data for the tests. Fortunately, the critical middle accelerometer functioned perfectly.

Before testing began, a sine sweep of frequencies was performed to characterize the tray and setup. The middle accelerometer followed the reference until the tray hit its natural frequency at about 520 Hz. This is well above the 35 Hz danger zone and very similar to the 593-1072 Hz expected from the FEM analysis (somewhere between simply supported and fixed boundary conditions). Discrepancies in this fundamental frequency can be accounted for by variations in

CHAPTER 7. TESTING OF PROTOTYPES

material, unpredictable manufacturing processes and actual boundary conditions that are difficult to accurately model.

Shake Test

The first test that was performed on the tray was a simulated launch. Using the Delta II spectrum as the baseline and following the General Environmental Verification Specifications (GEVS) manual published by NASA for expendable launch vehicles, a series of vibration tests were chosen. The tray was shaken from 20-2000 Hz at levels from 6.3 to 25 G_{rms} thereby meeting and exceeding the NASA protoflight qualification levels of 6 dB above the expected flight conditions (only $2 \times 8.7 = 17.4$ was required). The tray went through its natural frequencies causing rise to G_{rms} values of over 100! The response of the middle accelerometer at the 25 G_{rms} inputted spectrum is shown in Figure 7-1. This test, in compliance with the GEVS qualification standards, was performed for two minutes. After each shake, continuity checks were performed to verify the status of the electrical connections.

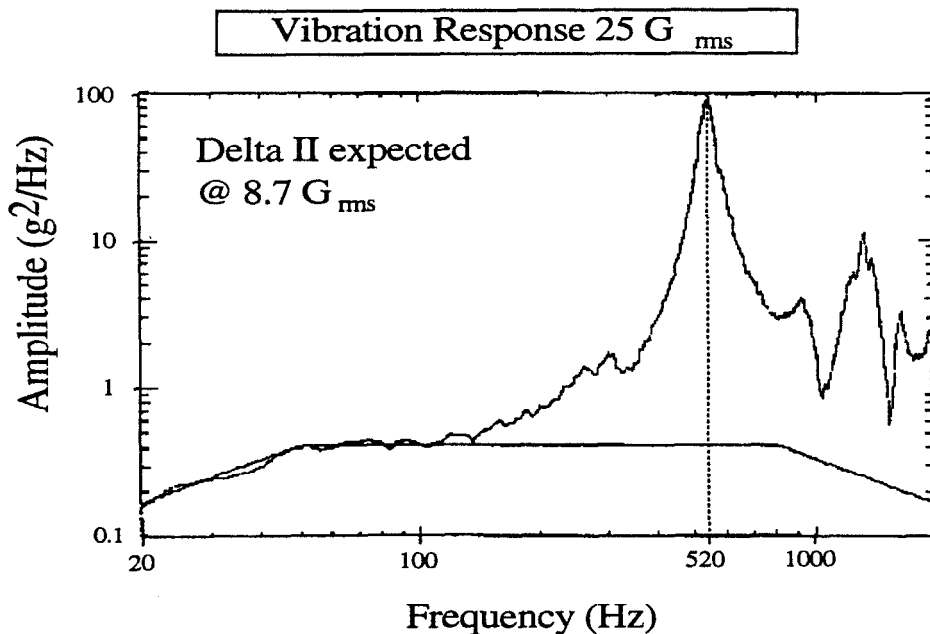


Figure 7-1 - Response of center of tray under random vibration

CHAPTER 7. TESTING OF PROTOTYPES

Thermal Cycling under Vacuum

In orbit, a spacecraft experiences huge temperature input changes. This, combined with a hard vacuum, can strain to failure even the most robust systems. Because of trapped voids, a hard vacuum can cause tremendous point sources of pressure and because of differential thermal expansions, components can be severely stressed. These effects are even more critical when dealing with delicate equipment like silicon detectors and wirebonds.

Thermal Equipment Setup

The support stand for the thermal tests was a simple bar on two sides of the tray that supported the tray above the test chamber floor. A series of four calibrated thermocouples were placed around the apparatus to record temperatures at various locations. Two sensors were used as references and placed on the walls of the test chamber. The other two thermocouples were placed on the tray, one at a corner and one in the center of the tray.

Before thermal cycling occurred, the testing rig was sealed in the thermal vacuum tank, and was brought to a 10^{-5} Torr pressure level over the span of an hour. In the time span of a launch (2 min.) the pressure decreased from 760 to 2 Torr, simulating a rapid fall to vacuum. This test is extremely important as any mistakes (large voids) produced during manufacturing could have resulted in a catastrophic explosion under the rapid evacuation.

Thermal/vacuum Tests

In order to prove that wirebonds will hold up under thermal cycling in this configuration, extensive thermal testing was performed. For protoflight qualifications [NASA GEVS], eight complete cycles are required, from +10 °C over the maximum temperature expected, to -10 °C below the coldest temperature expected. The GLAST detectors will operate (noisily) up to +45 °C and as cold as -35 °C. Hence, eight cycles were performed under vacuum from +55 °C to -45 °C. The vacuum level varied from 5×10^{-5} Torr (from typical outgassing at the hot condition) to as low as 5×10^{-6} Torr. Figure 7-2 shows the response of the middle and reference thermocouples through one of the eight identical cycles.

CHAPTER 7. TESTING OF PROTOTYPES

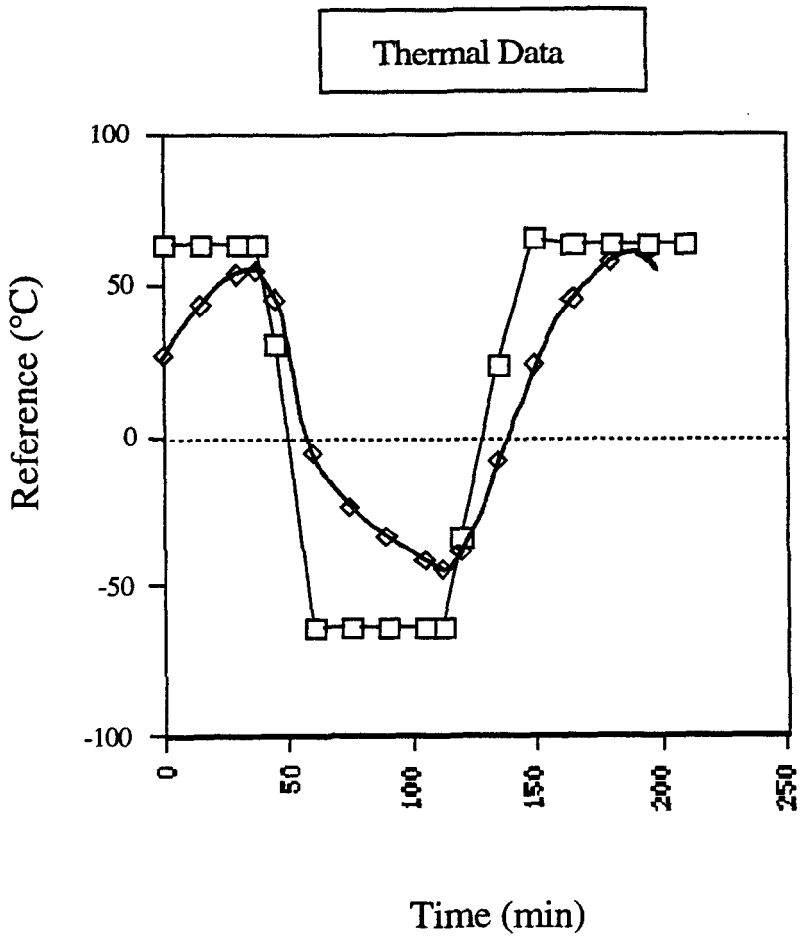


Figure 7-2 - Sample thermal vacuum temperature cycle

8 : Final Results

Post test

The continuity results were particularly impressive. All 3000 wirebonds, as well as the backplane connections, held up through the simulated launch at 25 G_{rms} for two minutes and survived through eight cycles under vacuum with a thermal cycle of 100 °C. In fact, there was no damage or other effect whatsoever to the tray of detectors through all of the environmental testing, verifying the robustness of the basic design of the tray and its manufacturing procedure. It also verifies that the use of wirebonding for mass electrical connections will work and that the use of z-axis conductive transfer adhesive is a viable method of connecting the back-planes.

CHAPTER 8. FINAL RESULTS

Mass Estimates

Table 8-1 below summarizes the masses of the various components in a tray.

Material	Thickness (microns)	Thickness (cm)	Area ratio (%)	X_o (cm)	Equivalent radiation length ^a	Weight (grams)
X layer Silicon	500	0.050	0.955	9.36	0.510%	67.10
Y layer Silicon	500	0.050	0.955	9.36	0.510%	67.10
Aluminum	1	0.0001	0.955	8.9	0.001%	0.16
Z axis adhesive ^b	50	0.005	0.825	2.71	0.152%	0.62
Copper	3	0.0003	0.083	1.43	0.002%	0.13
Kapton ^c	100	0.010	1.1	19.4	0.052%	5.07
Glue ^c	40	0.004	1.0	20	0.020%	2.41
Dry carbon facesheet	130	0.013	1.0	18.8	0.069%	23.53
Aluminum insert ^d	6350	0.635	0.101	8.9	0%	108.10
Honeycomb	6350	0.635	0.899	800	0.071%	6.89
Smooth carbon facesheet	250	0.025	1.0	18.8	0.133%	52.80
Wirebonds	750	0.075	0	8.9	0%	0.50
Total	8674	0.870			1.52%	334.4

a. Ratio or thickness to radiation length X_o . Reported as a percentage of equivalent radiation length.

b. Z axis Tape (3M 9703) is made us of Acrylic ($t=0.0032$ cm; $X_o=10$ cm; 0.032% of an equivalent radiation length), Silver ($t=0.0005$ cm; $X_o=1.5$ cm; 0.033% of an equivalent radiation length), and Nickel ($t=0.0013$ cm; $X_o=1.5$ cm; 0.087% of an equivalent radiation length), resulting in tape properties of $t=0.005$ cm, $X_o=2.71$ cm and 0.0152% of an equivalent radiation length.

c. Unknown radiation length

d. Closeout material is a concentrated mass that must be accounted for differently in the material audit

Table 8-1 - Mass and radiation lengths in tray

Table 8-2 below approximates the masses in the GLAST instrument.

Section	Tower mass	Instrument mass	Mass added for
Instrument			
Calorimeter			
<i>CsI</i>	53.26	2609.8	2923.0
<i>Structure</i>	1.00	49.0	54.9
<i>Photodiodes & electronics</i>	0.50	24.5	27.4
Total	54.76	2683.3	3005.3
Tracker (12 trays)			
<i>Si</i>	1.59	77.9	87.3
<i>Pb</i>	1.91	93.8	105.1
<i>Inserts/bolts</i>	1.32	64.7	72.4
<i>Tray structure</i>	1.10	54.1	60.6
<i>Preamps</i>	0.60	29.4	32.9
Total	6.53	319.9	358.3
Tower walls (4)	2.28	111.7	125.1
Wires, electronics, etc.	2.00	98.0	109.8
Instrument total	6.53	319.9	358.3
Spacecraft additional components			
Support grid		200.0	224.0
Space craft bus		600.0	672.0
Spacecraft total		4013.0	4494.5
Delta II 7920, 2-stage, 600km Circular Orbit, 28.7°			
Maximum allowable weight		4500.0	4500.0
Spacecraft weight (% of maximum)		88	100

Table 8-2 - Mass estimates for GLAST

Physics Performance Numbers

The performance of this design will be measured in how efficiently it will perform as a gamma-ray observatory track. The interaction probability is directly a function of the radiation length in the material audit. Table 8-1 lists the material audit and equivalent radiation length of a tray.

The 1.52% of a radiation length in this tray and layup design is sufficiently below the 5% specification to assure satisfactory use in an efficient instrument.

Concluding Remarks

This thesis has encompassed the design for the GLAST instrument tray, tower walls and structural grid. It has outlined the procedure for manufacturing a tray, laying up detectors and completing electrical connections. In addition, it has verified the performances of these designs using both analytical methods and rigorous environmental and mechanical testing.

This thesis work has provided a viable solution for the GLAST structural tray and the first cut at the design concept of the entire instrument.

I look forward to the completion and operation of the GLAST instrument. This was an exciting project to work on and collaborating with such an excellent team of people from all around the world was a real joy. I hope that GLAST will be a wonderful success and will help to unravel some of the mysteries of our Universe.

BIBLIOGRAPHY

- 1) Brooks P J, 1985, *Chartered Mechanical Engineer* , Sept. pgs. 36-40
- 2) Larson W J and Wertz J R, 1992, *Space Mission Analysis and Design*
- 3) Mcdonnell Douglas Corporation, 1987, *Delta II Commercial Spacecraft Users Manual*
- 4) National Aeronautics and Space Administration, 1990, *General Environmental Verification Specification (GEVS) Manual*
- 5) Tsai S W, 1980, *Introduction to Composite Materials*
- 6) Williamson M, 1990, *The Communication Satellite*
- 7) Wise P C, 1985, *International Astronautical Federal Congress* , IAF-85-373

APPENDIX A. ANSYS STATIC DEFLECTION AND FREQUENCY GRID CODE

APPENDIX A - ANSYS STATIC DEFLECTION AND FREQUENCY GRID CODE

```
/BATCH,LIST
!! ANSYS 5.2 FINITE ELEMENT ANALYSIS
!! GRID12.GEOM.LOG LAST REVISION 8/6/96 IN SLAC ANSYS
!! WRITTEN BY ALEX LUEBKE AND CHAD JENNINGS

!!*****
!!
!! DEFINES THE GEOMETRY FOR GLAST GRID ANALYSIS
!! STRUCTURAL, MODAL, THERMAL
!!
!! CODE GENERATES GEOMETRY AND STRUCTURAL BOUNDARY CONDITIONS
!! DIMENSIONS, MATERIALS, WEIGHTS, RESULTS IN EACH SUBSEQUENT SECTION
!!
!!*****

!!*****
!!      RESULTS SECTION (ALL NATURAL FREQUENCIES IN HZ)
!!      THICKNESS IS 1 CM RIB THICKNESS AND 25 CM TALL IN ALUMINUM
!!      GRID IS WEIGHTED UNDER 10 G LOAD FROM TOWERS
!!
!!      LOCKING THE GRID AT THE 3 OUTER SQUARE INTERFACES GIVES 3 CASE
!!
!!BOT_1 LOCKED (BOT_1 MEANS THE FIRST BC ON THE BOTTOM OF THE GRID)
!!      F1      = 256
!!      F2      = 442
!!
!!BOT_2
!!      F1      = 439
!!      F2      = 516
!!
!!BOT_3
!!      F1      = 153
!!      F2      = 196
!!
!!      MAXIMUM STRESS UNDER 10 G LOAD FROM TOWERS WITH B.C. #2 IS
!!      11.2 MPA WITH A MAXIMUM DEFLECTION OF 0.189 MM
!!
!!*****

/COM,ANSYS MEDIA REV. 5.2
/UNITS,SI      ! UNITS M,KG,SEC,N
/FILNAM,gridfreq
/PREP7      ! PREPROCESSOR PREP7

GRIDRIB = 0.01      ! THICKNESS OF GRID RIB IN METERS (1 CM)
VERTH = 0.25      ! HEIGHT OF GRID IN METERS
MOREH = 0.01      ! ADDED ELEMENTS FOR HEAT INPUT

!!!!!!!!!!!!!!!!!!!!!!!!!!!!!!!!!!!!!!!!!!!!!!!!!!!!!!!!!!!!!!!!!!!!!!!!!!!!!!
!! ANALYSIS TYPE AND MATERIAL PROPERTIES
```

APPENDIX A. ANSYS STATIC DEFLECTION AND FREQUENCY GRID CODE

```

!!!!!!!!!!!!!!!!!!!!!!!!!!!!!!!!!!!!!!!!!!!!!!!!!!!!!!!!!!!!!!!!!!!!!!!!!!!!!!!!!!!!!!!!!!!!!!!!!!!!!!!!!!!!!!!!!!!!!!!!
!! STRUCTURAL ELEMENTS
!!*****
!! STRUCTURAL ELEMENT NUMBER 1
ET,1,SHELL99,,,,,1 ! TYPE 1,ISOTROPIC WALL MATERIAL- USE SHELL
!!KEYOPT(2)=0 - NL,LSYM,LP1,LP2,EFS,BLANK(7),MAT,THETA,TK,MAT2,THETA2,TK2,ETC
KEYOPT,1,2,0 ! ET,1 - KEYOPT(2)=0
R,1,1 ! REAL 1,ONE LAYER
RMORE ! SKIP 6
RMORE,1,,GRIDRIB ! MAT 1, 0 DEG, 1 CM THICK WALL
MP,EX,1,7.0E10 ! MAT 1,AI 70 GPa ISOTROPIC MATERIAL
MP,EY,1,7.0E10
MP,EZ,1,7.0E10
MP,NUXY,1,0.3 ! AI POISSONS RATIO = 0.3
MP,GXY,1,2.6E10 ! AI RIGIDITY MODULUS = 26 GPa
MP,DENS,1,2.8E3 ! AI DENSITY = 2800 KG/M^3

!! STRUCTURAL ELEMENT NUMBER 2
ET,2,SHELL99,,,,,1 ! TYPE 2,ISOTROPIC WALL MATERIAL- USE SHELL
KEYOPT,2,2,0 ! ET,2 - KEYOPT(2)=0
R,2,1 ! REAL 2,ONE LAYER
RMORE ! SKIP 6
RMORE,2,,GRIDRIB ! MAT 2, 0 DEG, 1 CM THICK WALL
MP,EX,2,7.0E10 ! MAT 2,AI 70 GPa ISOTROPIC MATERIAL
MP,EY,2,7.0E10 ! MAT 1,AI 70 GPa ISOTROPIC MATERIAL
MP,EZ,2,7.0E10 ! MAT 1,AI 70 GPa ISOTROPIC MATERIAL
MP,NUXY,2,0.3 ! AI POISSONS RATIO = 0.3
MP,GXY,2,2.6E10 ! AI RIGIDITY MODULUS = 26 GPa
MP,DENS,2,2.8E3 ! AI DENSITY = 2800 KG/M^3
!!*****

!! THERMAL ELEMENTS
!!*****
!! THERMAL ELEMENT NUMBER 1
!ET,1,SHELL57 ! TYPE 1,THERMAL WALL MATERIAL- USE SHELL57
!R,1,GRIDRIB ! REAL 1,1 CM THICK = 0.00635 M
!MP,DENS,1,2.8E3 ! AI DENSITY = 2800 KG/M^3
!MP,KXX,1,200 ! AI HEAT 200 W/M/DEG C
!MP,KYY,1,200
!MP,KZZ,1,200

!! THERMAL ELEMENT NUMBER 2
!ET,2,SHELL57
!R,2,GRIDRIB ! REAL 2
!MP,DENS,2,2.8E3 ! AI DENSITY = 2800 KG/M^3
!MP,KXX,2,200 ! AI HEAT 200 W/M/DEG C
!MP,KYY,2,200
!MP,KZZ,2,200

!!*****

!!222222222222222222222222222222222222222222222222222222222222222222222222222222222222222222222222222
!! GENERATE GRID ELEMENTS - MODEL
!!222222222222222222222222222222222222222222222222222222222222222222222222222222222222222222222222222

VNUM = 2 !NUMBER OF VERTICAL ELEMENTS IN GRID
HNUM = 2 !NUMBER OF HORIZONTAL ELEMENTS IN TOWER GRID

HOR = 0.25 !LENGTH OF TOWER WALL/GRID LENGTH
K,1,0,0 !KEYPOINTS DEFINING BOUNDARY OF X WALL
K,2,0,VERTH,0
K,3,HOR,VERTH,0
K,4,HOR,0,0

K,5,0,0,0 !KEYPOINTS DEFINING BOUNDARY OF Y WALL
K,6,0,VERTH,0
K,7,0,VERTH,HOR

```


APPENDIX A. ANSYS STATIC DEFLECTION AND FREQUENCY GRID CODE

```

CM,BOT_1,NODES

NSEL,ALL                ! BOTTOM, NEXT PERIMETER
NSEL,S,LOC,X,HOR ! BOT_2 IS THE NAME OF THE NEXT INNER PERIMETER
NSEL,A,LOC,Z,HOR
NSEL,A,LOC,X,6*HOR
NSEL,A,LOC,Z,6*HOR
NSEL,U,LOC,Y,0.01,10
NSEL,U,LOC,X,0.99*HOR
NSEL,U,LOC,X,6.01*HOR,7*HOR
NSEL,U,LOC,Z,0.99*HOR
NSEL,U,LOC,Z,6.01*HOR,7*HOR

CM,BOT_2,NODES

NSEL,ALL                ! BOTTOM, NEXT PERIMETER
NSEL,S,LOC,X,HOR*2     ! BOT_3 IS THE NAME OF THE THIRD INNER PERIMETER
NSEL,A,LOC,Z,HOR*2
NSEL,A,LOC,X,5*HOR
NSEL,A,LOC,Z,5*HOR
NSEL,U,LOC,Y,0.01,10
NSEL,U,LOC,X,0.99*HOR
NSEL,U,LOC,X,5.01*HOR,7*HOR
NSEL,U,LOC,Z,0.99*HOR
NSEL,U,LOC,Z,5.01*HOR,7*HOR

CM,BOT_3,NODES

!!!!!!!!!!!!!!!!!!!!!!!!!!!!!!!!!!!!!!!!!!!!!!!!!!!!!!!!!!!!!!!!!!!!!!!!!!!!

ALLSEL
/VIEW,1,1,1,1
EPLIT

FINISH

/EOF

!! ANSYS 5.2 FINITE ELEMENT ANALYSIS
!! NATURAL FREQUENCY AND STATIC DEFLECTION ANALYSIS FOR GLAST GRID
!! GRID12.FREQ.LOG LAST REVISION 8/6/96
!! WRITTEN BY ALEX LUEBKE AND CHAD JENNINGS

!!!!!!!!!!!!!!!!!!!!!!!!!!!!!!!!!!!!!!!!!!!!!!!!!!!!!!!!!!!!!!!!!!!!!!!!!!!!
!!
!! MODAL ANALYSIS AND STRESS ANALYSIS OF GLAST GRID BUS
!! RUN THIS PROGRAM AFTER GRID12.GEOM.LOG
!! DIMENSIONS AND MATERIAL PROPERTIES FOUND IN GRID12.GEOM.LOG
!!
!! LOADING IS WEIGHT OF TOWERS UNDER 10 G ACCELERATION
!!
!!!!!!!!!!!!!!!!!!!!!!!!!!!!!!!!!!!!!!!!!!!!!!!!!!!!!!!!!!!!!!!!!!!!!!!!!!!!

/TITLE, 1ST, 2ND NAT. FREQ. OF 1X25X25 CM GLAST GRID, 2ND B.C.
!/TITLE, STRESS IN/AUTO
/PBC,U,0
/ERASE
ALLSEL
/PNUM,ELEM,1
/COLOR,ELEM,RED,1,448 ! SETS COLR OF OUTPUT DISPLAY
/NUMBER,1             ! TURNS OFF ELEMENT NUMBERING

/PBC,U,1             ! TURNS ON ALL BOUNDARY CONDITION MARKERS
/PBC,ACEL,1         ! TURNS ON GRAVITY VECTOR
/PSF,PRES,2
/DSCALE,ALL,0.005   ! AMOUNT OF DEFORMATION IN OUTPUT PLOT
/VIEW,1,1,1,1

```


APPENDIX A. ANSYS STATIC DEFLECTION AND FREQUENCY GRID CODE

```
/AUTO
/PBC,U,0
/ERASE
ALLSEL
/PNUM,ELEM,1
/COLOR,ELEM,RED,1,448      ! SETS COLR OF OUTPUT DISPLAY
/NUMBER,1                  ! TURNS OFF ELEMENT NUMBERING

!/PBC,U,1                  ! TURNS ON ALL BOUNDARY CONDITION MARKERS
!/PBC,ACEL,1              ! TURNS ON GRAVITY VECTOR
!/PSF,PRES,2
!/DSCALE,ALL,0.005        ! AMOUNT OF DEFORMATION IN OUTPUT PLOT
/VIEW,1,1,1,1

SET,,1                      ! PLOT FIRST, LOWEST NATURAL FREQUENCY
PLDISP,2

!SHELL,TOP                ! GET STRESS ON TOP FACESHEET
!PLNSOL,S,INT

/VIEW,2,0,1,0
/WINDOW,1,OFF

/WINDOW,2,0.2,1,-1,-0.2
/PBC,U,1
SET,,2                      ! GET SECOND LOWEST NATURAL FREQUENCY
/TITLE, 1ST, 2ND NAT. FREQ. OF 1X25X25 CM GLAST GRID, 2ND B.C.
/NOERASE
PLDISP,2                  ! PLOT MODE W/ UNDEFORMED OUTLINE
EPlot
/WINDOW,2,OFF

/WINDOW,ALL,ON            ! LEAVE IN THIS CONDITION FOR DISPLAY OPTIONS
/PBC,U,0

/EOF
```

APPENDIX B. ANSYS TRAY CODES

APPENDIX B - ANSYS TRAY CODES

```
/BATCH,LIST
!! ANSYS 5.2 FINITE ELEMENT ANALYSIS
!! NATURAL FREQUENCY ANALYSIS FOR COMPOSITE GLAST TRAY
!! TRAYS.THESIS.LOG LAST REVISION 8/6/96
!! WRITTEN BY ALEX LUEBKE
!!
!!*****
!!
!! TWO DIMENSIONAL SHELL MODAL ANALYSIS OF COMPOSITE GLAST TRAY
!! TRAY IS MODELED AS 8.3 MIL THICK CARBON WEAVE FACESHEETS ON BOTH SIDES
!! OF A 1/4" THICK NOMEX HONEYCOMB CORE (3/8" CELL).
!!
!! FOR TRAY WEIGHT OF 159 GRAMS
!! INCLUDING COMPOSITES, ONE LAYER DETECTORS, ETC.
!! SIMULATING TESTED CONDITION
!! FOR CLAMPED BOUNDARY CONDITION.
!! THE RESULTS SHOW THAT THE LOWEST NATURAL
!! FREQUENCY EXPERIENCED BY THE TRAY IS 947 HZ (2ND = 1847 HZ)
!! FOR SIMPLY SUPPOERTED BOUNDARY CONDITION.
!! THE RESULTS SHOW THAT THE LOWEST NATURAL
!! FREQUENCY EXPERIENCED BY THE TRAY IS 473 HZ (2ND = 1199 HZ)
!!
!! ADDING ANOTHER 67 GRAMS FOR ANOTHER LAYER OF DETECTORS
!! AND ANOTHER 192 G FOR THE CONVERTER LAYER (0.56*0.05*24.6^2*11.35)
!! GIVING A TOTAL MASS OF 418 GRAMS EVENLY SPREAD OVER THE TRAY :
!! FOR CLAMPED BOUNDARY CONDITION.
!! THE RESULTS SHOW THAT THE LOWEST NATURAL
!! FREQUENCY EXPERIENCED BY THE TRAY IS 584 HZ (2ND = 1138 HZ)
!! FOR SIMPLY SUPPOERTED BOUNDARY CONDITION.
!! UNDER 1 G ACCELERATION, THE RESULTS SHOW THAT THE LOWEST NATURAL
!! FREQUENCY EXPERIENCED BY THE TRAY IS 292 HZ (2ND = 739 HZ)
!!
!!*****
Z = 10                ! ACCELERATION FOR DEFLECTION ANALYSIS

/COM,ANSYS REVISION 5.2
/UNITS,SI            ! UNITS IN M,KG,SEC,N
/PREP7              ! PREPROCESSOR
/TITLE,1ST, 2ND NAT. FREQ. OF GLAST TRAY,FULL LOAD, S.S.
! /TITLE,X STRESS IN OUTER PLY OF GLAST TRAY, S.S., 10 G'S

!!!!!!!!!!!!!!!!!!!!!!!!!!!!!!!!!!!!!!!!!!!!!!!!!!!!!!!!!!!!!!!!!!!!!!!!!!!!!!!!!!!!!!!!!!!!!!!!!!!!!!!!!!!!!!!!!!!!!!!!!!!!!!!!
!! ANALYSIS TYPE AND MATERIAL PROPERTIES
!!!!!!!!!!!!!!!!!!!!!!!!!!!!!!!!!!!!!!!!!!!!!!!!!!!!!!!!!!!!!!!!!!!!!!!!!!!!!!!!!!!!!!!!!!!!!!!!!!!!!!!!!!!!!!!!!!!!!!!!!!!!!!!!

ET,1,SHELL99,,,,,1 ! TYPE 1, COMPOSITE TRAY MATERIAL
KEYOPT,1,2,0        ! ET,1 - KEYOPT(2)=0
R,1,3              ! REAL 1,THREE LAYERS
RMORE              ! SKIP 6
!! LAYER 1,3 AT 0 DEG 8.3 MIL'S THICK,LAYER 2,0 DEG 0.635 CM THICK (1/4" CORE)
RMORE,1,,2.1E-4,,6.35E-3
RMORE,1,,2.1E-4    ! MAT,THETA,THICK
```


APPENDIX B. ANSYS TRAY CODES

```
/COLOR,ELEM,RED,1,100    ! SETS COLR OF OUTPUT DISPLAY TO RED
/NUMBER,1                ! TURNS OFF ELEMENT NUMBERING

SET,,1                   ! PLOT FIRST, LOWEST NATURAL FREQUENCY
PLDISP,2

!SHELL,BOT              ! GET STRESS ON TOP FACESHEET
!PLNSOL,S,X

/PBC,U,0
/NOERASE
/WINDOW,1,OFF
/WINDOW,2,0.2,1,-1,-0.2
SET,,2                   ! GET SECOND LOWEST NATURAL FREQUENCY
/NOERASE
PLDISP,2                ! PLOT MODE W/ UNDEFORMED OUTLINE
/WINDOW,2,OFF
/WINDOW,1,ON             ! LEAVE IN THIS CONDITION FOR DISPLAY OPTIONS

!EOF
```

APPENDIX C. ANSYS TOWER CODES

APPENDIX C - ANSYS TOWER CODES

```
/BATCH,LIST
!! ANSYS 5.2 FINITE ELEMENT ANALYSIS
!! NATURAL FREQUENCY ANALYSIS FOR 4 WALL GLAST TOWER W/ TRAYS, CSI CALORIMETER
!! TOWER1.GEOM.LOG LAST REVISION 8/6/96
!! WRITTEN BY ALEX LUEBKE
!!
!!*****
!! TWO DIMENSIONAL SHELL MODAL ANALYSIS OF GLAST TOWER
!! FOUR BERYLLIUM WALLS ENCLOSE THE TOWER
!! 12 LOADED COMPOSITE TRAYS SPACED 3 CM APART ENCOMPASS THE TRACKER
!! CSI CALORIMETER MODELED AS SEVEN HORIZONTAL TRAYS EACH 3 CM THICK WITH
!! THE MECHANICAL PROPERTIES OF LEAD
!!
!! THE RESULTS SHOW THAT THE LOWEST NATURAL FREQUENCY EXPERIENCED BY
!! THE TOWER IS 604 HZ (2ND = 1217 HZ).
!!
!! UNDER A HORIZONTAL 10 G LOAD, THE DEFLECTION AT THE END OF THE TOWER
!! IS 13.6 MICRONS (0.136E-4 M)
!! AND THE MAXIMUM STRESS IS 10.4 MPA (0.104E8 - ELEM SOLUTION, SHELL,BOT)
!! TENSION AND COMPRESSION ON THE BOTTOM EDGES OF THE TOWER
!!
!!*****

/COM,ANSYS REVISION 5.2
/UNITS,SI ! UNITS IN M,KG,SEC,N
/FILENAME,towerfreq
/PREP7 ! PREPROCESSOR

!!!!!!!!!!!!!!!!!!!!!!!!!!!!!!!!!!!!!!!!!!!!!!!!!!!!!!!!!!!!!!!!!!!!!!!!!!!!!!!!!!!!
!! ANALYSIS TYPE AND MATERIAL PROPERTIES
!!!!!!!!!!!!!!!!!!!!!!!!!!!!!!!!!!!!!!!!!!!!!!!!!!!!!!!!!!!!!!!!!!!!!!!!!!!!!!!!!!!!

ET,1,SHELL99,,,,,,,,1 ! TYPE 1,ISOTROPIC WALL MATERIAL- USE SHELL
!! KEYOPT(2)=0->NL,LSYM,LP1,LP2,EFS,BLANK(7),MAT,THETA,TK,MAT2,THETA2,TK2,ETC
KEYOPT,1,2,0 ! ET,1 - KEYOPT(2)=0
R,1,1 ! REAL 1,ONE LAYER
RMORE ! SKIP 6
RMORE,1,,0.002 ! LAYER 1, 0 DEG, 2 MM THICK WALL

MP,EX,1,3.18E11 ! MAT 1,Be = 318 GPa ISOTROPIC MATERIAL
MP,EY,1,3.18E11
MP,EZ,1,3.18E11
MP,NUXY,1,0.02 ! Be POISSONS RATIO = 0.02
MP,GXY,1,1.56E11 ! Be RIGIDITY MODULUS G = 156 GPa
MP,DENS,1,1.848E3 ! Be DENSITY = 1.848 G/CM^3

ET,2,SHELL99,,,,,,,,1 ! TYPE 1, COMPOSITE TRAY MATERIAL
KEYOPT,2,2,0 ! ET,1 - KEYOPT(2)=0
R,2,3 ! REAL 1,THREE LAYERS
RMORE ! SKIP 6
!! LAYER 1,3 AT 0 DEG 8.3 MIL'S THICK,LAYER 2,0 DEG 0.635 CM THICK (1/4" CORE)
RMORE,2,,2.1E-4,3,,6.35E-3
```


APPENDIX C. ANSYS TOWER CODES

```

K,20,0,CSIH+TRAKH,BASE

K,21,0,CSIH,0           ! KEYPOINTS DEFINING BOUNDARY OF CSI TRAY
K,22,BASE,CSIH,0
K,23,BASE,CSIH,BASE
K,24,0,CSIH,BASE

L,1,2                   ! LINES BETWEEN KEYPOINTS IN CSI
L,2,3
L,3,4
L,4,1
L,1,5
L,5,6
L,6,2
L,5,8
L,6,7
L,7,8
L,4,8
L,3,7

ADD=8
L,1+ADD,2+ADD          ! LINES BETWEEN KEYPOINTS IN TRACKER
L,2+ADD,3+ADD
L,3+ADD,4+ADD
L,4+ADD,1+ADD
L,1+ADD,5+ADD
L,5+ADD,6+ADD
L,6+ADD,2+ADD
L,5+ADD,8+ADD
L,6+ADD,7+ADD
L,7+ADD,8+ADD
L,4+ADD,8+ADD
L,3+ADD,7+ADD

L,17,18                ! DEFINE LINES FOR TRAY
L,18,19
L,19,20
L,20,17

MORE = 4
L,17+MORE,18+MORE     ! DEFINE LINES FOR CSI TRAYS
L,18+MORE,19+MORE
L,19+MORE,20+MORE
L,20+MORE,17+MORE

!!*****
!! MATCHES NUMBER OF CSI TRAYS
VNUM = 7               !DEFINE NUMBER OF VERTICAL ELEMENTS ALONG CSI WALL
!!*****
VTRAK = 13            !DEFINE NUMBER OF VERTICAL ELEMENTS ALONG TRACKER WALL
HNUM = 4              !DEFINE NUMBER OF HORIZONTAL ELEMENTS ALONG WHOLE WALL
!!*****

LESIZE,1,,VNUM        ! BREAK APART LINES FOR CSI
LESIZE,2,,HNUM
LESIZE,3,,VNUM
LESIZE,4,,HNUM
LESIZE,5,,HNUM
LESIZE,6,,VNUM
LESIZE,7,,HNUM
LESIZE,8,,HNUM
LESIZE,9,,HNUM
LESIZE,10,,VNUM
LESIZE,11,,HNUM
LESIZE,12,,HNUM

ADD2 = 12
LESIZE,1+ADD2,,VTRAK ! BREAK APART LINES IN TRACKER

```

APPENDIX C. ANSYS TOWER CODES

```

LESIZE,2+ADD2,,,HNUM
LESIZE,3+ADD2,,,VTRAK
LESIZE,4+ADD2,,,HNUM
LESIZE,5+ADD2,,,HNUM
LESIZE,6+ADD2,,,VTRAK
LESIZE,7+ADD2,,,HNUM
LESIZE,8+ADD2,,,HNUM
LESIZE,9+ADD2,,,HNUM
LESIZE,10+ADD2,,,VTRAK
LESIZE,11+ADD2,,,HNUM
LESIZE,12+ADD2,,,HNUM

LESIZE,1+ADD2+ADD2,,,HNUM      ! BREAK APART LINES FOR TRAY
LESIZE,2+ADD2+ADD2,,,HNUM
LESIZE,3+ADD2+ADD2,,,HNUM
LESIZE,4+ADD2+ADD2,,,HNUM

LESIZE,1+ADD2+ADD2+MORE,,,HNUM    ! BREAK APART LINES FOR CSI TRAY
LESIZE,2+ADD2+ADD2+MORE,,,HNUM
LESIZE,3+ADD2+ADD2+MORE,,,HNUM
LESIZE,4+ADD2+ADD2+MORE,,,HNUM

TYPE,2                          ! GENERATE TRAYS SHOULD BE COMPOSITE OF 2&3
REAL,2

PLUS1 = 0
!! GENERATE AN AREA OUT OF LINES FOR TRAY
A,1+ADD+ADD,2+ADD+ADD,3+ADD+ADD,4+ADD+ADD
AMESH,1+PLUS1

!! DUPLICATE TRAYS DOWNWARD TO MAKE TOTAL OF 12 TRAYS 3 CM APART
NSEL,S,LOC,Y,CSIH+TRAKH
ESEL,S,TYPE,,2
NGEN,VTRAK,1000,ALL,,,0,-DIST,0 ! 12 TRAYS
EGEN,VTRAK,1000,ALL

TYPE,4                          ! GENERATE CSI TRAYS
REAL,4
MAT,4
PLUS1 = 1
!! GENERATE AN AREA OUT OF LINES FOR CSI TRAY
A,1+ADD+ADD+MORE,2+ADD+ADD+MORE,3+ADD+ADD+MORE,4+ADD+ADD+MORE
AMESH,1+PLUS1

!! DUPLICATE TRAYS DOWNWARD TO MAKE TOTAL OF 7 CSI TRAYS 3 CM APART
ESEL,S,TYPE,,4

!!*****
NGEN,VNUM,1000,ALL,,,0,-DIST,0
EGEN,VNUM,1000,ALL
!!*****

TYPE,1                          ! GENERATE TOWER WALLS
REAL,1
MAT,1
PLUS2 = PLUS1+1
A,1,2,3,4      ! GENERATE AN AREA OUT OF LINES FOR CSI WALLS
AMESH,1+PLUS2      ! MESH CSI WALL 1
A,1,2,6,5
AMESH,2+PLUS2      ! MESH CSI WALL 2
A,5,6,7,8
AMESH,3+PLUS2      ! MESH CSI WALL 3
A,8,7,3,4
AMESH,4+PLUS2      ! MESH CSI WALL 4

ADD3 = 4
!! GENERATE AN AREA OUT OF LINES ON TRACKER WALLS
A,1+ADD,2+ADD,3+ADD,4+ADD

```


APPENDIX C. ANSYS TOWER CODES

```
/POST1                ! POSTPROCESSING PHASE
/AUTO
/NSSEL,S,LOC,X,BASE
/NSSEL,A,LOC,Z,BASE
/NSSEL,A,LOC,Y,CSIH+TRAKH
/ESLN,1
/PBC,U,1

/ERASE
/PNUM,ELEM,1
/COLOR,ELEM,RED,1,640 ! SETS COLR OF OUTPUT DISPLAY
/NUMBER,1             ! TURNS OFF ELEMENT NUMBERING
/VIEW,1,0,0,1
/VIEW,2,1,1,1
/WINDOW,1,LEFT
/WINDOW,2,RIGHT

/WINDOW,ALL,OFF

/WINDOW,1,ON
SET,,1                ! GET FIRST NATURAL FREQUENCY SIDE VIEW
/DSCALE,,0.2          ! 20% DEFLECTION RATIO
PLDISP,2              ! PLOT MODE W/ UNDEFORMED OUTLINE
/WINDOW,1,OFF

/WINDOW,2,ON
/NOERASE

SET,,1                ! GET FIRST NATURAL FREQUENCY
/DSCALE,,0.2          ! 20% DEFLECTION RATIO

PLDISP,2              ! PLOT MODE W/ UNDEFORMED OUTLINE

/WINDOW,2,OFF

/WINDOW,ALL,ON
/ERASE

!! DISPLAY OUTPUT AS NEEDED, SET,LIST FOR NATURAL FRQUENCIES
```

APPENDIX D. ANSYS THERMAL AND RADIATION GRID CODES

APPENDIX D - ANSYS THERMAL AND RADIATION GRID CODES

```
/BATCH,LIST
!! GRID13.THERM.LOG LAST REVISION 8/6/96 IN SLAC ANSYS
!! RUN THIS CODE AFTER GRID12.GEOM.LOG
!! WRITTEN BY ALEX LUEBKE AND CHAD JENNINGS

!!*****
!!
!! FOR A 1 CM THICK, 25 CM TALL STRUCTURAL/THERMAL ALUMINUM GRID (196 KG)
!! DISSIPATING 645 W OF ENERGY TO DEEP SPACE THROUGH
!! 3.36 M^2 OF RADIATOR AREA (0.6 METER TALL, 80% PACKING FACTOR)
!! AROUND GLAST GIVES A TEMPERATURE DIFFERENCE ACROSS THE GRID AS
!! 28 DEG C (-23.5 C TO 4.6 C)
!! AND FOR A 12.8 DEC C TEMPERATURE RISE ALONG TOWER WALL GIVES
!! THE MAXIMUM TEMPERATURE (AT TOP OF TOWER) IN GLAST AS
!! 17.4 DEG C
!! AND A MINIMUM TEMPERATURE AT TOP OF TOWER AS
!! -10.7 C
!!
!!*****

!!!!!!!!!!!!!!!!!!!!!!!!!!!!!!!!!!!!!!!!!!!!!!!!!!!!!!!!!!!!!!!!!!!!!!!!!!!!
!! THERMAL ANALYSIS SECTION
!!!!!!!!!!!!!!!!!!!!!!!!!!!!!!!!!!!!!!!!!!!!!!!!!!!!!!!!!!!!!!!!!!!!!!!!!!!!

!! HEAT INPUT TO GRID IS FROM
!! 300 MICRO WATTS PER CHANNEL FOR
!! 249 CHANNELS PER STRING OF DETECTORS WITH
!! 8 DETECTORS PER TRAY AND
!! 12 TRAYS PER TOWER AND
!! 49 TOWERS IN GLAST
!! WITH A CALORIMETER IN EACH TOWER GENERATING
!! 5 WATTS OF POWER AND EACH TOWER COMPUTER GENERATING
!! 1 WATT OF POWER GIVES A TOTAL HEAT INPUT TO THE GRID AS
!! 645 WATTS
!!

/PREP7                ! PREPROCESSOR PREP7
/TITLE,THERMAL ANALYSIS OF GLAST STRUCTURAL GRID

MORE = 2
!! THERMAL ELEMENT 3 - COVERPLATE FOR HEATINPUT TO GRID
ET,1+MORE,SHELL57      ! TYPE 3,THERMAL COVER MATERIAL- USE SHELL57
R,1+MORE,GRIDRIB       ! REAL 3, ANY THICKNESS
MP,DENS,1+MORE,0       ! NO MASS
MP,KXX,1+MORE,200     ! K ~ INFINITE

!! THERMAL ELEMENT 4 - COVERPLATE FOR HEATINPUT TO GRID
ET,2+MORE,SHELL57      ! TYPE 4,THERMAL COVER MATERIAL- USE SHELL57
R,2+MORE,GRIDRIB       ! REAL 4, ANY THICKNESS
MP,DENS,2+MORE,0       ! NO MASS
```


APPENDIX D. ANSYS THERMAL AND RADIATION GRID CODES

```

ESEL,S,TYPE,,4          ! DUPLICATE FULL Y WALL IN X
NGEN,8,10000,ALL,,,HOR,0,0
EGEN,8,10000,ALL

ESEL,ALL                ! MERGE ALL NODES, ELEMENTS AND KEYPOINTS
NSEL,ALL
NUMMRG,NODE
NUMMRG,ELEM
NUMMRG,KP
NUMCMP,NODE
NUMCMP,ELEM
NUMCMP,KP
FINISH

NSEL,ALL
/VIEW,1,-1,1,1
EPLT
FINISH

!!!!!!!!!!!!!!!!!!!!!!!!!!!!!!!!!!!!!!!!!!!!!!!!!!!!!!!!!!!!!!!!!!!!!!!!!!!!!!!!!!!!!!!!!!!!!!!!!!!!!!!!!!!!!!!!!!!!!!!!
!! SOLUTION PHASE
!!!!!!!!!!!!!!!!!!!!!!!!!!!!!!!!!!!!!!!!!!!!!!!!!!!!!!!!!!!!!!!!!!!!!!!!!!!!!!!!!!!!!!!!!!!!!!!!!!!!!!!!!!!!!!!!!!!!!!!!

/SOLU

!! GENERATE HEAT INPUT FROM WALLS
!! POWER GENERATED/TRAY = 300E-6*249*8 = 0.6 WATTS
!! POWER FROM CALORIMETER/TOWER = 5 WATTS
!! POWER/TOWER = 0.6*12 + 5 = 12.2 WATTS
!! 49 TOWER = 597.8 WATTS ~ 600 WATTS FROM PREAMPS
!! CALORIMETER INPUT PER TOWER = 5 WATTS
!! COMPUTER INPUT PER TOWER = 1 WATT
!! FOR TOTAL POWER INPUT AS 645 WATTS
!! HEAT INPUT INTO HEAT ELEMENT OF AREA 8*2*7*HOR*0.01 = 0.28 M^2
!! FLUX = 645/0.28 = 2304 W/M^2 (HEAT)

WATTS = 3.0E-4          ! POWER/CHANNEL (W)
CHAN = 249              ! CHANNELS/STRING
STRING = 8              ! NUMBER OF STRINGS
TRAYP = WATTS*CHAN*STRING ! POWER/TRAY
TRAYS = 12             ! NUMBER OF TRAYS
TRACKP = TRAYS*TRAYP   ! POWER IN TRACKER SECTION
CALP = 6               ! WATTS/TOWER IN CALORIMETER
TOWERP = TRACKP+CALP   ! POWER/TOWER
NUMSIDE = 7            ! NUMBER OF TOWERS ON SIDE
NUMTOWER = NUMSIDE*NUMSIDE ! NUMBER OF TOWERS IN INSTRUMENT
BUS = 0                ! WATTS FROM BUS TO GRID
TOTAL = NUMTOWER*TOWERP + BUS ! TOTAL HEAT INPUT INTO GRID
HEAT = TOTAL/(16*7*0.01*HOR) ! HEAT FLUX INPUT

ALLSEL
ESEL,S,TYPE,,3
ESEL,A,TYPE,,4
NSLE,S
SFE,ALL,1,HFLUX,,HEAT
ALLSEL

FINISH

/EOF

/BATCH,LIST
!! GRID13.RAD.LOG RUN AFTER GRID12.GEOM.LOG AND GRID13.THERM.LOG
!! LAST REVISION 8/6/96 IN SLAC ANSYS
!! WRITTEN BY ALEX LUEBKE

!! MODEL FOR RADIATION TO FREE SPACE
!! NO HEAT INPUT FROM ANY SOURCES

```


APPENDIX D. ANSYS THERMAL AND RADIATION GRID CODES

```

/REP7
!! DEFINE DIFFERENCE BETWEEN CELCIUS AND KELVIN
!! WE WORK IN CELCIUS BUT RADIATION REQUIRES AN ABSOLUTE KELVIN
TOFFST,273

*DO,I,0,VNUM

      N,(I+1)*2001,-HOR,I*VERTH/VNUM,-HOR
      N,(I+1)*2002,-HOR,I*VERTH/VNUM,(NUMSIDE+1)*HOR
      N,(I+1)*2044,(NUMSIDE+1)*HOR,I*VERTH/VNUM,(NUMSIDE+1)*HOR
      N,(I+1)*2086,(NUMSIDE+1)*HOR,I*VERTH/VNUM,-HOR

      FILL,(I+1)*2001,(I+1)*2002,(NUMSIDE+2)*HNUM-1,(I+1)*2003,1
      FILL,(I+1)*2002,(I+1)*2044,(NUMSIDE+2)*HNUM-1,(I+1)*2045,1
      FILL,(I+1)*2044,(I+1)*2086,(NUMSIDE+2)*HNUM-1,(I+1)*2087,1
      FILL,(I+1)*2086,(I+1)*2001,(NUMSIDE+2)*HNUM-1,(I+1)*2128,1

*ENDDO

! RADIATION LINKS
SBC = 5.67E-8      ! STEFAN-BOLTZMANN CONSTANT = 5.67E-8 W/(M^2*K^4)
FORM = 1 ! AREA FORM FACTOR = 1
EMIS = 0.8        ! RADIATOR EMISSIVITY - 0.8
PACK = 0.8        ! PACKING FACTOR FOR RADIATORS
HI = 0.6 ! METERS HIGH OF RADIATOR AROUND GLAST

!! RADIATION AREA FACTOR FOR EMISSION SURFACE TO BE AT 0 DEG C
P = 0.04167*HI*PACK      ! FOR 168 SPACE NODES GIVES 1 M DEEP RADIATOR
H = 1                    ! EXTRA AREA SCALING FACTOR

ET,5,LINK31      ! RADIATION LINK
TYPE,5
REAL,5

ESEL,NONE
NSEL,S,LOC,X,7*HOR,8*HOR
NSEL,A,LOC,Z,-HOR,0
NSEL,A,LOC,Z,7*HOR,8*HOR
NSEL,A,LOC,X,-HOR,0
NSEL,U,LOC,Y,0.001,2*VERTH

! AREA,FORM FACTOR,EMISSIVITY,SBC
R,5,P*H,FORM,EMIS,SBC

!! GENERATE ELEMENTS
T = 0
      E,2001,1

      E,362+(T),2005+(2003*T)
      E,46+(T),2006+(2003*T)
      E,365+(T),2007+(2003*T)
      E,91+(T),2008+(2003*T)
      E,368+(T),2009+(2003*T)
      E,136+(T),2010+(2003*T)
      E,371+(T),2011+(2003*T)
      E,181+(T),2012+(2003*T)
      E,374+(T),2013+(2003*T)
      E,226+(T),2014+(2003*T)
      E,377+(T),2015+(2003*T)
      E,271+(T),2016+(2003*T)
      E,380+(T),2017+(2003*T)

E,2044,357
E,2086,42
E,2002,316

E,527,2089

```

APPENDIX D. ANSYS THERMAL AND RADIATION GRID CODES

E,312,2090
E,524,2091
E,267,2092
E,521,2093
E,222,2094
E,518,2095
E,177,2096
E,515,2097
E,132,2098
E,512,2099
E,87,2100
E,509,2101

E,44,2130
E,36,2131
E,38,2132
E,30,2133
E,32,2134
E,24,2135
E,26,2136
E,18,2137
E,20,2138
E,12,2139
E,14,2140
E,6,2141
E,8,2142

E,323,2047
E,321,2048
E,329,2049
E,327,2050
E,335,2051
E,333,2052
E,341,2053
E,339,2054
E,347,2055
E,345,2056
E,353,2057
E,351,2058
E,359,2059

ESEL,S,TYPE,,5 ! SELECT ELEMENTS TO DUPLICATE
NSLE,ALL

NGEN,3,10000,ALL,,,0,VERTH/2,0 ! DUPLICATE SPACE NODES
EGEN,3,10000,ALL ! DUPLICATES RADIATION LINKS

NSEL,S,LOC,X,-HOR
NSEL,A,LOC,X,8*HOR
NSEL,A,LOC,Z,-HOR
NSEL,A,LOC,Z,8*HOR
ESEL,S,TYPE,,5
NSLE,U

NDEL,ALL

NSEL,ALL
NUMMRG,NODE
NUMCMP,NODE

FINISH

/SOLU
NEQIT,40

!OUTPR,ALL,1
!OUTPR,VENG,NONE

APPENDIX E - MATLAB THERMAL CODE FOR WALL

```

% START OF CODE
% One dimensional MATLAB thermal analysis for GLAST wall
% Updated 7/23/96 - Match conditions in ANSYS code for comparison
% Written by Alex Luebke
% Thermal13.m in Thesis Thermal
clear;clc
disp('7/23/96, thermal13.m, A. Luebke');
%
% System:
% Three Beryllium walls 2 mm thick 60 cm tall and 25 cm wide to
% conduct heat from 12 trays at nearly 0.6 watts per tray.
%
%*****
% ASSUMPTIONS
%*****
% 1) Steady state conduction
% 2) One dimensional conduction
% 3) Isothermal preamp chip
% 4) Constant properties at all temperatures/conditions
% 5) Radiation to deep space at zero degrees Kelvin (0 K)
% 6) 0.5 cm distance from chip to wall (conduction distance)
% 7) Contact resistance is through DC 340 grease at 100 kN/m^2 pressure
% (C x 228 for safety!) gives 0.5 C temp rise across contacts.
% 8) Five cm conduction panel at base of towers to pipe heat to radiators
% 9) 30% increase in heat for end of life
%
%-----
% MATERIAL PROPERTIES
%-----
% k = thermal conductivity (Watts/cm/deg celcius)
% Baseline is Be
k = 2.18;           % Be W/cm/C
rho = 1.9e-3;      % rho = density of Be (kg/cm^3)

disp(['Material is Be, k = ' num2str(k) ' W/cm/C'])

%*****
% CONTACT PROPERTIES
%*****
% Aluminum/Aluminum with Dow Corning 340 grease ~ 100 KN/m2 pressure
% = 0.07 cm^2 C/W
% APPROXIMATE VALUE! q = kA dt/dx, dx/k = C = A dt/q, dt = C q/A, 0.07x228 = 16
% Use 16 to get 1.27 deg C temp rise across contact to match FEM

Contact = 12      ;           % cm^2 deg C/Watt
% APPROXIMATE VALUE!

disp(['Contact resistance is = ' num2str(Contact) ' cm^2 deg C/Watt']);

%*****
% GEOMETRY

```

APPENDIX E. MATLAB THERMAL CODE FOR WALL

```

#####
ThickWall = 0.2;           % thickness of tower wall material (cm)
LengthWall = 25;          % length of tower wall (cm)
HeightWall = 60;          % height of tower wall (cm)
OneWallArea = ThickWall*LengthWall;
% minimum vertical conductive area in single wall in (cm^2)
TwoWallArea = 2*OneWallArea;   % conductive area for two walls (cm^2)
ThreeWallArea = 3*OneWallArea; % conductive area for three walls (cm^2)
FourWallArea = 4*OneWallArea;  % conductive area for four walls (cm^2)
ThickTray = 0.25*2.54;         % thickness of tray 1/4" (honeycomb) (cm)
BetweenTrays = 3;             % vertical distance between preamps (cm)
TraysTower = 12;              % number of trays/tower
Htrack = TraysTower*BetweenTrays; % height of tracker section (cm)
HCsl = HeightWall-Htrack;      % height of Csl section (cm)
NumWallsTower = 4;            % number of walls/tower for weight
NumTowersSide = 7;            % grid size of towers in GLAST
NumTowersTotal = NumTowersSide^2; % total # towers in (square) GLAST
WeightWalls = NumTowersTotal*NumWallsTower*HeightWall*OneWallArea*rho;
% weight of wall material (kg)
MaxNumTowers = 4;
% number of towers heat has to travel along to get to radiator
MaxDist = MaxNumTowers*LengthWall;
% d = worst distance from tower to radiator (cm)

disp(['Thickness of wall is ' num2str(ThickWall) ' cm']);
disp(['Height of tower wall is = ' num2str(HeightWall) ' cm']);
disp(['Weight of all walls = ' num2str(WeightWalls) ' kg']);
%disp(['Temperature measured at ' num2str(MaxDist) ' cm from radiator']);

%%%%%%%%%%
% THERMAL RESISTANCES
RBetweenChips = BetweenTrays/(ThreeWallArea*k);
% thermal resistance of wall between chips (C/W)
Chip2Wall = 0.5; % distance from chip to wall through material (cm)
RChip2Wall = Chip2Wall/(ThreeWallArea*k);
% thermal resistance of metal from chip to wall (C/W)
% ASSUMPTION!
BaseArea = 71; % cm^2, 5 cm thick bottom conduction panel (5*175*4/49 = 71)
RTowerRadiator = MaxDist/(BaseArea*k);
% worst thermal resistance of metal from tower to radiator (C/W)
% ASSUMPTION!

%=====
% POWER
%=====
WattsChannel = 300e-6; % #Watts/channel
EOL = 1.3; % 30% increase in power at end of life
TrayPower = WattsChannel*249*4*2*EOL; % power generated/tray (Watts)
% #microWatts/channel*249 channels/string*4 strings/layer*2 layers
TowerPower = TrayPower*TraysTower; % #watts/tower
TotalPower = NumTowersTotal*TowerPower;
% total power generated by preamps in GLAST (Watts)

disp(['Watts/channel = ' num2str(WattsChannel*1e6) ' micro-watts']);
disp(['Watts/tower = ' num2str(TowerPower) ' watts']);
disp(['Total power from preamps in GLAST = ' num2str(TotalPower) ' watts']);

%-----
% RADIATOR TEMPERATURE
%-----
% ASSUMPTION!
TRadiator = 273;% temperature of radiation surface on spacecraft (deg K)
% ASSUMPTION!

%+++++
% ANALYSIS SECTION
%+++++

```

APPENDIX E. MATLAB THERMAL CODE FOR WALL

```

% NOTES
% Transient heat transfer analysis - thermal circuit method
%  $Q=k*A*dt/dx=k*A*Vo/y=Vo/$ Thermal resistance= $Vo/R$ ,  $R=y/(k*A)$ 
%  $Vo=I*R$ ,  $I=Vo/R$ ,  $q=V/R$ :  $Vo$  corresponds to temperature difference
% Temperature drop across thermal resistance equiv. to  $q$ 
%  $Vo=I*R \rightarrow dt=Q*R=T1-T2$ ,  $T1=T2+Q*R$ 
% Add resistance from Q to wall = + Ra+C
% Design: trays connected to continuous wall
% Define wall temperature = T(101) + (deg celcius)
% Worst case temperature from middle tower to radiator surface
% Heat is transferred down three walls = ThreeWallArea
% Radiators at 0 Celcius

% Tbase = temperature rise along baseplate (deg C)
%Tbase=(TRadiator-273)+TowerPower*
%(Contact/(ThreeWallArea)+RTowerRadiator+Contact/BaseArea);
Tbase = 0; % bypass grid analysis, base of tower forced to 0 deg C
TCsl = TowerPower*(HCsl-BetweenTrays)/(k*ThreeWallArea);
% temp rise along Csl section of wall (deg C)

T(TraysTower+101) = Tbase+TowerPower*(HCsl/(k*ThreeWallArea));
% temp at base of tracker

    for i=TraysTower:-1:1;
        T(i+100) = T(i+101)+i*TrayPower*RBetweenChips;
            % Resistance between trays on wall
    T(i)=T(i+100)+TrayPower*(Contact/(ThreeWallArea)+RChip2Wall+Contact/(ThreeWallArea));
        % Change in temp. = Told+Q*Rtot
    end

TrakTempRise = T(1)-TCsl-Tbase;           % = Max temp rise in tracker

%%%%%%%%%%%%%%%%%%%%%%%%%%%%%%%%%%%%%%%%%%%%%%%%%%%%%%%%%%%%%%%%%%%%%%%%
% PRINT TEMPERATURES
%%%%%%%%%%%%%%%%%%%%%%%%%%%%%%%%%%%%%%%%%%%%%%%%%%%%%%%%%%%%%%%%%%%%%%%%
disp(' ');
disp('Temp in tracker(top down) Temp of preamp chips (top Down)');
disp('-----');
    for i=1:TraysTower;
        str1=['Twall(' num2str(i+100) ') = ' num2str(T(i+100)) ];
        str2=[' deg C, Tchip(' num2str(i) ') = ' num2str(T(i)) ' deg C'];
        disp([str1 str2]);
    end

disp(' ');
%disp(['Temp rise along from radiator to base of tower = ' num2str(Tbase) ' deg C']);
disp(['Temp rise along Csl section of wall = ' num2str(TCsl) ' deg C']);
disp(['Temp rise (Max) to farthest chip in tracker ' num2str(TrakTempRise) ' deg C']);
disp(['Max temperature in GLAST tower = ' num2str(T(1)) ' deg C']);
disp('NOTE: this is for conduction down an average of three walls');

%-----
% RADIATION CONSTANTS
%-----
% Stefan-Boltzmann Constant for Radiation
sigma=5.670e-12; % sigma = watts/cm^2/deg K

% Sample radiator material - Aluminized teflon 10.0 mil type A -
% Teflon x vacuum deposited on aluminum (6403800 Sheldahl)
% alpha = 0.1, epsilon = 0.85 use alpha = 0.1, epsilon = .8
alpha = 0.1; % alpha <= 0.1 (absorptivity), 1.0 = perfect blackbody
epsilon = 0.8; % e >=0.8 (emissivity), 1.0 = perfect blackbody
TSpace = 3; % temperature of free space radiation "surface" (3 deg K)

% Power dissipated by one wall = q = epsilon*RadArea*sigma*TRadiator^4,
% (TRadiator in deg K)
RadArea = TotalPower/(epsilon*sigma*TRadiator^4);
% total radiation surface area (cm^2)

```

APPENDIX E. MATLAB THERMAL CODE FOR WALL

```
Circumference = NumTowersSide*LengthWall*4;
% circumferential distance around GLAST
HRadSurf = RadArea/Circumference;
% vertical height of radiation surface

disp(' ');
%disp(['ASSUMTION, temperature of radiative surface is
%' num2str(TRadiator-273) ' deg C']);
%disp(['Total radiative area = ' num2str(RadArea/1e04) ' m^2']);
%disp(['Height of radiator surfaces around GLAST = ' num2str(HRadSurf) ' cm']);

% END OF CODE
```

APPENDIX F. ANSYS THERMAL WALL FEM

APPENDIX F - ANSYS THERMAL WALL FEM

```
/BATCH,LIST
!! ANSYS 5.2 FINITE ELEMENT ANALYSIS
!! THERMAL ANALYSIS OF STEADY STATE TEMPERATURES DOWN GLAST WALL
!! WALLTEMP5.THESIS.LOG
!! LAST REVISION 7/10/96 - COMMENTS UPDATED

!!*****
!! TWO DIMENSIONAL GLAST THERMAL WALL WITH HEAT INPUT FROM 12 TRAYS,
!! INCLUDING CONTACT RESITANCES.
!! HEAT COMES FROM THE AMPLIFICATION OF 249 CHANNELS FROM 8 SILICON
!! STRIP DETECTORS EACH GENERATING 300 MICRO-WATTS OF POWER
!! INCREASING BY 30% AT END OF LIFE.
!! THE 3 WALLS ARE 2 MM THICK AND 60 CM TALL BERYLLIUM WITH 12 HEAT INPUTS
!! SPACED APART BY 3 CM.
!! THE RESULTS SHOW THAT THE MAXIMUM TEMPERATURE RISE ALONG THE TOWER
!! IS 12.8 DEG C.
!!*****

/UNITS,SI ! UNITS IN METERS, C, WATTS
/COM,ANSYS REVISION 5.2
/PREP7 ! PREPROCESSOR
/TITLE,CONDUCTION ANALYSIS OF GLAST WALL

!!!!!!!!!!!!!!!!!!!!!!!!!!!!!!!!!!!!!!!!!!!!!!!!!!!!!!!!!!!!!!!!!!!!!!!!!!!!!!
!! GENERATE GLAST WALL CONDUCTION GEOMETRIC MODEL WITH CONTACT ELEMENTS
!!!!!!!!!!!!!!!!!!!!!!!!!!!!!!!!!!!!!!!!!!!!!!!!!!!!!!!!!!!!!!!!!!!!!!!!!!!!!!

ET,1,PLANE55 ! THERMAL ELEMENT FOR WALLS
MP,KXX,1,2.18E2 ! BE THERMAL CONDUCTIVITY, K = 2.18 W/CM(C)

ET,2,PLANE55 ! CONTACT RESISTANCE ELEMENTS
MP,KXX,2,0.5 ! 1.27 DEG TEMPERATURE RISE ACROSS EACH CONTACT

Y = 0.01 ! ADD ONE CM OF HEIGHT TO WALL FOR THERMAL CONTACT
K,1,0,0.20+Y ! INPUT KEYPOINTS THAT DEFINE GEOMETRY
K,2,0,0.23+Y
K,3,0.002,0.23+Y
K,4,0.002,0.224+Y
K,5,0.002,0.20+Y
K,6,0.004,0.23+Y
K,7,0.01035,0.23+Y
K,8,0.004,0.232+Y
K,9,0.01035,0.232+Y
K,10,0.01035,0.224+Y
K,11,0.004,0.224+Y
K,12,0.002,0.002+Y
K,13,0,0.002+Y
K,14,0,0
K,15,0.002,0

L,1,2 !DRAW LINES BETWEEN THE KEYPOINTS TO DRAW OUTLINES
L,2,3
L,3,4
```


APPENDIX F. ANSYS THERMAL WALL FEM

```
L,4,5
!! LINE 5
L,5,1
L,3,6
L,6,11
L,11,4
L,6,7
!! LINE 10
L,7,10
L,10,11
L,6,8
L,8,9
L,9,7
!!LINE 15
L,5,12
L,12,13
L,1,13
L,13,14
L,14,15
L,15,12
```

```
ENUM = 5                                !DEFINE NUMBER OF ELEMENTS
```

```
WIDTH = 1
```

```
CSI = 33
```

```
!BREAK UP LINES TO DEFINE SECTIONS
```

```
LESIZE,1,,,ENUM
```

```
LESIZE,2,,,WIDTH
```

```
LESIZE,3,,,WIDTH
```

```
LESIZE,4,,,ENUM-WIDTH
```

```
LESIZE,5,,,WIDTH
```

```
LESIZE,6,,,1
```

```
LESIZE,7,,,WIDTH
```

```
LESIZE,8,,,1
```

```
LESIZE,9,,,WIDTH
```

```
LESIZE,10,,,WIDTH
```

```
LESIZE,11,,,WIDTH
```

```
LESIZE,12,,,1
```

```
LESIZE,13,,,WIDTH
```

```
LESIZE,14,,,1
```

```
LESIZE,15,,,CSI
```

```
LESIZE,16,,,WIDTH
```

```
LESIZE,17,,,CSI
```

```
LESIZE,18,,,WIDTH
```

```
LESIZE,19,,,WIDTH
```

```
LESIZE,20,,,WIDTH
```

```
!! AREA 1
```

```
A,1,2,3,4,5
```

```
!! AREA 2
```

```
A,4,3,6,11
```

```
!! AREA 3
```

```
A,6,7,10,11
```

```
!! AREA 4
```

```
A,6,8,9,7
```

```
!! AREA 6
```

```
A,5,12,13,1
```

```
!! AREA 7
```

```
A,12,13,14,15
```

```
TYPE,1
```

```
! GENERATE TRACKER SECTION
```

```
REAL,1
```

```
MAT,1
```

```
AMESH,1
```

```
AMESH,3
```

```
TYPE,2
```

```
REAL,2
```

```
MAT,2
```

```
AMESH,2
```


APPENDIX F. ANSYS THERMAL WALL FEM

FINISH

```
/POST1                ! POST-PROCESSING OF OUTPUT
/AUTO
SET
NSEL,ALL
/PBC,TEMP,1
/PSF,HFLUX,,1
/ERASE

/WINDOW,1,LEFT        ! MAKE 3 OUTPUT WINDOWS
/WINDOW,2,RTOP
/WINDOW,3,RBOT

!/TRIAD,OFF           ! TURNS OFF X,Y TRIAD
!/PLOPTS,FRAME,OFF   ! TURN ON WINDOW FRAMES
!/PLOPTS,INFO,ON

/WINDOW,ALL,OFF

/WINDOW,1,ON
/NOERASE
PLNSOL,TEMP           ! DISPLAY CONTOUR PLOT OF TEMPERATURES ON WALL
/WINDOW,1,OFF

/WINDOW,2,ON
/NOERASE
EPLLOT                ! SHOWS MODEL DETAILS
/WINDOW,2,OFF

/WINDOW,3,ON
/NOERASE
PLNSOL,TEMP           ! DISPLAY CONTOUR PLOT OF TEMPERATURES ALONG CSI
/WINDOW,3,OFF

!/PLOPTS,FRAME,ON
!/PLOPTS,INFO,OFF

!/PLOPTS,LEG3,ON

!/NOERASE
!/WINDOW,ALL,ON

!/ZOOM
!/NOERASE
!/PLNSOL,TEMP
!/WINDOW,ALL,OF
!/WINDOW,1,ON
!/NOERASE
!/ZOOM
!/PLNSOL,TEMP
!/WINDOW,1,OFF

/PPRSOL              ! FOR 1 M DEEP WALL TOTAL ENERGY = 0.8*1.3*12 = 12.48 W
```

APPENDIX G - IDL CODE FOR ON ORBIT TEMPERATURES

```
pro glast
; IDL analysis
; On orbit thermal analysis for GLAST
; Adapted from analysis in "Space Mission Analysis and Design,
; Wertz and Larson, Microcosm, Inc, Torrance Ca and Kluwer Academic Publishers
; Second edition, 1995 pgs 420-424
; 80 % packing factor for radiator second surface mirrors
; 600 km orbit, variable radiator height and power generation
; Full sun or no sun capabilities
; Written by Jeff Tobin (Lockheed-Martin) and Alex Luebke
;*****
;
;
; Results
;
; No sun, 645 watts power generated (corresponding to grid transfer only)
; 0.6 meter high radiator no eol compensation, 80% packing factor, 3.36 m^2
; no IR from earth, coldest condition - to match ANSYS code
; Temperature : -20.2 deg C
;
; Full sun, 645 watts power generated (corresponding to grid transfer only)
; 0.6 meter high radiator eol (10%) compensation included, 80% packing factor
; IR from earth included, expected hot condition for just grid
; Temperature range: -10, +20 deg C
;
; No sun, 1000 watts power generated (for full satellite)
; 1 meter high radiator eol compensation (absorptivity does not matter)
; included, 80% packing factor
; IR from earth, expected cold condition for full satellite
; Temperature range: -17, -1 deg C
;
; Full sun, 1000 watts power generated (for full satellite)
; 1 meter high radiator eol compensation (absorptivity = 0.1)
; included, 80% packing factor
; IR from earth, expected hot condition for full satellite
; Temperature range: -14, +15.5 deg C
; (for 1.5 meter radiator, -40, 0 deg C)
;
; Full sun, 1000 watts power generated (for full satellite)
; 1 meter high radiator eol compensation (absorptivity = 0.25 for eol)
; included, 80% packing factor
; IR from earth, expected hot condition for full satellite
; Temperature range: -14, +37 deg C
;
;*****
; To run:
; IDL> .run glast
; IDL> glast
; ~/idl/glast.ps is output file
```

APPENDIX G. IDL CODE FOR ON ORBIT TEMPERATURES

```

;set_plot, 'x' ;outputs graph to screen
portrait, 'ps', FILENAME='~/idl/two.eol.thesis.ps' ;outputs graph to postscript file

hi = 2 ; height of radiator surface (m)
Qw = 1000.0 ; power generated by instrument at end of life (W)
;Gs = 0. ; energy input from sun during eclipse (W/m^2)
Gs = 1358. ; energy input from full exposure to sun (W/m^2)
;qi = 0. ; no infrared (IR) from earth
qi = 237. ; IR energy absorbed from Earth (W/m^2)

trak = 0.4 ; height of tracker (m)
wi = 1.75 ; width of instrument (m)
dp = wi ; depth of instrument (m)
pacfact = 0.8 ; packing factor for radiator mirrors (%)

areaRad = wi * hi * pacfact ; radiator surface area (m^2)

Re = 6378. ; radius of Earth (km)
sigma = 5.67e-8 ; Stefan-Boltzmann constant (W/m^2/k^4)
H = 600. ; altitude of spacecraft orbit above surface (km)

sn_p = Re / ( Re + H ) ; sine of anglar radius of Earth
p = asin( sn_p ) ; angular radius of Earth (angle to tangent of horizon)

Gearth = qi * sn_p^2.0 ; IR energy flux at altitude of GLAST

Ka = 0.664 + 0.521*p - 0.203*p^2.0
; reflection of collimated incoming solar energy off a spherical Earth

a = 0.3 ; percentage of direct solar energy reflected off the Earth

alb = a * Ka * sn_p^2.0 ; solar energy reflected off Earth (albedo)

d2rad = asin(1.) / 90.0 ; conversion form degrees to radians

eol = 0.1 ; 10% reduction in properties at end of life (%)
Erad = 0.8 - 0.8 * eol ; IR emissivity at end of life
Arad = 0.25 ; IR absorptivity at end of life (0.25 at worst eol)
Eblnk = 0.01 ; IR emissivity of thermal blanket
Ablnk = 0.01 ; IR absorptivity of thermal blanket

e = fltarr(10) ; 10 surfaces for emittance
a = fltarr(10) ; 10 surfaces for absorptance
area = fltarr(10) ; 10 areas, 4 tracker sides, 4 radiator sides, top and bottom
nrm = fltarr(3,10) ; surface normal directions
temp = fltarr(10,10) ; end game temperatures

; IR Emissivity of areas , four bottom panels are radiators, rest is blanketed
; 0,2,4,6,8,9 are blanketed
; 1,3,5,7 are radiator
e(0) = Eblnk
e(1) = Erad
e(2) = Eblnk
e(3) = Erad
e(4) = Eblnk
e(5) = Erad
e(6) = Eblnk
e(7) = Erad
e(8) = Eblnk
e(9) = Eblnk

; Solar Absorbptivity
; 0,2,4,6,8,9 are blanketed
; 1,3,5,7 are radiator
a(0) = Ablnk
a(1) = Arad
a(2) = Ablnk

```

APPENDIX G. IDL CODE FOR ON ORBIT TEMPERATURES

```

a(3) = Arad
a(4) = Ablnk
a(5) = Arad
a(5) = Arad
a(6) = Ablnk
a(7) = Arad
a(8) = Ablnk
a(9) = Ablnk

; Total area
area(0) = wi * trak
area(1) = areaRad
area(2) = wi * trak
area(3) = areaRad
area(4) = wi * trak
area(5) = areaRad
area(6) = wi * trak
area(7) = areaRad
area(8) = wi * dp
area(9) = wi * dp

; Surface normal directions
nrm(*,0) = [1., 0., 0.] ; x
nrm(*,1) = nrm(*,0)
nrm(*,2) = [0., 1., 0.] ; y
nrm(*,3) = nrm(*,2.)
nrm(*,4) = [-1., 0., 0.] ; -x
nrm(*,5) = nrm(*,4)
nrm(*,6) = [0., -1., 0.] ; -y
nrm(*,7) = nrm(*,6)
nrm(*,8) = [0., 0., 1.] ; z
nrm(*,9) = [0., 0., -1.] ; -z

for th = 0, 9 do begin ; 0 to 90 degrees

  theta = th * 10.0
; theta = float( th )

  theta_rad = theta * d2rad
  c_theta = cos( theta_rad )
  s_theta = sin( theta_rad )

  for ph = 0, 9 do begin

    phi = ph * 10.0
; phi = float( ph )

    phi_rad = phi * d2rad
    c_phi = cos( phi_rad )
    sun_dir = [ [c_phi * c_theta], [c_phi * s_theta], [sin( phi_rad )] ]
    rth_dir = -sun_dir

    Qi = 0.0 ; no heat in yet
    Ri = 0.0 ; none radiated off yet

    for i = 0, 9 do begin ; each surface

      sdot = max( [ 0., sun_dir # nrm(*,i) ] );can't have negative area factor
      edot = max( [ 0., rth_dir # nrm(*,i) ] )
      Qs = Gs*area(i)*sdot*a(i)
      Qc = Gearth*area(i)*edot*e(i)
      Qa = Gs*alb*area(i)*edot*a(i)

      Qi = Qi + Qs + Qc + Qa

      Ri = Ri + area(i)*e(i)

    endfor
  endfor

```

APPENDIX G. IDL CODE FOR ON ORBIT TEMPERATURES

```
Qt = Qi + Qw      ;Plus instrument power dissipation
temp(th, ph) = ( Qt / ( sigma * Ri ) ) ^ 0.25

endfor

endfor

temp = temp - 273.15
;fine_t = rebin(temp, 500, 500)
;tvsc1, fine_t
;tv, fine_t

surface, temp, xtitle='Azimuth (longitude, 0-90 deg)', ytitle='Elevation (latitude, 0-90 deg)', ztitle = 'Deg C'

;xyouts, 6., 2.0, 'No Sun,'
;xyouts, 6., 1.7, '1 Kw power'
;xyouts, 6., 1.4, '1.0 m radiator'
xyouts, 1, 8, 'GLAST on-orbit temperatures: Full Sun 2.0 m rad (0.25 alpha)'
portrait,'ps'./CLOSE
end
```